



Developmental Problems and Their Solution for the Space Shuttle Main Engine Alternate Liquid Oxygen High-Pressure Turbopump: Anomaly or Failure Investigation the Key

R.S. Ryan and L.A. Gross



Developmental Problems and Their Solution for the Space Shuttle Main Engine Alternate Liquid Oxygen High-Pressure Turbopump: Anomaly or Failure Investigation the Key

*R.S. Ryan and L.A. Gross
Marshall Space Flight Center • MSFC, Alabama*

TABLE OF CONTENTS

	Page
I. INTRODUCTION	1
II. GENERAL	3
III. FAULT TREE/LOGIC DIAGRAM/ACTIONS/GENERAL VIBRATION AND BEARING TEAMING	5
IV. HIGH-SYNCHRONOUS VIBRATION	13
A. Dynamic Characteristics of Turbomachinery	13
B. Rotordynamic Characteristics of ATD Lox Pump	16
V. BEARING WEAR	40
VI. OVERALL CONCLUSION/SUMMARY	67
REFERENCES.....	69
BIBLIOGRAPHY	70

LIST OF ILLUSTRATIONS

Figure	Title	Page
1.	ATD high-pressure oxidizer turbopump (HPOTP)	3
2.	Turbomachinery rotordynamics.....	4
3.	Rotordynamic correlation	5
4.	FTA symbols	6
5.	Typical fault tree (ignition energy for a sugar dust explosion in a sugar refinery)	7
6.	Cause and effect fishbone diagram.....	8
7.	HPOTP synchronous vibration fault tree.....	9
8.	Bearing distress investigation fault tree.....	10
9.	HPOTP synchronous vibration fault tree team	12
10.	HPOTP sample fault tree	12
11.	Linear resonance response	14
12.	Nonlinear resonance response	15
13.	Bearing force versus deflection	15
14.	System response.....	17
15.	PEBB/damper seal	18
16.	Vibration response scenarios	19
17.	Typical vibration response.....	20
18.	HPOTP synchronous vibration resolution process	21
19.	MSFC/Pratt & Whitney vibration team	22
20.	ATD rotordynamic interactions	22
21.	HPOTP synchronous vibration problem characteristics.....	23
22.	Reduced critical team synergistic effects	23

LIST OF ILLUSTRATIONS (Continued)

Figure	Title	Page
23.	Critical tracks near the pump rotating speed (pump configuration 3-1A).....	25
24.	Critical tracks near the pump rotating speed (pump configuration 4-1D).....	25
25.	Hot-fire data of radial synchronous acceleration versus pump speed	26
26.	ATD HPOTP deadband interaction	26
27.	Analytical sideband simulation.....	27
28.	Damper seal stiffness versus convergence ratio	28
29.	Pump end ball bearing stiffness as a function of bearing tilt.....	29
30.	Increased inducer tip clearance reduced synchronous forcing function with no loss in suction performance margin	30
31.	ATD HPOTP synchronous flow dynamics.....	31
32.	ATD synchronous vibration fix summary	32
33.	HPOTP vibration configuration study plan	34
34.	SSME/ATD HPOTP unit 06-2 vibration	35
35.	Unit 03-1A vibration envelope for turbopump without corrective fixes (03-1) and intermediate corrective fix (03-1A)	36
36.	Synchronous vibration onset eliminated from operating range	37
37.	1X synchronous trackings versus time	38
38.	1X synchronous trackings versus time—unit 7-2A.....	39
39.	End-to-end runs of two of the development pumps.....	41
40.	Bearing coolant flow temperature	51
41.	Bearing coolant temperature rise	51
42.	SSME/ATD HPOTP pump end ball bearing experience before corrective solution.....	52
43.	Bearing life	53
44.	Bearing wear parameters	53

LIST OF ILLUSTRATIONS (Continued)

Figure	Title	Page
45.	Operation of misaligned bearing	56
46.	Cage thermal model of bearing distress scenario	57
47.	Loss of lubrication bearing failure simulation	58
48.	CFD analysis of ATD bearing coolant flows	61
49.	Stribeck curve (coefficient of friction versus viscosity by velocity/pressure).....	62
50.	Lox EHD film thickness analysis	62
51.	PEBB outer race piloted cage	64
52.	SSME/ATD HPOTP bearing configuration	65

TECHNICAL PAPER

DEVELOPMENTAL PROBLEMS AND THEIR SOLUTION FOR THE SPACE SHUTTLE MAIN ENGINE ALTERNATE LIQUID OXYGEN HIGH-PRESSURE TURBOPUMP: ANOMALY OR FAILURE INVESTIGATION THE KEY

I. INTRODUCTION

The space shuttle main engine (SSME) alternate turbopump developmental (ATD) program, particularly the high-pressure oxidizer pump, has experienced problems that were program threatening. The problem solutions, in a timely manner, were key to program continuation and success. This was accomplished using a concurrent engineering-multidiscipline team with members from NASA/MSFC, Pratt & Whitney, Rocketdyne, and special consultants as needed. This paper serves two purposes: (1) to demonstrate the formal failure investigation and solution approach and (2) to provide documentation of the basic problems and their solutions.

The key to correcting deficiencies is having a sound supporting technology program and the use of a concurrent Government-contractor engineering team coupled with the formal fault tree approach. It is the nature of engineers to want to make intuitive jumps and to check out a proposed solution without using a formal guided approach. As powerful as intuition is, this approach generally results in additional problems, costly additional changes, and operational constraints. This is because high-performance systems, such as the oxidizer turbopump, are finely tuned systems balanced between conflicting or competing parameters such as cost, weight, performance, and reliability. The authors' experience is replete with examples of synergistic effects resulting from small changes which lead to other problems or performance loss. In order to deal with this synergism, sensitivity analysis has to be accomplished in order to first understand the cause and second to arrive at a problem fix. This task becomes a part of the formal failure investigation.

A fault tree analysis method is a good choice to establish the problem cause or causes and to define a properly balanced solution. This formalized approach consists of a set of basic steps that have known characteristics.¹ The steps are:

- (1) Define the basic characteristics of the system
- (2) Derive a cause and effect by failure modes and effects analysis (FMEA) or fault tree (can use the fishbone)
- (3) Develop a logic diagram to resolve the fault tree (rule in or out potential causes)
- (4) Conduct analyses and tests to resolve the fault tree (formalized actions)
- (5) Determine the cause or causes
- (6) Recommend potential fixes.

The characteristics of this process are:

- (1) Formal fault tree closure matrix
- (2) Develop supporting data files
- (3) Date all papers (evolutionary change history)
- (4) No “eureka’s”
- (5) Formal, dated, personalized action items
- (6) Lessons learned conclusions.

Two problems experienced by the ATD liquid oxygen (lox) pump are discussed in this paper: (1) high-synchronous vibration and (2) bearing degradation and short bearing life. These problems are of special interest because they illustrate the fundamental aspects of balancing complex, interactive, nonlinear performance parameters (technical issues) during design and development, requiring a concurrent engineering team using the formalized fault tree approach.

The technical aspects of these interacting performance parameters, as well as the fault tree approach, are very instructive as lessons learned for future projects. Some of the interesting parameters are: rotordynamics (response and stability), flow efficiency, induced environments (thermal, vibration, flow), bearing characteristics (cooling, lubrication, materials, etc.), and geometric characteristics. These can be summarized under five major headings:

- (1) Hydrodynamics: performance and induced environments
- (2) Rotordynamics: balance, vibration, stability
- (3) Bearings: characteristics and life
- (4) Housing and support structure (stiffness and flow geometrics)
- (5) Damping seals: characteristics and performance.

This paper will discuss the two development problems, (1) vibration and (2) bearing life—how they were approached, the technical issues, and the solutions implemented. Both of the problems are closely related and are nonlinear in nature, with many strong interactions. Understanding the associated sensitivities and the resulting trades was essential to solving the problems without introducing other problems. Taguchi design of experiments was used to augment and guide diagnostic testing. The underlying principle is: high-performance machines are a compromise, a balancing act; hence, solving one problem, as a minimum, reduces the margins in another area—many times at the expense of performance, cost, and reliability.

II. GENERAL

Turbopumps (oxidizer and fuel) are used to increase pressures to the levels required in the combustion chambers of high specific impulse (ISP) liquid rocket engines. The SSME uses a two-stage pump system and a dual combustion cycle to achieve very high ISP (453 s). The high-pressure lox pump, the subject of this paper, has a three-stage turbine driven by hydrogen/oxygen combustion products that powers two liquid oxygen pumps on a common shaft. The larger of the two pumps, a double-suction pump with integral inducers, supplies oxygen at 4,000 lb/in² to the main combustion chamber. The smaller pump supplies lox at 8,000 lb/in² for combustors driving the engine turbines. A cross-section of the turbopump is shown in figure 1.

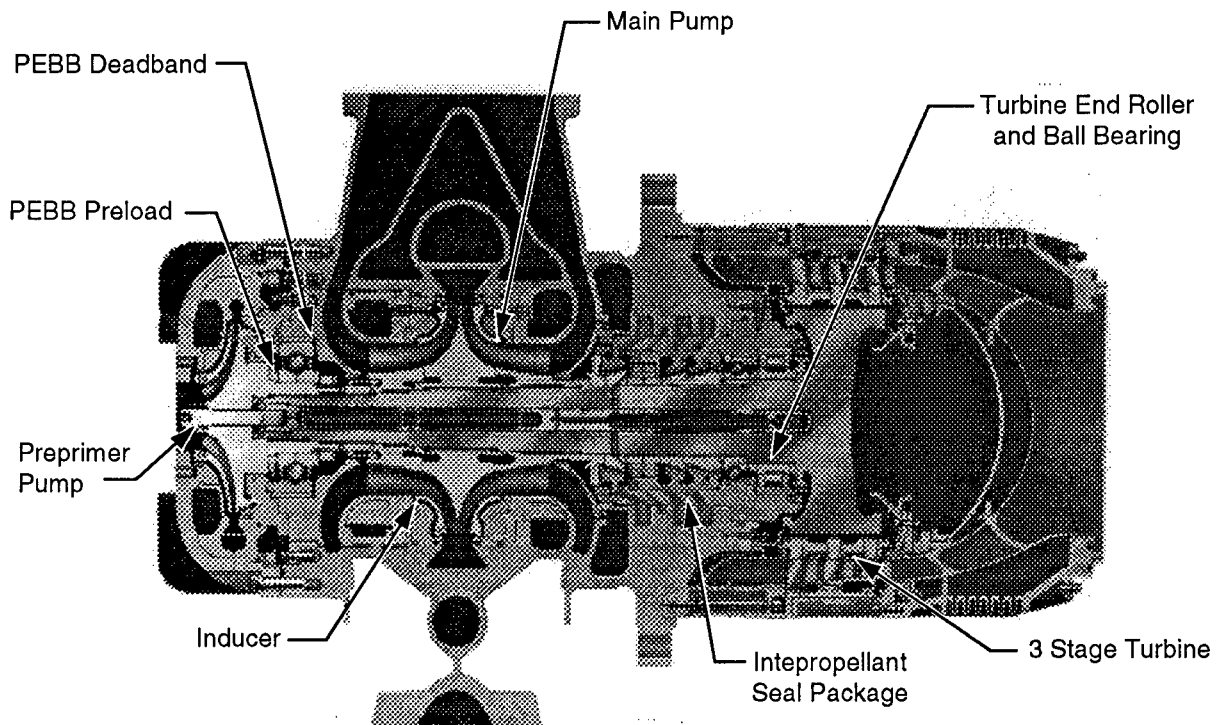


Figure 1. ATD high-pressure oxidizer turbopump (HPOTP).

The rotor is supported by a roller bearing on the turbine end, and a ball bearing and damping seal on the pump end. Axial thrust is controlled during operation by a double-acting balance piston on the shrouds of the main pump impeller. Transient axial thrust is controlled by the two ball bearings. The ball bearings are preloaded with a spring axially to ensure proper ball race contact. In order to guarantee axial movement capability, the ball bearings are built with a clearance between the outer race and bearing support structure. The purpose of the damping seal is to provide damping for rotordynamic modes, ensuring low vibration and stability. Designing the damping seal to provide fluid stiffness results in creating a parallel support system on the pump end. This parallel load path produces interactions and system trades that must be tuned and balanced.

The pump operates over a speed range of 0 to 24,500 r/min. Temperatures in the turbine are approximately 1,500 °R with an inlet pressure of 4,800 lb/in². A purge seal system is located between the pumps and turbine to prevent hydrogen from mixing with oxygen during operation.

The above characteristics are obtained in a system of minimum size and weight. The pump has high-energy density and operates at a high speed. The conflicting requirements between the performance requirements and minimum weight lead to a finely tuned system. The result is a fine balance between performance (ISP, flow, pressure), stability, weight, and lifetime, as well as the unwanted rogue forces that affect its own system and the rest of the engine system.

This brings into play several specialized disciplines such as structural analysis, structural dynamics, rotordynamics, thermal, fluid flow, bearings, seals, materials, and performance in a highly interactive and sensitive manner. Generally, design analysis cannot fully replicate this phenomenon because analysis is just models built around approximate assumptions and incomplete data. An example is shown in figure 2. The output of the models is the turbomachinery characteristics that can be understood by varying the various design parameters. In the final analysis, the only complete characterization is the hot firing of the turbomachinery system. This means that specialized tests (structure, flow, etc.), using special instrumentation, are run to quantify parameters for the models and to certify the system. The results of the analysis are then correlated with the hot-fire data (obtained using special instrumented development hardware) to baseline the models for design use. In addition, hardware tear down and inspection provide further correlation and insight (fig. 3). Through this process of dispersed parameter analysis supported by specialized tests to define the parameters correlated to development hot-fire data (dispersed to understand margins) and hot-fire hardware inspections, a balanced design is accomplished. Similar design, analysis, and correlation cycles are followed for all of the key aspects of the turbomachine. The important fact to remember is that the pump operates as a system, not a set of independent disciplines, in a highly interactive manner.

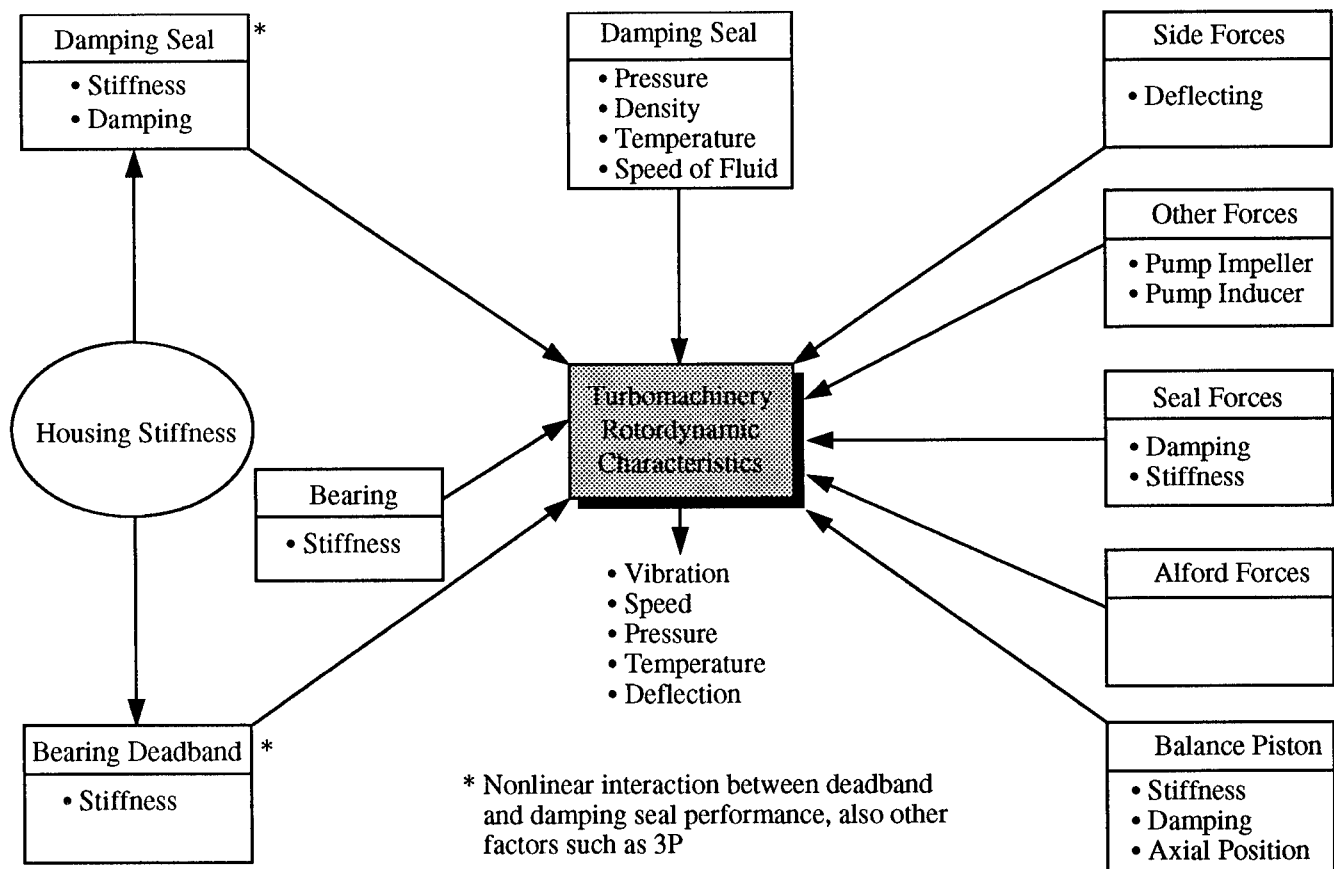


Figure 2. Turbomachinery rotordynamics.

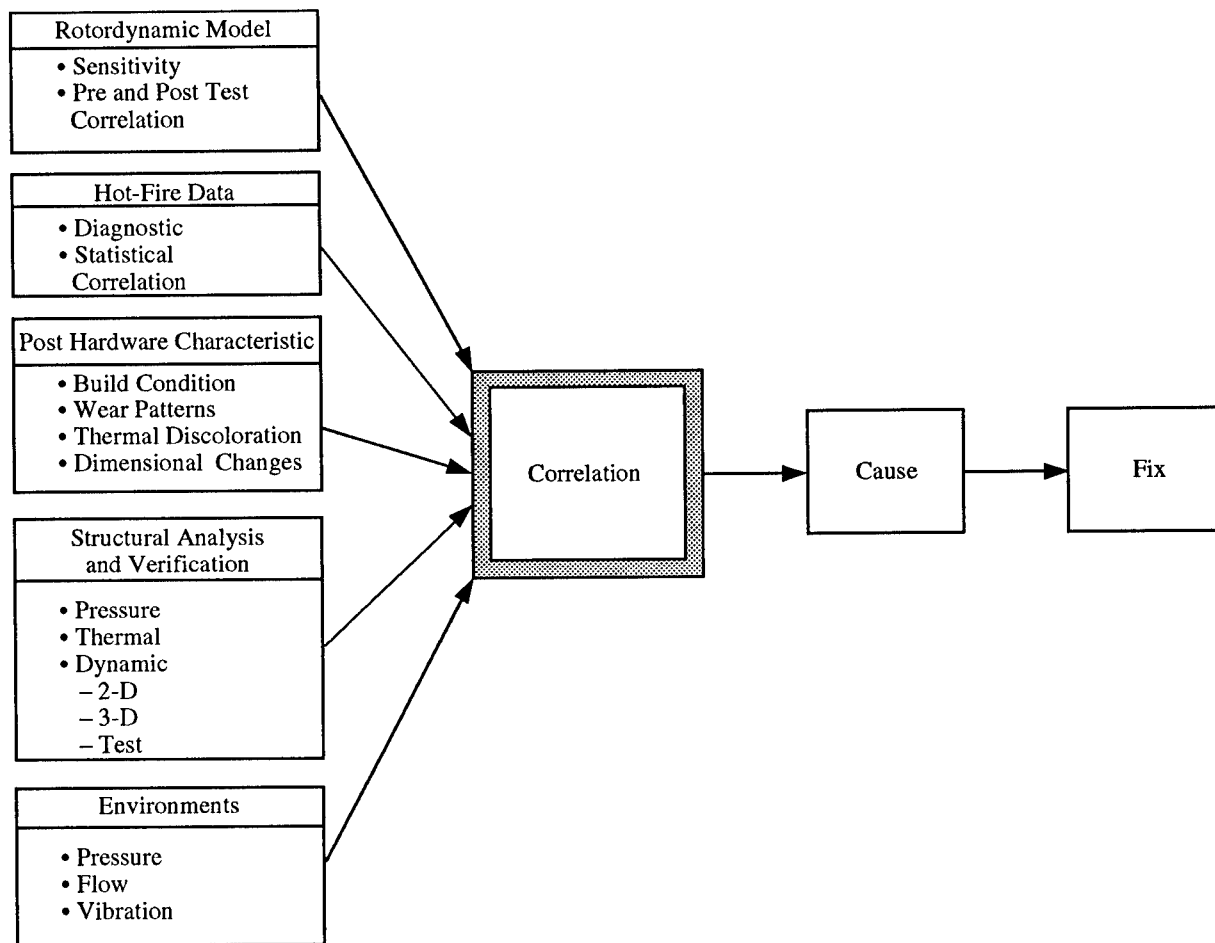


Figure 3. Rotordynamic correlation.

During development, when problems occur due to this fine tuning of design parameters, a formal procedure must be followed to ensure proper understanding of the system and the correct solutions. This approach is the fault tree with supporting logic diagrams, analyses, and tests. The next section discusses this approach.

III. FAULT TREE/LOGIC DIAGRAM/ACTIONS/GENERAL VIBRATION AND BEARING TEAMING

Determining the cause and the solution to developmental problems experienced in space programs is most efficiently accomplished using a concurrent engineering-multidiscipline team employing fault trees with support logic diagrams and formal action items. The concurrent engineering-multidiscipline team is necessary to ensure communications and understanding.

The fault tree approach focuses the activity by requiring the use of supporting data to formally close all branches not contributing to the problem. These data are acquired by analyses, special tests, and system tests. The point to remember is that all analyses and special tests are merely models of the real thing and are based on many assumptions. The only true data are obtained from instrumented system tests and inspection and evaluation of the hardware after these tests. In the final analysis, the hardware has the answer. The problem is our ability to read it. One usually reads

it based on the theories one understands, which emphasizes the need to have all plausible theories investigated and understood. Consultants can help greatly in this area.

The fault tree approach (fishbone diagrams can be used in place of the fault tree) requires a thorough understanding of the system. Based on this understanding, all the potential causes and contributing parameters are identified. Using these causes, a fault tree is laid out that identifies the path of the potential causes. Figure 4 shows the elements of a fault tree. Figure 5 is an example of a fault tree developed for a dust explosion in a sugar mill. Figure 6 is an example of a fishbone diagram for cause and effect for categorizing mistakes. How and which of these to use depends on the problem and the team. Many times the symbols described can be eliminated resulting in a straight-line cause tree, simplifying the layout of work.

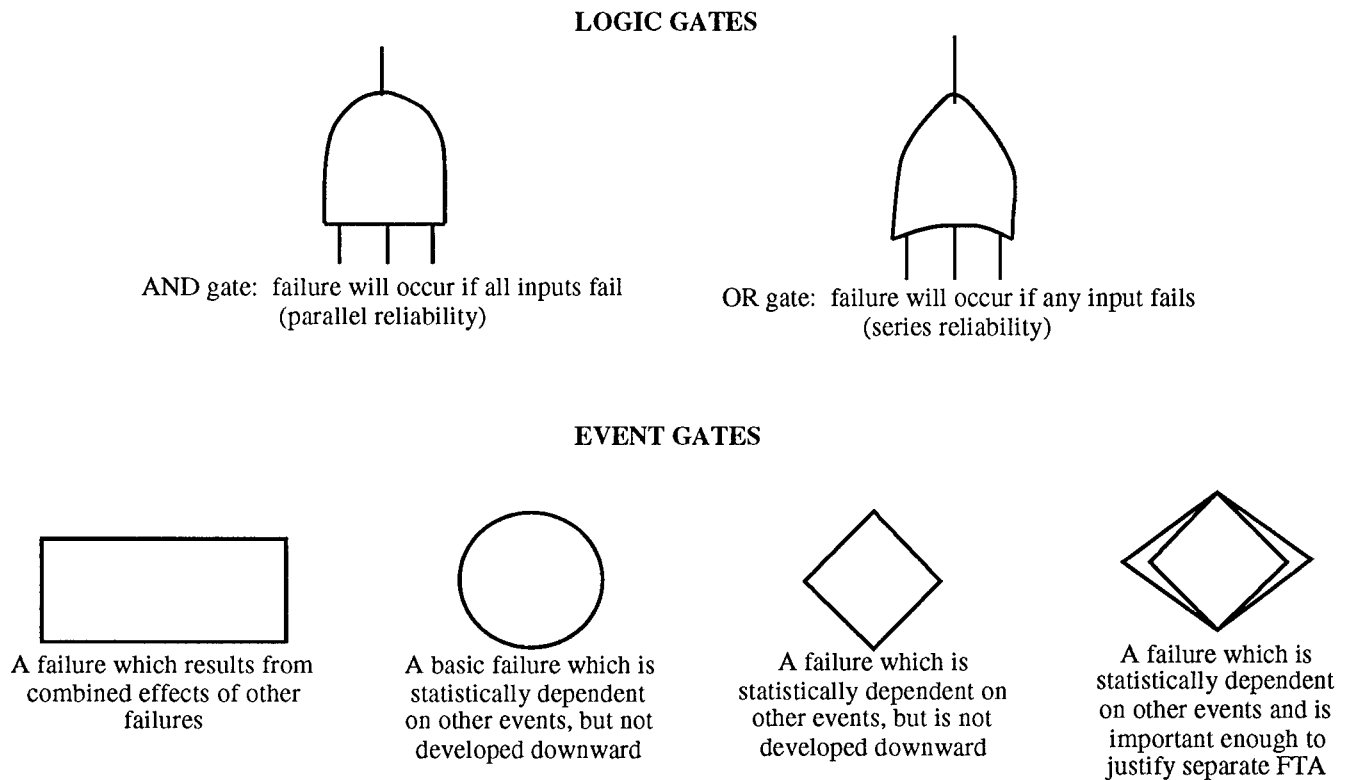


Figure 4. Fault tree analysis (FTA) symbols.

This straight-line approach, in conjunction with logic flow diagrams, was used by both the vibration and bearing teams. Figure 7 is the fault tree for the vibration team, and figure 8 is the fault tree for the bearing life team. The teams' compositions included NASA, Pratt & Whitney, Rocketdyne, and several consultants, in all disciplines including structures, flow, thermal, manufacturing, etc. In all cases, a formal action item list and fault tree closure matrix were used in conjunction with logic networks. Design of experiments was used to guide diagnostic testing.

The teams functioned in two distinct ways. First, the team members spent several days together at the Pratt & Whitney plant to lay out the fault tree and start the process. The teams reconvened in face-to-face meetings at critical path decision points. Second, a biweekly teleconference was held with all members participating to discuss action item results and to fine tune the plan.

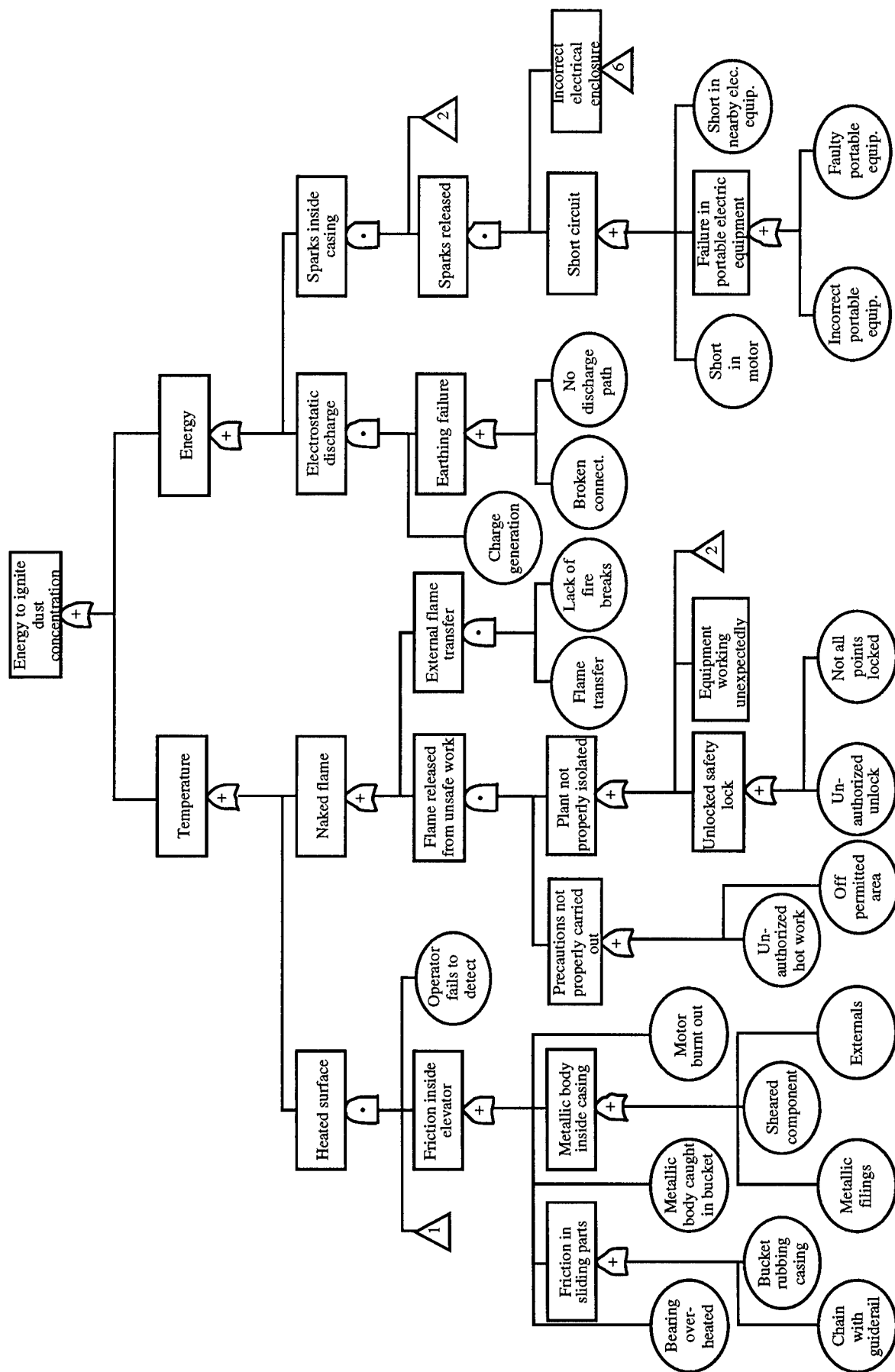


Figure 5. Typical fault tree (ignition energy for a sugar dust explosion in a sugar refinery).

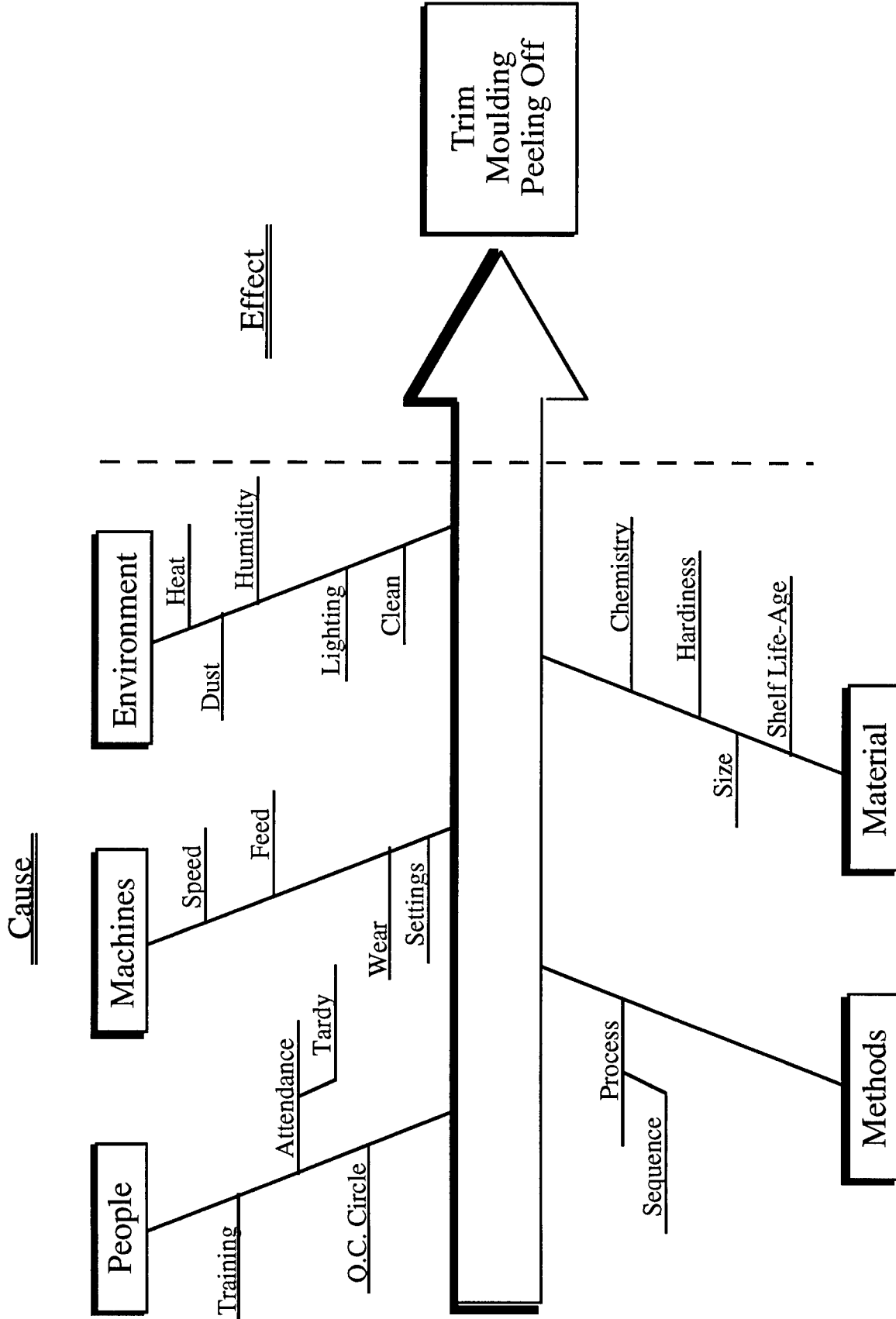


Figure 6. Cause and effect fishbone diagram.

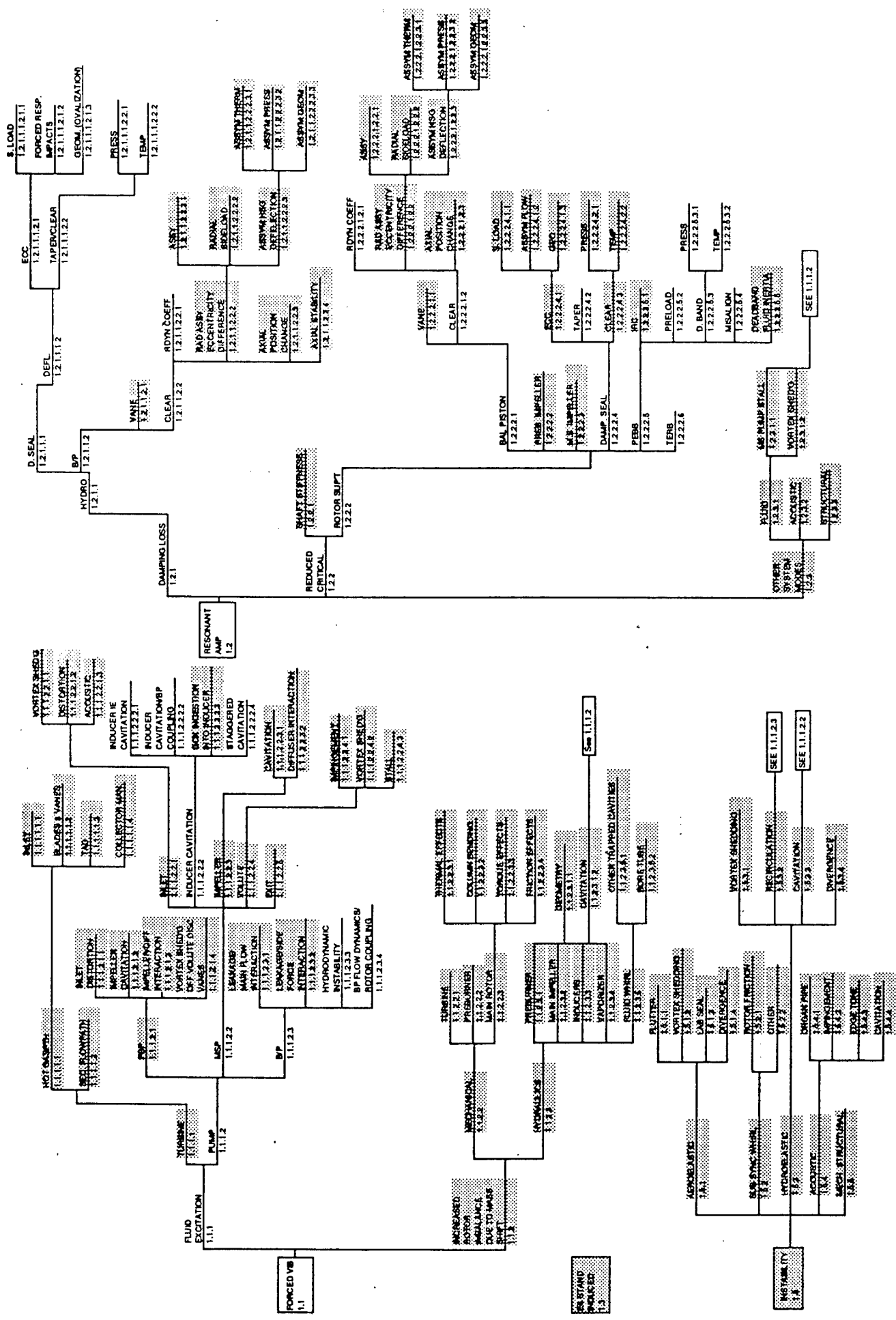
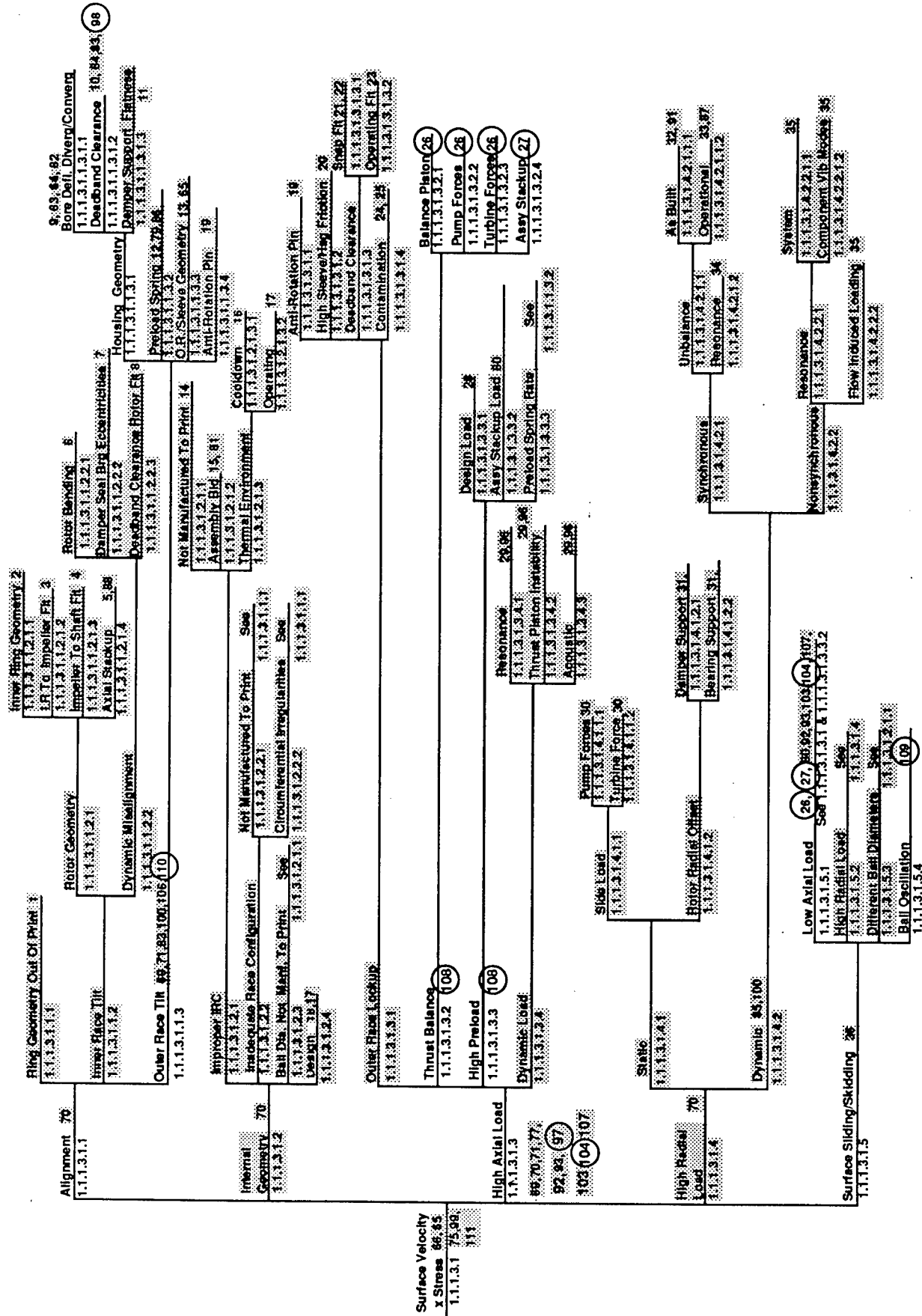


Figure 7. HPTP synchronous vibration fault tree.



This teleconferencing approach was chosen so that the engineers could be at their home station and have access to computer programs and test facilities. This dual approach of periodic face-to-face meetings supplemented with teleconferences was very successful; particularly with the efficiency of electronic data transfer between individual computers and fax machines. This allowed complete utilization of test and other facilities at MSFC and Pratt & Whitney and the variously honed skills their respective engineers and managers provided.

The major problem that the teams had to deal with was declaring success or partial success and thus discarding the formal process. It is mandatory that the process be completed, not accepting any "eureka's." Engineers by nature like to use intuition and solve the problem without the burden of the formal process. The history of aerospace problems dictates that the formal process as outlined be used. Figure 9 shows this formal process by breaking out the fault tree by work breakdown structure (WBS) numbers with comments and actions. Figure 10 is a typical action item tracking matrix.

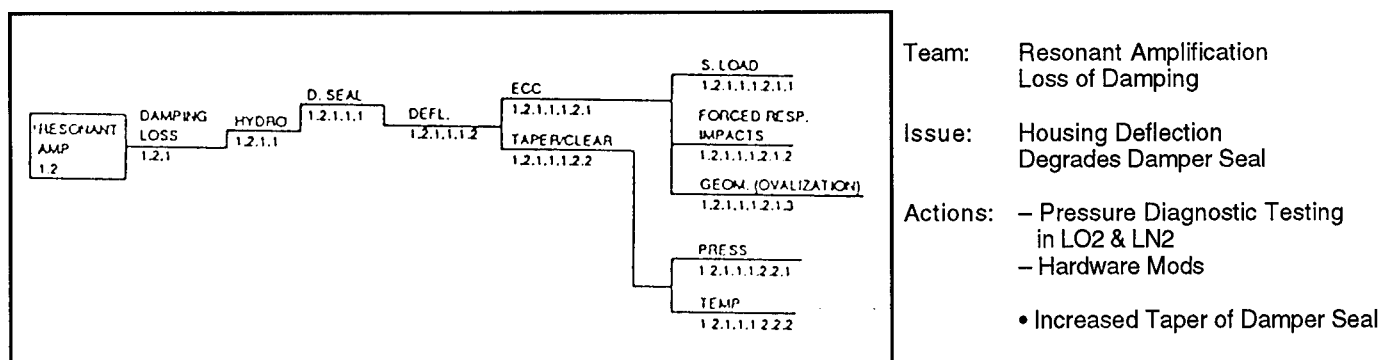


Figure 9. HPOTP synchronous vibration fault tree team.

Cause	Support	Refuting	Action	Disposition	
1.1	Forced Vib				
1.1.1	Fluid Excitation				
1.1.1.1	Turbine				
1.1.1.1.1	Hot Gas Path	O4-1D ran to 111% with no sync step. Turbine run to very high power, indicating no turbine fluid driver.	Assess Kistler data in turnaround duct (Action 1.5.1)	Not credible	
1.1.1.1.1.1	Inlet	Thick & thin inlet struts are potential sources for vortex shedding.	Vortex shedding frequencies are probably high.	Calculate inlet vane vortex shedding frequencies (Action 1.1.1.16)	Not credible (>1,000 Hz)
1.1.1.1.1.2	Blades & Vanes	Blades and vanes potential sources of vortex shedding, unsteady separation.	Same as above	Same as above	Not credible
1.1.1.1.1.3	TAD	Struts & splitter are potential sources of vortex shedding or stall.	Same as above	• Same as above • TAD separation freq. --/= 10-100 Hz	Not credible
1.1.1.1.1.4	Collector Manifold	None	EB collector does not include LOX head exchanger. High vibrations not seen on G-3 flange. GFE vanes/hot gas manifold geometry same as current flight hardware.		Not credible

SAMPLE

Figure 10. HPOTP sample fault tree.

IV. HIGH-SYNCHRONOUS VIBRATION

Several instances of unacceptable synchronous vibrations have occurred during development of the ATD oxidizer turbopump. Initially, there was a high vibration that built up over a short period of time and caused premature shutdown of the turbopump. This problem was corrected by: (1) ensuring that the bearing-support-housing-to-outer-race clearance remained slightly convergent; (2) increasing the mean-bearing-outer-race-to-support-housing clearance; (3) ensuring that the damping seal was convergent to maintain adequate stiffness and damping; and (4) reducing the inducer hydrodynamic forcing function. These changes reduced vibrations to acceptable levels and allowed long-duration development testing to proceed. While the synchronous level was reduced, a distinct vibration sensitivity occurred in which multiple shifts in synchronous level persisted during the turbopump operation. This sensitivity was of concern because of the possibility that shifts were symptoms of a marginally acceptable vibration condition which would eventually precipitate high-level vibrations in a turbopump. The problem was corrected by (1) tightening the turbine roller bearing deadbands and retention, and (2) increasing the stiffness of the damping seal after extensive data correlation showed these to be the most likely sources of the problem.

A. Dynamic Characteristics of Turbomachinery

The nature of turbomachinery is very complex with many interacting parameters. In general, this set of interactions is very sensitive to small changes. This is especially true for the rotordynamics discipline and particularly for high-performance systems such as the SSME high-pressure pumps. Rotordynamics for these pumps is very complex and is highly nonlinear. There are many forcing functions that are derived from the fluid forces of the liquid being pumped and the turbine forces associated with the hot-gas power system. Forces also exist due to the structural system such as unbalance, friction, and vibration. The turbomachinery system is composed of the pressure vessel, rotor supports, shafts, impellers, turbine, and damping devices all of which combine to make the rotordynamic system. Childs² and Rao³ discuss these various aspects representing the rotordynamics characteristics.

In general, all dynamic phenomena can be classified in three ways: (1) forced oscillations where the frequency content of the natural or induced forces drive the dynamics of the system; (2) instabilities where the forces increase with increasing amplitude of response, creating a negative feedback (instability) further increasing the response; and (3) transient response. These three types of responses can be illustrated with a single mass spring damper system. Also, this same simple model can be used to help understand the oxidizer pump vibration problem by making several analogies. It should be pointed out however, that the actual rotordynamic system's nonlinearities precludes a complete analogy using this simple system.

To derive this simple approach, the assumption has to be made that one can represent each of the pump's dynamic system modes as uncoupled modes represented by individual uncoupled second-order differential equations. These equations can be linear or nonlinear in nature. The resulting equations have the form

$$M\ddot{X}(t) + C\dot{X}(t) + KX(t) = F(t) . \quad (1)$$

This equation for the rotordynamic analogy is complex in that M includes everything that makes up the effective system mass for a given mode, such as that part of the fluid mass which adds

to the structural mass. The damping is the total system damping, both positive and negative, that arises from the structure, the flowing fluids, and flowing gases. In turbomachinery, some of the damping terms are negative and can produce instabilities. Examples are: turbine tip seal forces and shaft internal friction.⁵⁻¹¹ The stiffness term has the same inherent complexities because stiffness can arise from seals, bearings, structure, etc. The degree to which one can approximate this combination into the single mean, damping, stiffness coefficient determines how much insight this simple system can provide. However, an approximate representation provides the insight and guides the understanding, and can provide a simple theoretical basis for interpreting information and data.

As stated previously, the response of this system can be placed in three categories: (1) forced response, (2) instability, and (3) transient, each of which is prevalent in rotating machinery. Each of these three types of responses can be linear or nonlinear in nature. Because the fault tree ruled out the instability early, leaving only the forced and transient response categories, it is prudent that one understands the basics of both the linear and nonlinear nature of forced response (transient response is a special type of forced response where the force or deflection is applied or released, then the structure rings out or decays from this energy pulse input).

1. Linear System. The assumptions that have to be made for this linear system analogy to hold is that there are no structural clearances (all parts in contact), and that the fluid forces are linear. In this case, the M , C , and K are a function of the operating conditions which are generally a function of time. Further, it is best to freeze these conditions at any one point in time assuming that the time changes are slow and do not significantly influence the frozen time point approximation. In this case, the response varies only as a function of the forcing function amplitude, the ratio of system frequency to the forcing function frequency, and the damping (fig. 11).

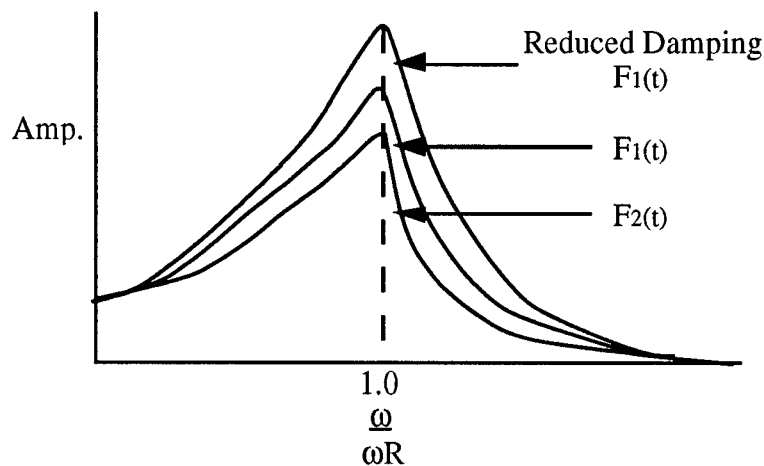


Figure 11. Linear resonance response.

The choices open to reduce the amplitude of a forced linear system are to: (1) reduce forcing function amplitude, (2) increase system damping, (3) shift system's natural frequency away from resonance with the forcing function, and (4) shift forcing function away from the system natural frequency. Obviously in a linear system, any combination of the above can be utilized to change the response amplitude.

2. Nonlinear System. Nonlinear systems are more complex and more difficult to interpret. Nonlinearities can be due to clearances, amplitude dependency, or time dependency. In turbomachinery, the main effect is clearance and amplitude dependency. The characteristic frequency curve

as was shown on figure 11 changes drastically. To illustrate the change, a stiffness hardening and softening system are chosen as examples. This case curve is only valid for one given nonlinearity type. Nonlinearities other than softening or hardening would look different, as well as the effect of the forces on hardening or softening stiffness. Examples of amplitude-sensitive nonlinearities are shown in the resonance curves in figure 12.

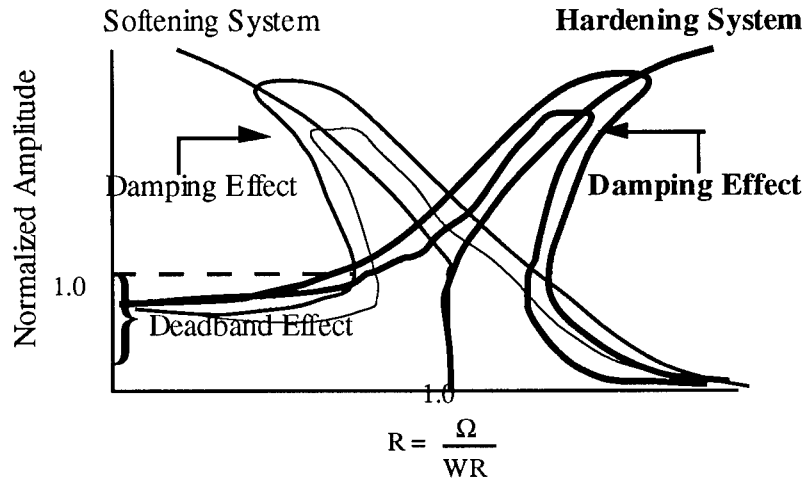


Figure 12. Nonlinear resonance response.

Rotating machinery can have a nonlinear bearing stiffness characteristic caused by rolling contact bearings moving within the housing clearance. As the bearing comes into full contact with the housing, a significant increase in stiffness will occur. Large changes in amplitude of the machine vibrations will result if the machine is operating near the critical speed, either before or after engagement of the bearing with the housing support (fig. 13). In a dynamic situation, there is

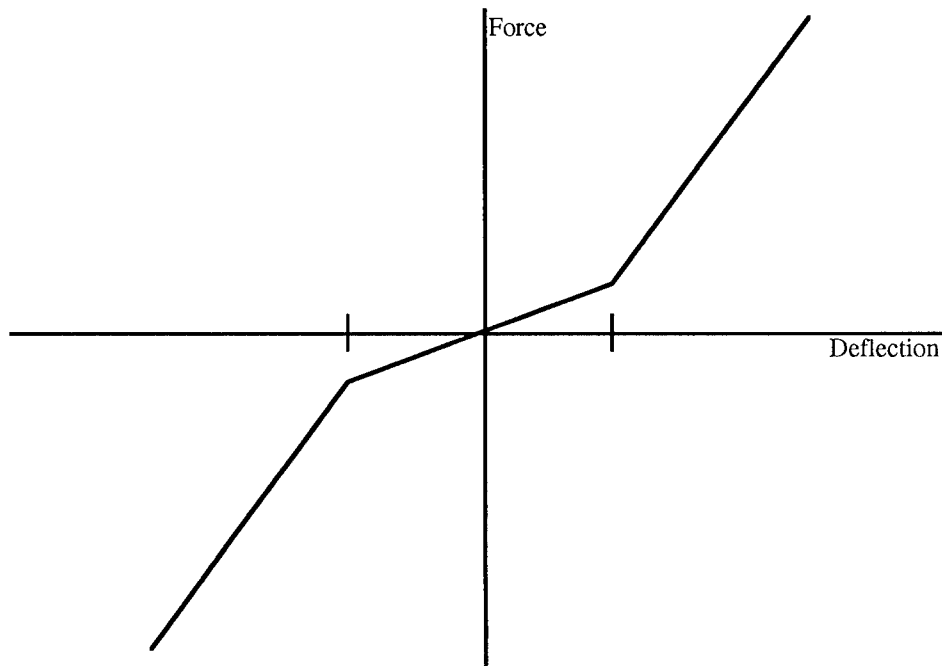


Figure 13. Bearing force versus deflection.

a back-and-forth motion between the clearance that produces an amplitude-varying stiffness. This is a function of the shaft orbit position creating a very complex nonlinear system. The simple analog of a planar nonlinearity does not attempt to show this effect. For example, the stiffness before clearance is taken up (if two springs are parallel) is:

$$K_1 = K_T . \quad (2)$$

After the clearance is taken up, the stiffness is:

$$K_1 + K_2 = K_T . \quad (3)$$

This equation becomes:

$$M\ddot{X} + C\dot{X} + [K_1 + K_2(X \geq X_1)]X = A \sin \Omega t . \quad (4)$$

As a result, the stiffness is highly nonlinear, producing the typical beating-wave forms instead of pure sine waves. Ideally, turbomachinery should operate subcritical; thus, when K_2 kicks in, the critical frequency is always above the operating range. Otherwise, if the operating point for K_1 is supercritical, then when the clearance is taken up, the frequency moves toward, or through, the operating range.

This implies that it is hard to use a simple analog to model the problem accurately, and one must rely on empirical data evaluation and nonlinear rotordynamic simulations. In fact, this is the only way the system is accurately represented without compromising assumptions. The test data are complete and the simulation is an approximation. The nonlinear rotordynamic simulation does, however, allow a good understanding of the sensitivity of the system to parameter variations and illustrates the basic physics of the system. The major problem in rotordynamic nonlinear simulations is the determination and quantification of the input data such as seal forces, rotor fluid forces, and Alford forces. The dynamic characteristics of rolling element bearings and structural dynamics are also difficult to accurately model.

3. Instabilities. The common title given to most rotordynamic instabilities is whirl. Whirl can be caused by the hot-gas forces, fluid forces, or frictional forces in the structural system. Because the shaft is rotating at high speeds, these modes can set up as either forward or backward whirl. The instabilities are caused by the forces and displacement generated by the motion being out of phase such that they add energy to the system. Whirl modes usually exist at some fraction of the synchronous speed around 60, 90 percent, etc. Because it was easily shown by analysis and the hot-fire data that no instabilities exist in the ATD lox pump, instabilities will not be discussed any further in this report. Many references exist, such as references 2, 4, 5, 6, 12, and 13.

B. Rotordynamic Characteristics of ATD Lox Pump

1. Characteristics. Reviewing the ATD lox pump configuration, it is clear that it is a highly coupled system. Rotordynamically, it is composed of a very rigid shaft supported by three elements radially and three longitudinally. The three radial supports are: (1) damping seal, (2) ball bearing (pump end), and (3) turbine end roller bearing (fig. 1). Because the damping seal is located adjacent to the pump-end ball bearing, and the seal has significant stiffness, a dual load path exists. The ball bearing stiffness comes into play when rotor forces are great enough to cause a displacement of seal stiffness large enough to move the bearing through the deadband and engage it with the support

housing. This creates a nonlinear spread and displacement-sensitive system requiring tuning and balancing for successful operation. All bearings are constrained and supported by the housing.

On one end of the shaft is the turbine that produces the rotary power and it is very hot. The other end contains the preburner and main stage pumps, both at cryogenic temperatures. Seals between the different areas are necessary to separate oxygen and the fuel-rich hot gas, and to provide performance. All these elements either determine stiffness and mass dynamic characteristics or they generate forces such as unbalance or fluid (damping and stiffness) as well as structural damping. Additionally, the pump-end ball bearing has a preload spring that ensures the correct axial load for successful bearing operation. A separator between the inner and outer races keeps the balls apart.

Figure 14 summarizes the rotordynamic characteristics to be considered in the turbopump. A detailed nonlinear rotordynamic simulation¹⁴ has been formulated and implemented to simulate the interactions of all these coupled parameters and/or subsystems. Because of the high-performance requirements, the system becomes a finely tuned and balanced system between these various parameters. The simulation can be linearized to produce frequencies, damping, and stability. The nonlinear formulation normally produces time responses as does the hot-fire instrumentation, which can be analyzed and evaluated using standard data processing techniques. These include analog amplitude plots versus time, root mean square (RMS) amplitude plots versus time, point time spectral analysis, and isoplots (frequency spectrums versus time). It is important for analysis/test correlation to utilize common data evaluation techniques for both.

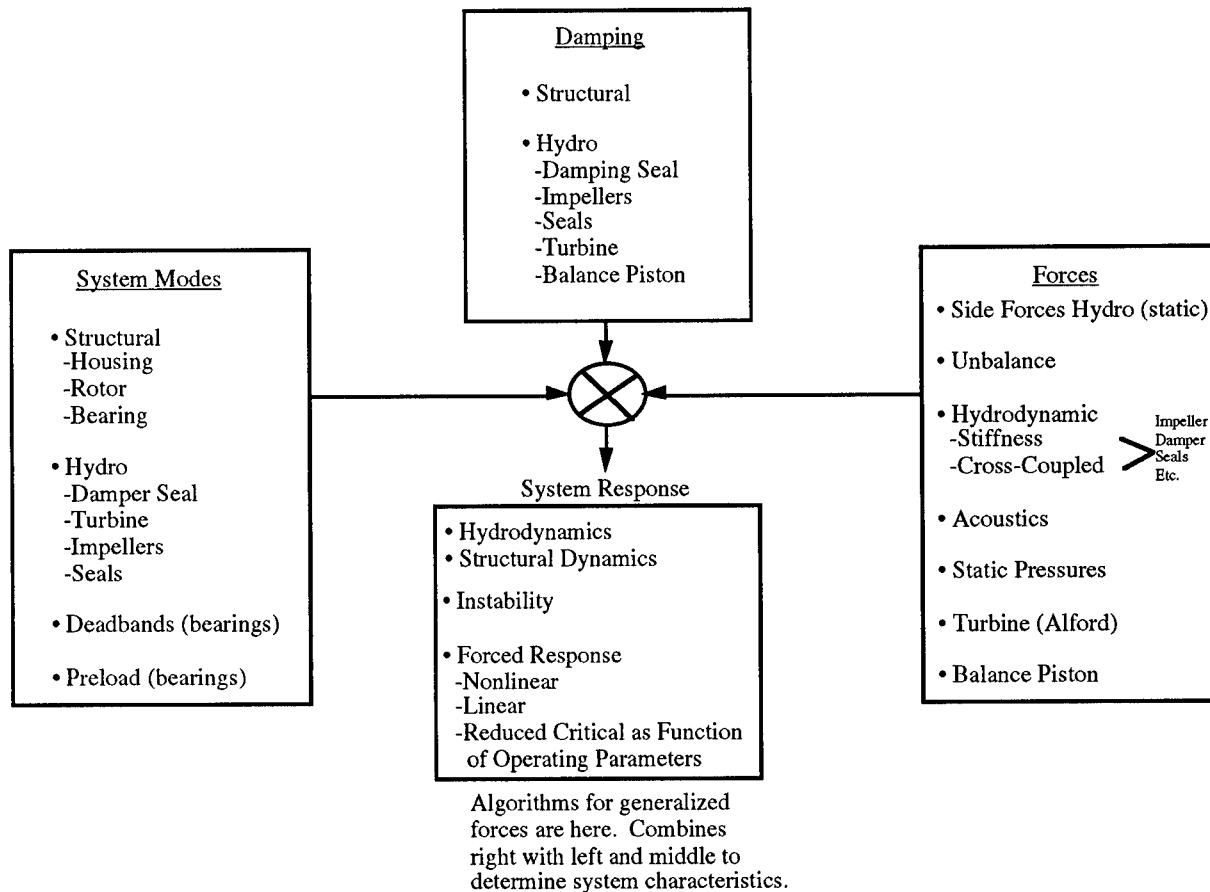


Figure 14. System response.

2. High-Synchronous Vibration Cause. The ATD lox pump was designed to have its critical modes well above its critical speed, plus to have a strong damper seal to augment the rotor system damping. The stiffness for the rotor support is a combination of both the bearings and the damper seal. The damper and pump-end ball bearing are located adjacent to each other, providing parallel load paths (fig. 15). This complicates the dynamic characteristics, simulation, and understanding in that the pump criticality is essentially determined by the damper spring until rotor deflection is large enough to transverse the bearing deadband and allow engagement of the bearing with the housing. Because the damper seal has substantial stiffness, the pump can operate without the bearing adding stiffness. Additionally, frictional hang-up of the bearing outer race in the housing and unfavorable tilting of bearing outer race relative to the rotor may significantly reduce the radial stiffness of the ball bearing. In operations, the critical mode (fig. 16) has been in the operational speed range, creating the high synchronous vibration. A typical vibration response is shown in figure 17. The lower critical radial stiffness resulted in a premature cutoff by the engine redline protection system. The other undesirable vibration did not result in redline shutdown and was named "vibration sensitivity." Vibration sensitivity was a catch-all term applied to synchronous vibration shifts of 1 to 2 g's, and spikes which could not be related to any changes in physical or operational characteristics of the turbopump. While not of themselves harmful, the potential for their being a precursor to unacceptable vibration made them a major concern during development.

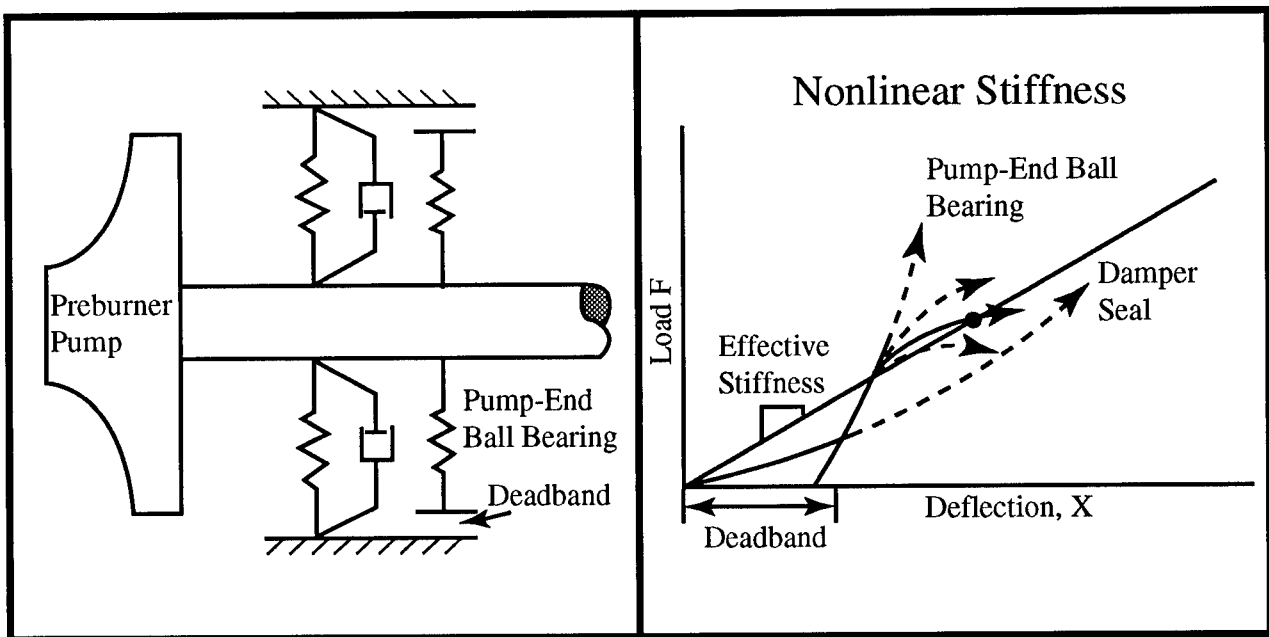
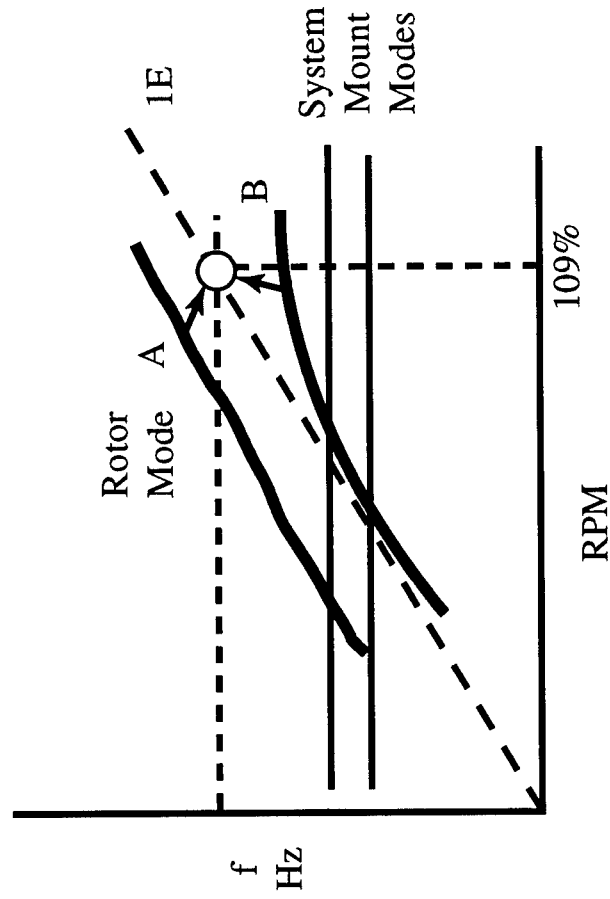
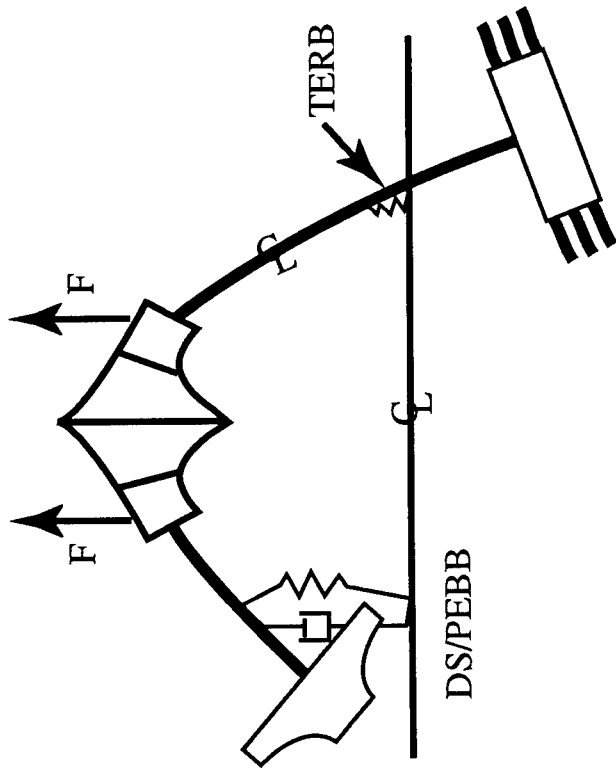


Figure 15. PEBB/damper seal.

The bearing must have some small clearance relative to the housing support in order to allow axial shaft motion resulting from operating point changes. Operating point changes cause a change in the pressure forces acting on the rotor elements that is corrected by a balance-compensating piston that requires rotor motion. The bearing inner race, which is part of the rotor, moves axially with the rotor. If the bearing outer race does not track the rotor (hang-up is the term used to describe this condition), the bearing can overload to failure or lose radial stiffness depending on the direction of the rotor motion. The preload spring action against the bearing outer race maintains the proper axial load for long bearing life.



Postulate to Explain Vibration Response

- Two Scenarios: A - Rotor mode drops onto the operating point
- B - Rotor mode increases onto the operating point

Figure 16. Vibration response scenarios.

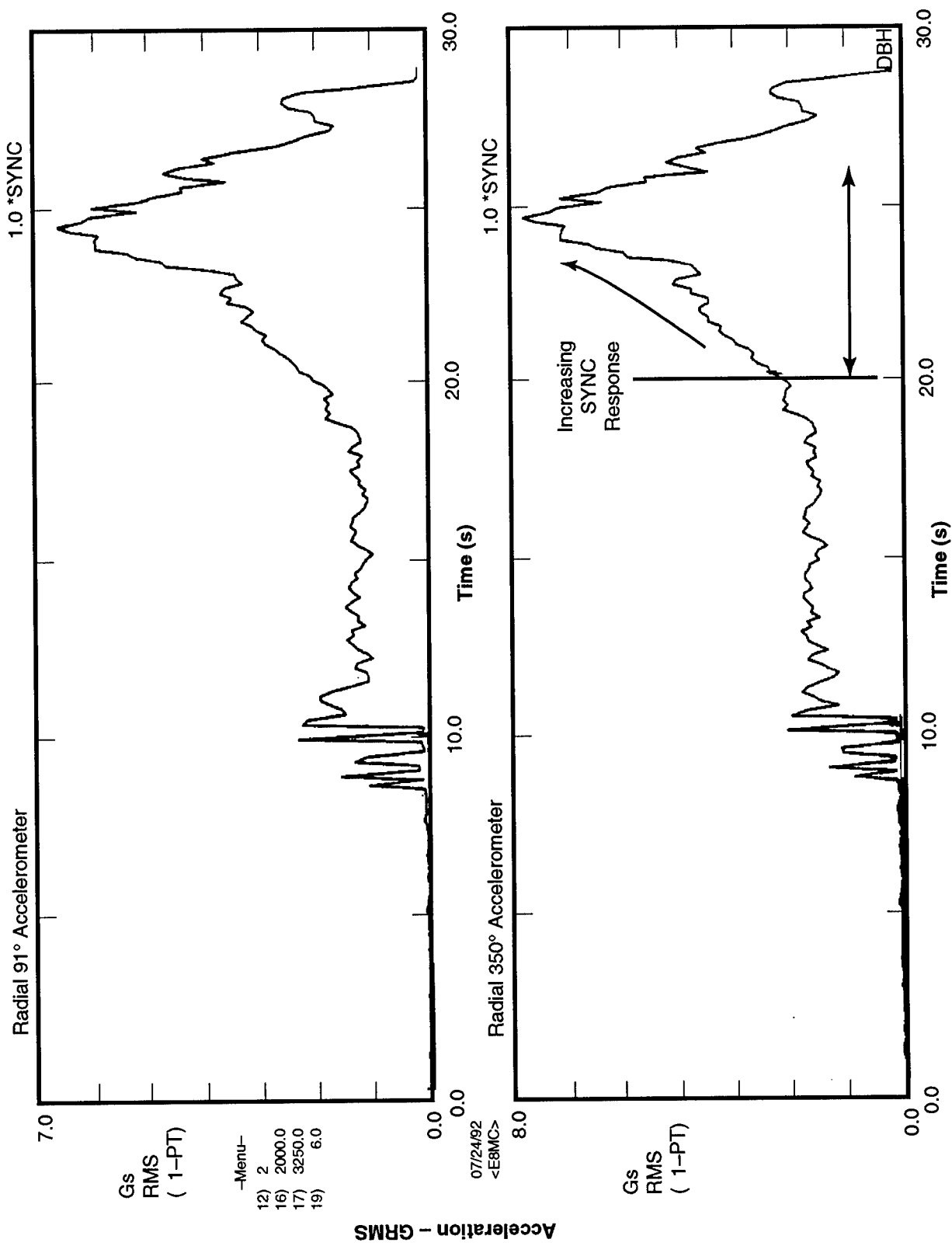


Figure 17. Typical vibration response.

As mentioned previously, the ATD HPOTP experienced high-synchronous vibration during development that reached levels which were considered to be unsafe and premature test termination had to be initiated. The characteristics of this response were originally interpreted as a nonlinear jump due to the compressed time scale. Expansion of the scale showed the response to be that of a tuned (resonance) lightly damped system. Figure 17 shows typical vibration response of the pumps as power (speed) is increased. After months of fine-tuning build clearances, and several redesigns, without affecting the problem, a vibration team was formed in May 1992 to understand and solve the problem (see earlier discussion).

Application of the fault tree and the logic diagram to the problem (figs. 18, 19, and 20) identified three primary sources of the vibrations: (1) a criticality in the operating speed range of the pump, (2) inadequate rotor damping, and (3) high dynamic forcing functions (section IV). The conclusion drawn by the team (figs. 21 and 22) was that a system mode resonant condition is the principal source of high vibration, with amplifiers arising from a hydrodynamic forcing function and reduced damping. There were two potential ways the criticality could be in the operation range. The first was due to the ball bearing tilting in the wrong direction, greatly reducing the bearing stiffness and, thus, causing the critical speed to drop into the operating speed range; second bearing hang-up, causing load stiffness.

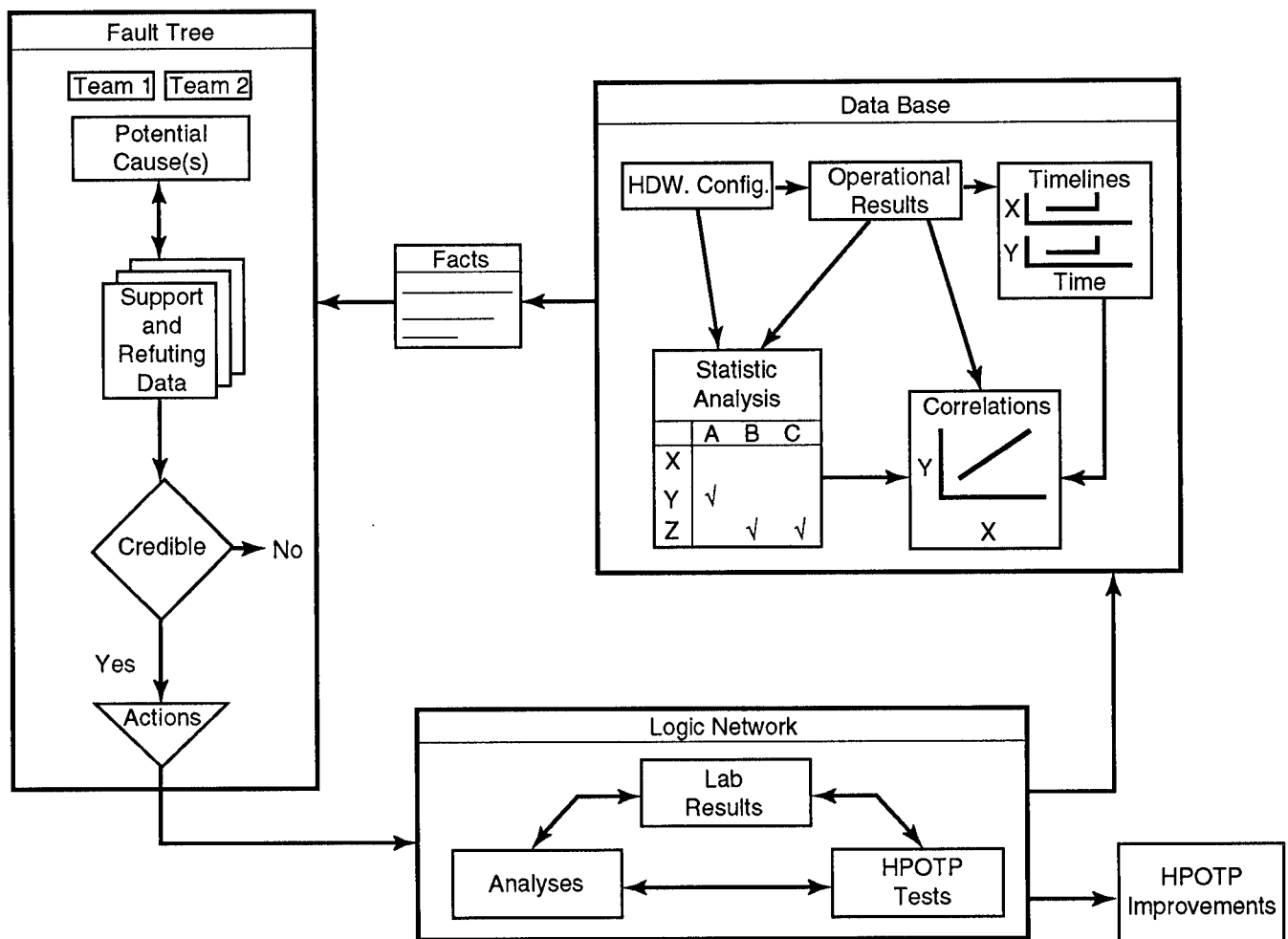


Figure 18. HPOTP synchronous vibration resolution process.

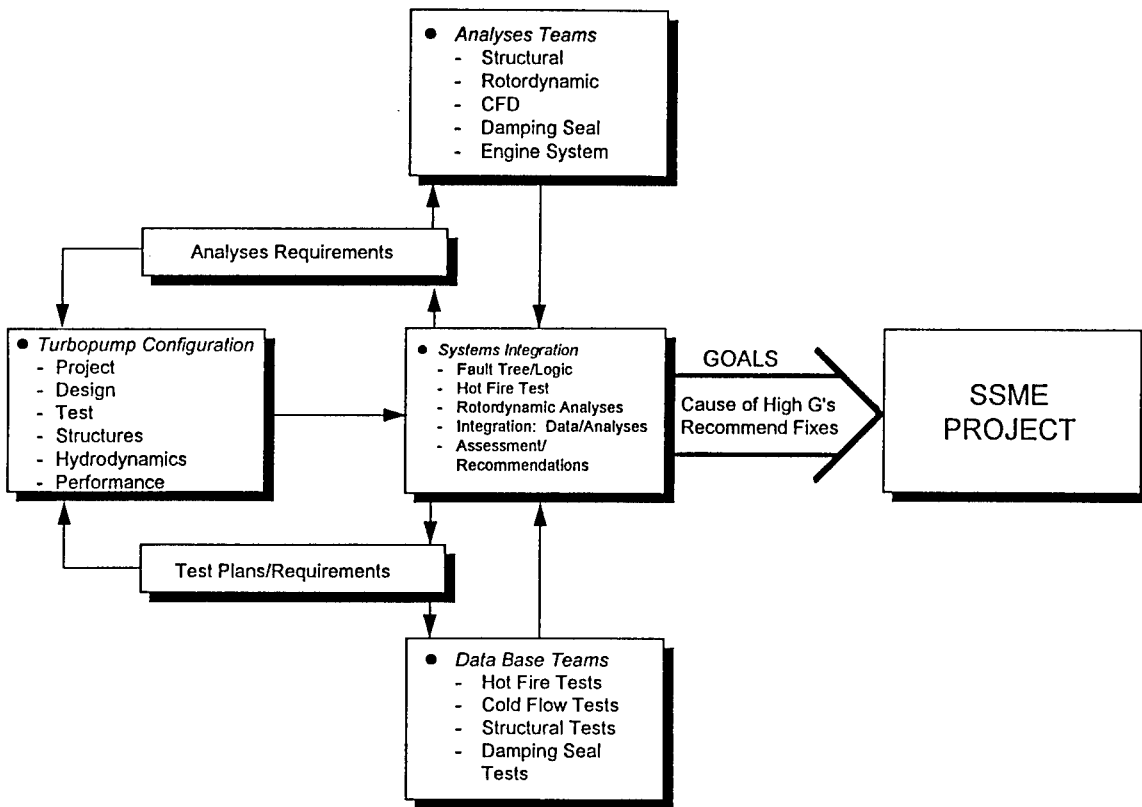


Figure 19. MSFC/Pratt & Whitney vibration team.

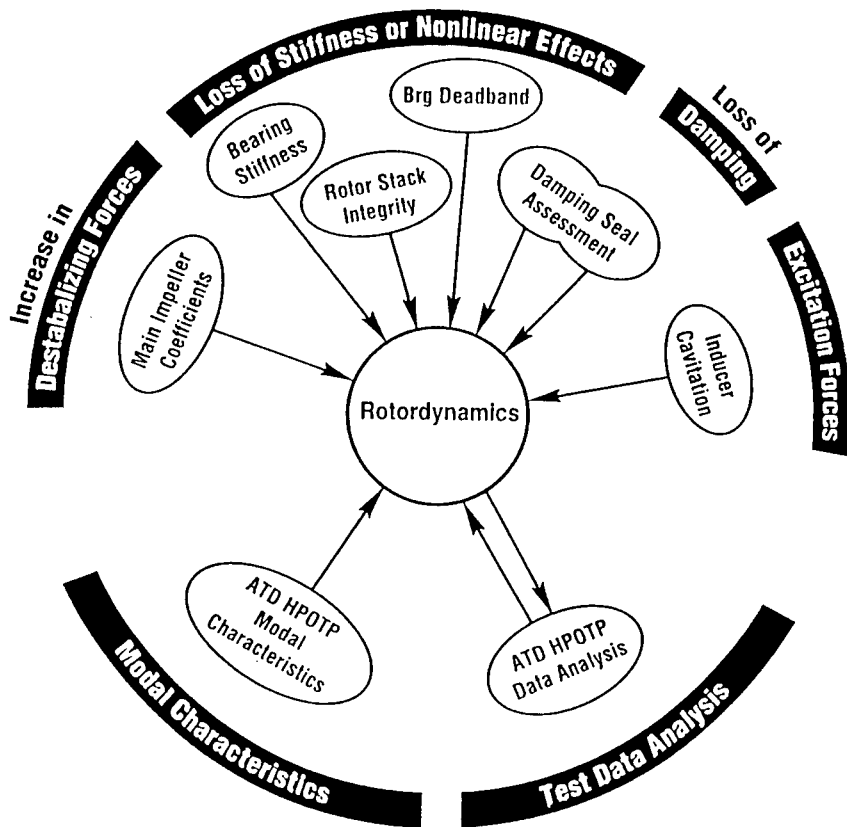
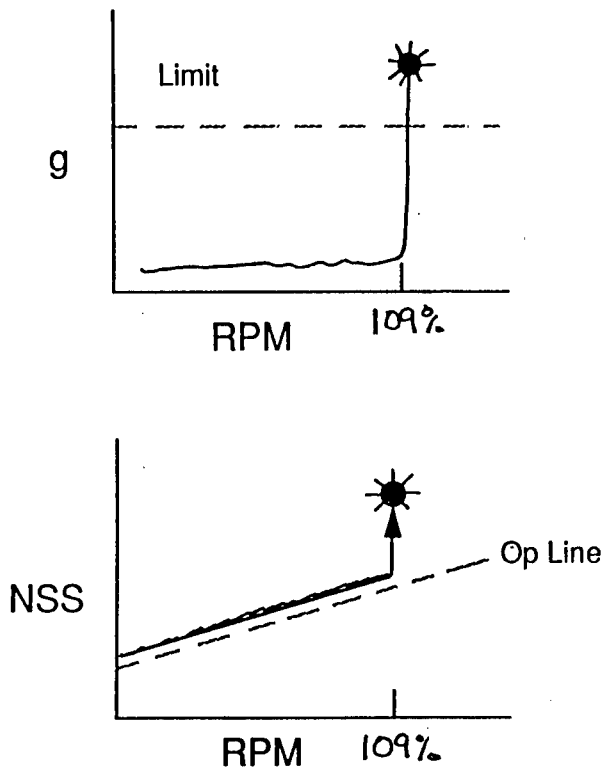


Figure 20. ATD rotordynamic interactions.



- Synchronous frequency vibration
- Sudden increase to over limit (g's)
- Suction specific speed (NSS) sensitivity
- Increasing inducer cavitation is the major change with NSS

Figure 21. HPOTP synchronous vibration problem characteristics.

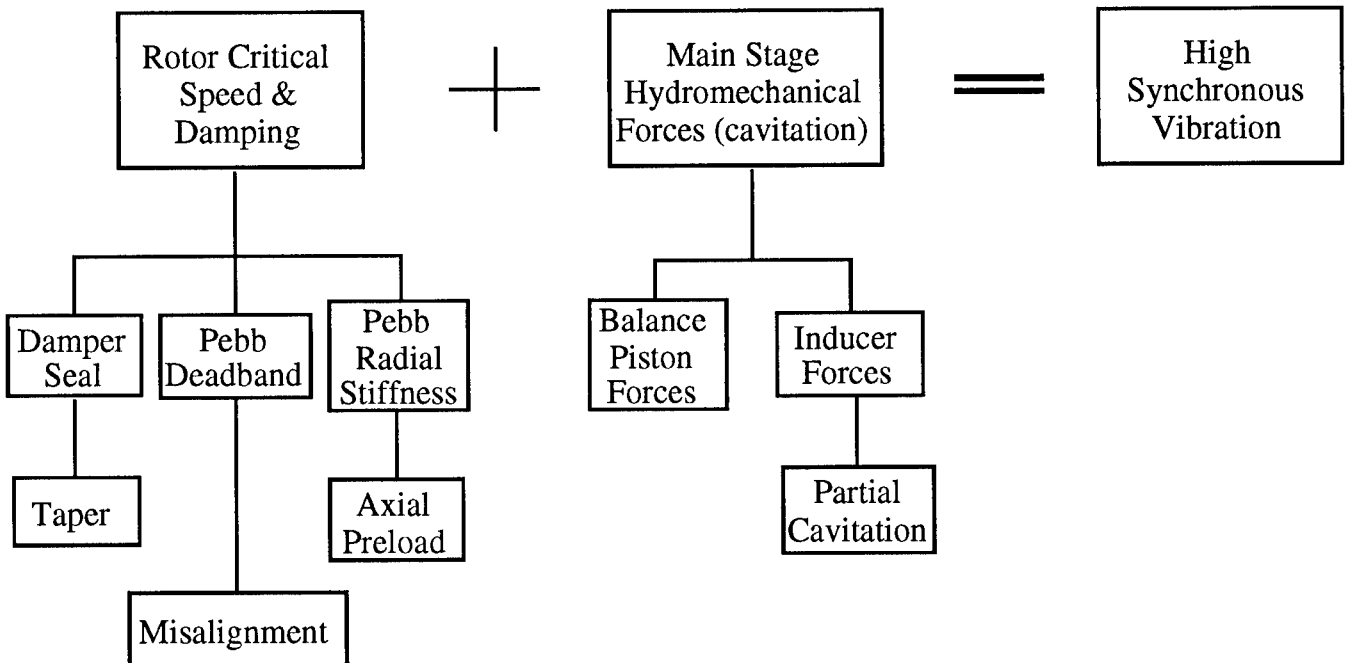


Figure 22. Reduced critical team synergistic effects.

As discussed earlier, the vibration cause and fix was derived by using the fault tree and logic diagrams (fig. 18). This figure shows the interaction between the fault tree, logic network, and databases obtained from analysis, hot firing of the pump or engine system, and a special laboratory test used to develop problem causes and resolution fixes. Notice how highly interactive and iterative this process is. Figure 19 further clarifies this process, showing the various analyses teams, database team, pump configurations, and systems integration. These type charts must be tailored for any problem being studied.

a. Criticality in Operating Range. Clearly, there have been pump criticalities in the operating speed range. The speed and sensitivity depends on the damper seal stiffness and the bearing deadband tilt and hang-up. These modes are system modes involving the dynamics of the total turbopump system. Many times, these are referred to, or classified, as either a housing or rotor mode. All this implies is that more of the motion/deflection is associated with that element; however, the total system is participating and is important (fig. 20).

These system modes are very complex and nonlinear and are a function of the structural characteristics, the fluid characteristics, the hot gas characteristics, and special element characteristics such as bearings, seals, and damping seals (fig. 22). The nonlinearities arise because the fluid characteristics are functions of speed squared hydrodynamic (e.g., cavitation), and the deadbands and clearances between structural elements. Figure 21 shows the typical HPOTP synchronous vibration characteristics indicating fluid cavitation dependence. Inspection of some bearings after hot-fire operation clearly indicates that the bearing sleeve-to-housing clearance never closed and the sleeve never engaged the housing. Hence, the stiffness from rotor support was primarily due to the roller bearing on the turbine end and the damping seal on the pump end. If this assumption is made and the system modes calculated in a linear model, there is a strong criticality that tracks near the pump rotating speed (figs. 23 and 24). Notice, depending on the damping seal stiffness, how close the pump mode (critical) is to the operating speed. Figure 23 is for pump configuration 3-1A which had a stiffer damper seal than configuration 4-1D, which is shown on figure 24. Obviously, this analysis assumes no ball bearing stiffness. With nonlinear stiffness (ball bearing moving in and out of its deadband), the critical frequency would increase and could become subcritical. Linear criticalities for different pumps have different damper seal stiffness. The dashed line is pump speed, the others are pump modes, with the heavy line illustrating the pump criticality.

There are other modes in the operating range that are not sensitive to operating conditions and are generally low-gain modes. By plotting hot-fire data of acceleration versus pump speed (fig. 25), it is possible to interpret the results as a resonance; however, other interpretations of the data are possible. Typically during the runs of the early pump configurations, synchronous sidebands are present. These are probably caused by nonlinear amplitude resolution. Figure 26 shows this pictorially for these conditions: (1) the static load predominates, holding the rotor and bearing against the housing; (2) the dynamic and static load are equal, showing the rotor/bearing moving in and out of contact with the housing; and (3) the dynamic load is greater than the static load, showing full contact around the orbit. A simulation of this effect shows the amplitude modulations and the sidebands (fig. 27).

One hypothesis was that the damping seal operating conditions could be such that the seal was divergent. In this case, the stiffness and damping provided by the seal was low. Figure 28 shows how the stiffness varies with the divergence and where the different pumps have operated. Changing the seal to a convergent operating condition could shift the criticality out of the operating range, depending on other clearances and flow conditions. Also, the convergent seal provides more damping, resulting in a potential increase in the vibration margin.

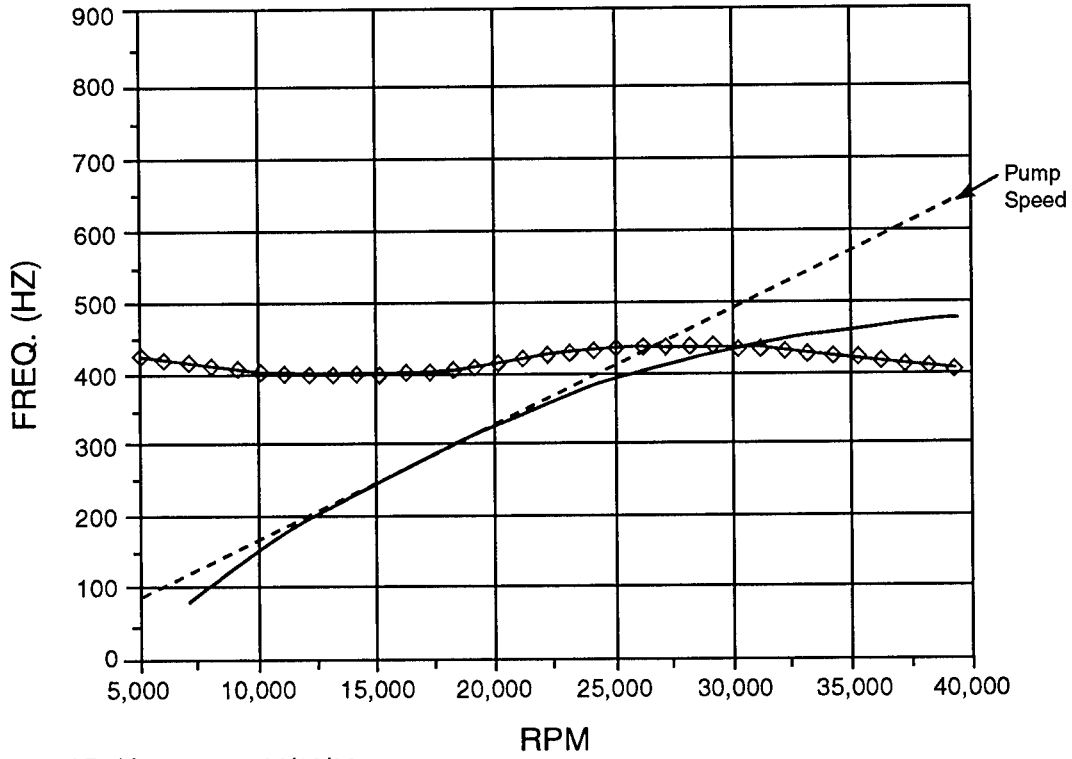


Figure 23. Critical tracks near the pump rotating speed (pump configuration 3-1A).

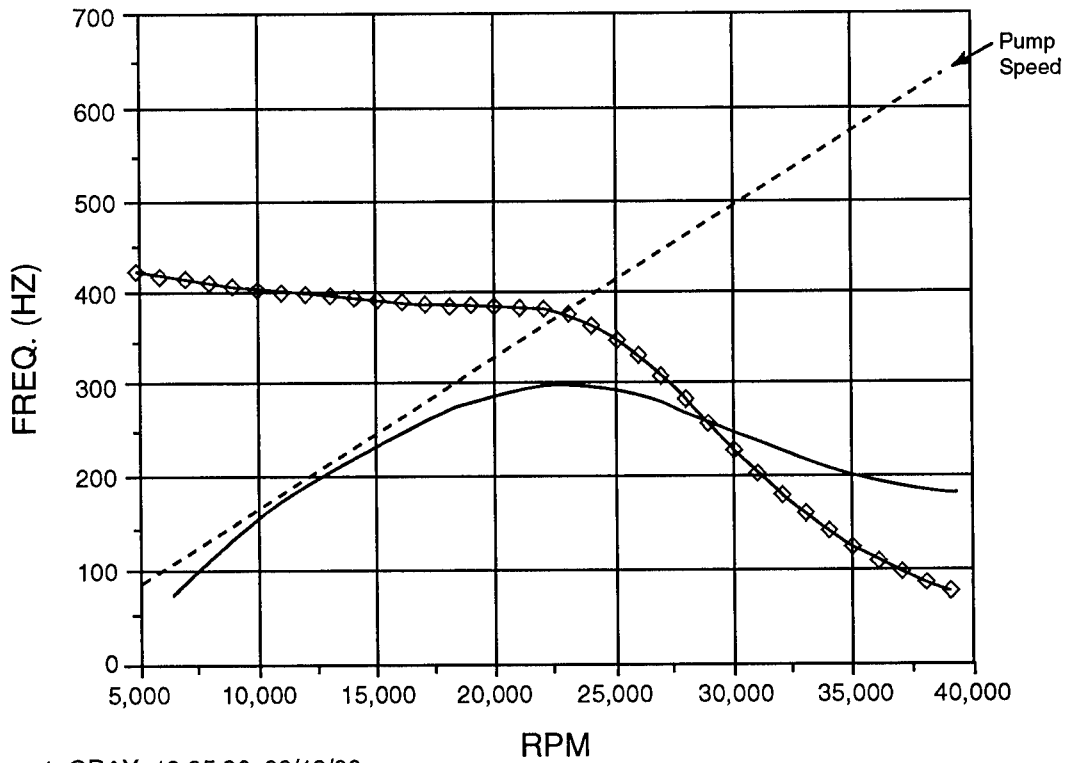


Figure 24. Critical tracks near the pump rotating speed (pump configuration 4-1D).

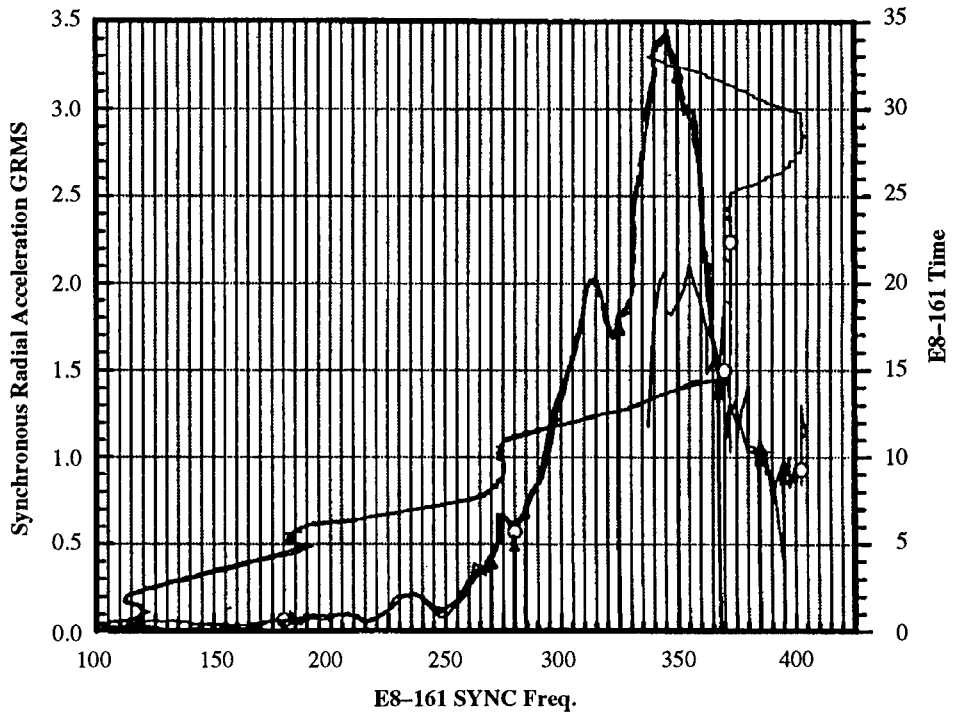
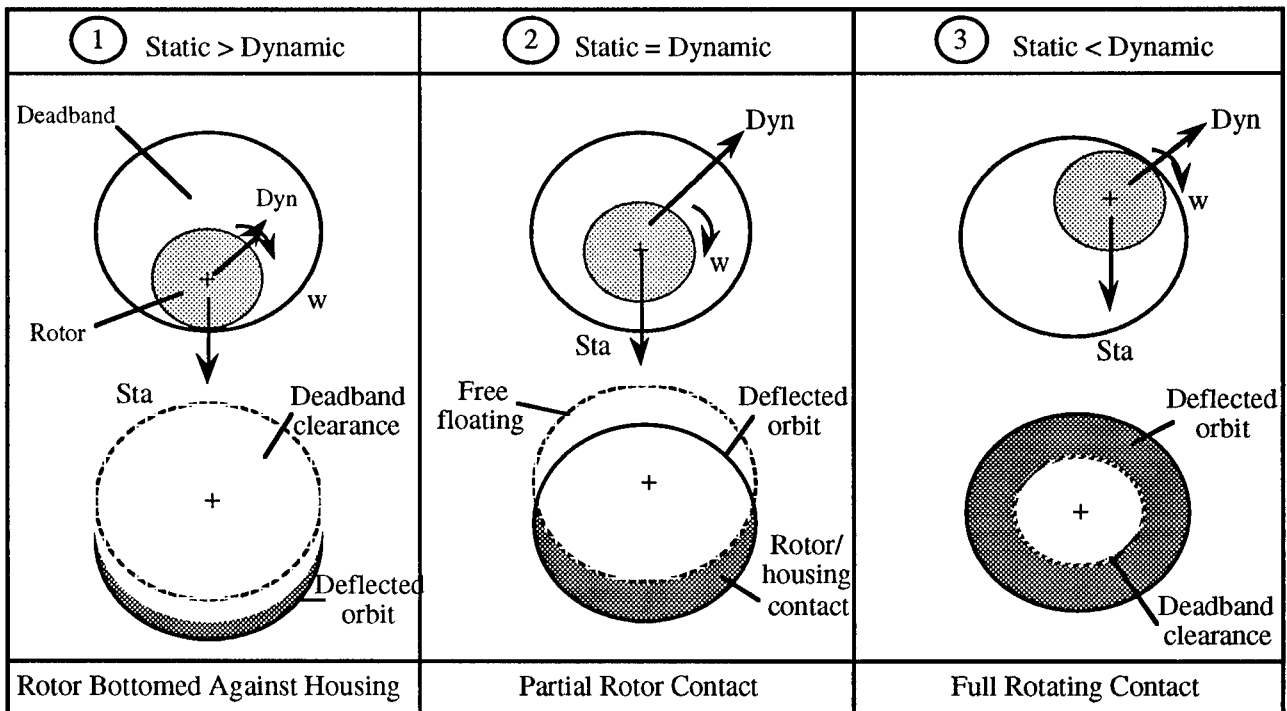


Figure 25. Hot-fire data of radial synchronous acceleration versus pump speed.

Rotor/housing contact dependent on static/dynamic load ratio, deadband clearance, and damper seal stiffness



Sta = Static load
 Dyn = Dynamic load
 w = Whirl

Figure 26. ATD HPOTP deadband interaction.

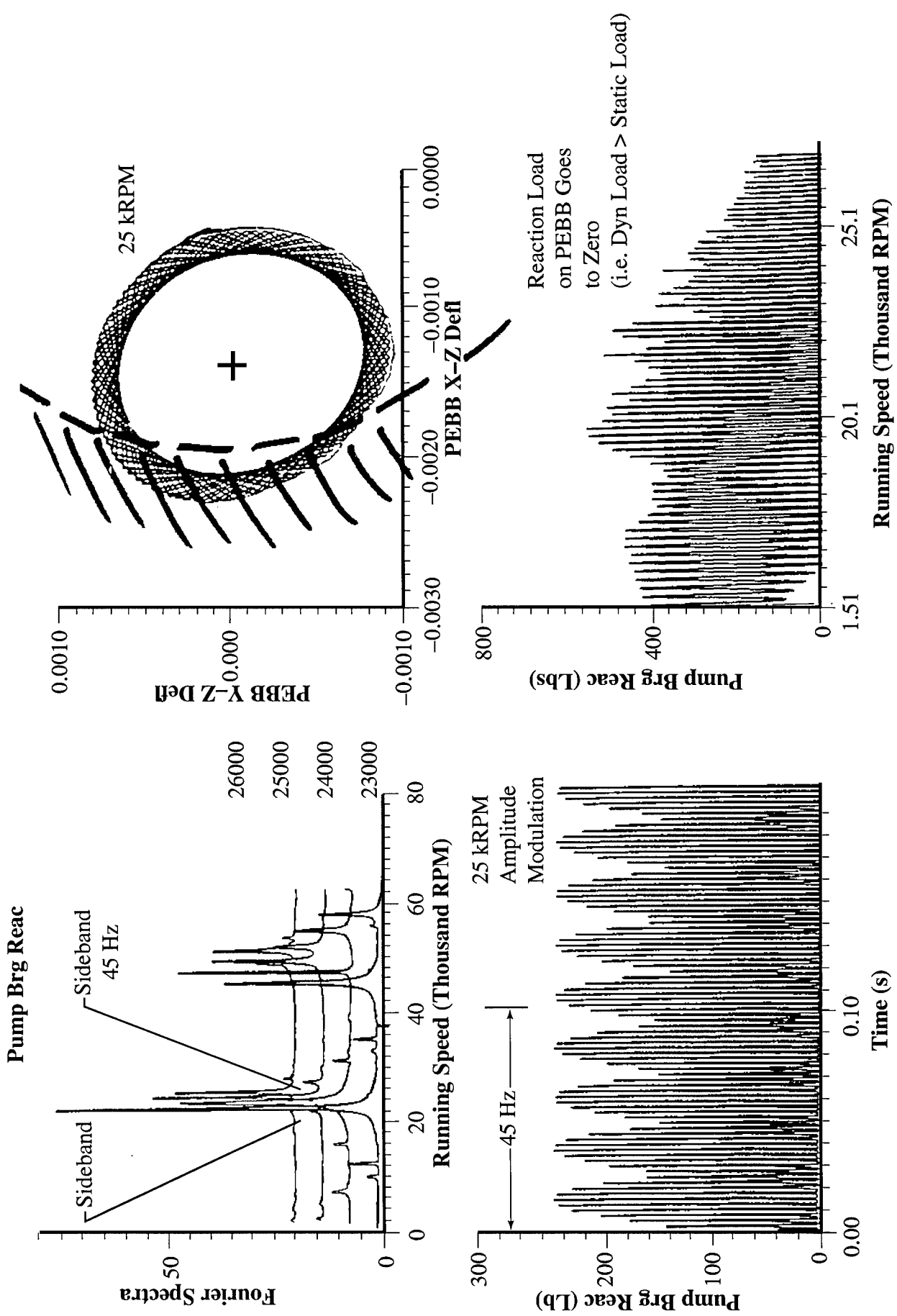


Figure 27. Analytical sideband simulation.

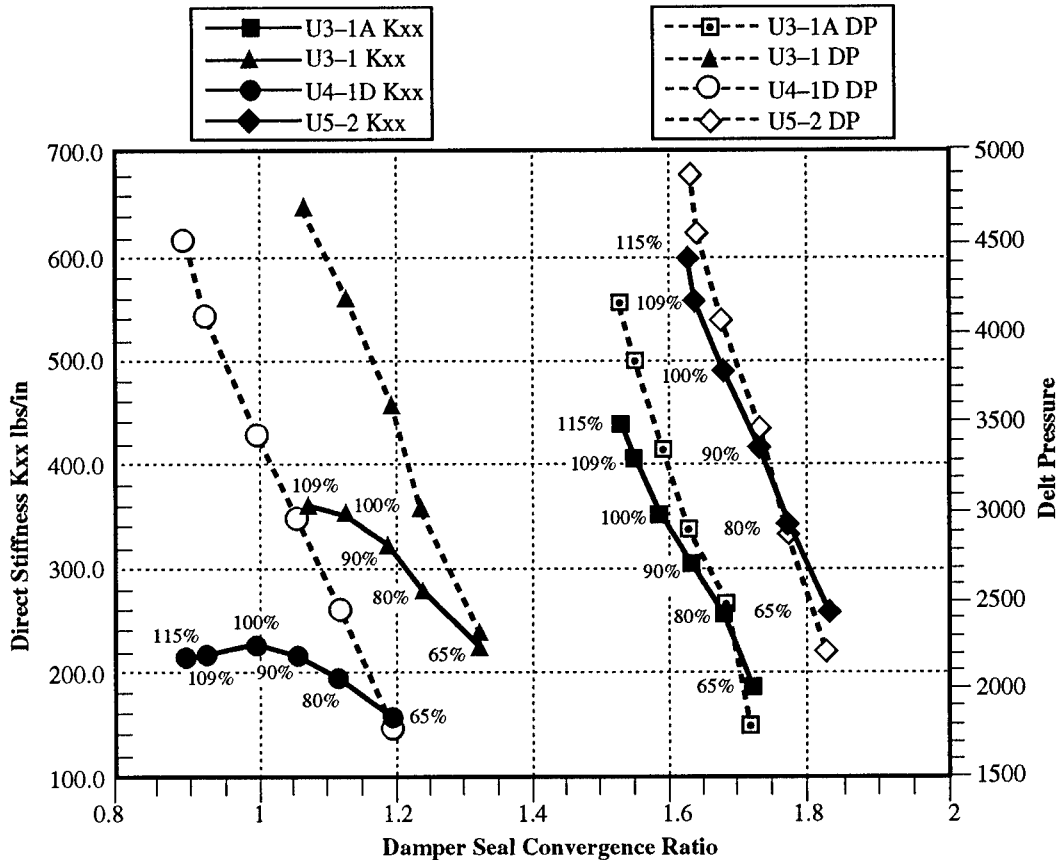


Figure 28. Damper seal stiffness versus convergence ratio.

Another theory that had much support had to do with the relative tilt of the ball bearing between the housing and the rotor shaft. In this configuration, the bearing was not running flat, which creates nonlinear stiffness characteristics for the bearing. The bearing was making contact at the pump end due to the bearing support (housing) being divergent with power increases. Figure 29 shows how the bearing softens with radial deflection as a function of bearing tilt in this direction. Hardware changes were made to control the damping seal characteristics and to open up the deadband of the bearing so that the bearing tilted properly and did not hang up. These changes were made and that significantly shifted the point at which high vibration occurred. At this point, it was concluded that the hydrodynamic forcing function was too large, driving the response. Changes were made (next section) that greatly reduced the forcing function and essentially eliminated the high vibration.

b. Hydrodynamic Forces. Evaluation of the hot-fire data has shown the presence of a significant hydrodynamic forcing function at one-time, two-times, and three-times synchronous frequency. These data were obtained through special instrumentation using Kistler pressure transducers. As a result, a major effort was conducted in computational fluid dynamics (CFD) analysis and water flow testing to understand the source of these forces and to determine a fix. The flow testing was accomplished in the MSFC water flow facility (fig. 30).

Results of the CFD and flow testing showed the source to be the inducer clearances and shape. Figure 31 shows the flow test cavity, pump configuration, CFD results, and flow test result used to verify the hydrodynamic force phenomenon. Figure 32 depicts some of the various changes

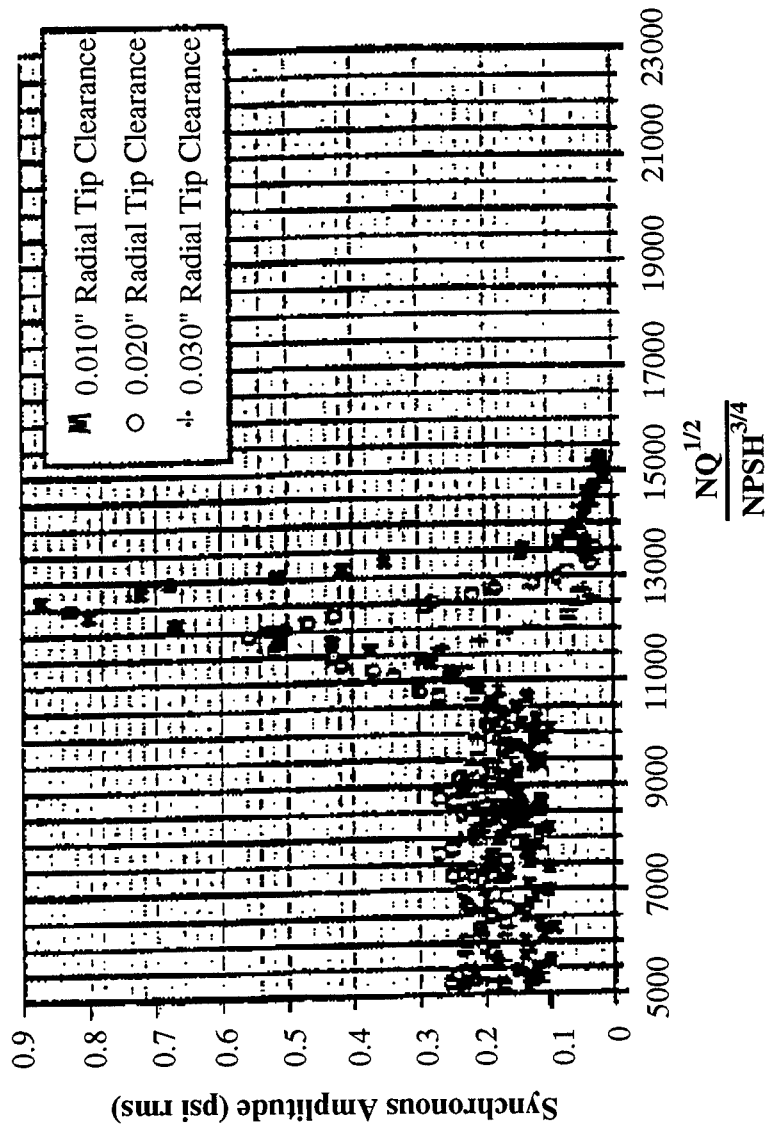
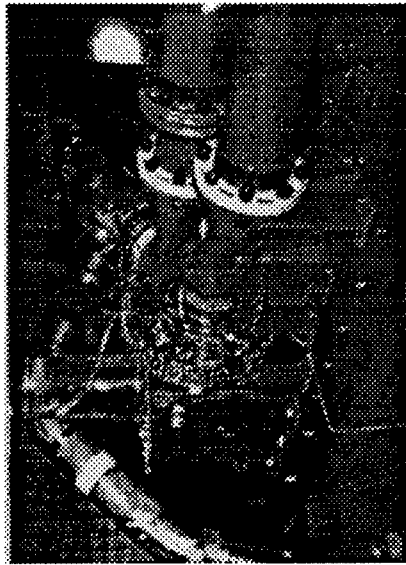
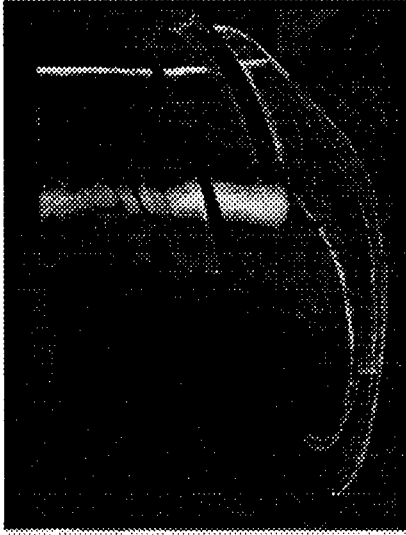


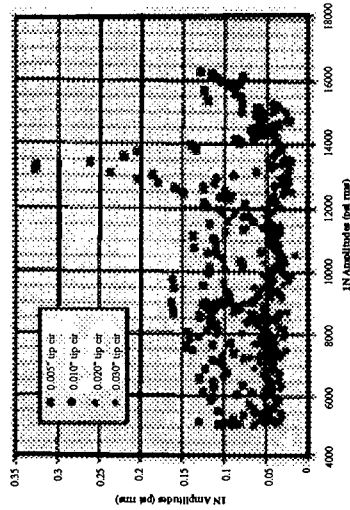
Figure 30. Increased inducer tip clearance reduced synchronous forcing function with no loss in suction performance margin.



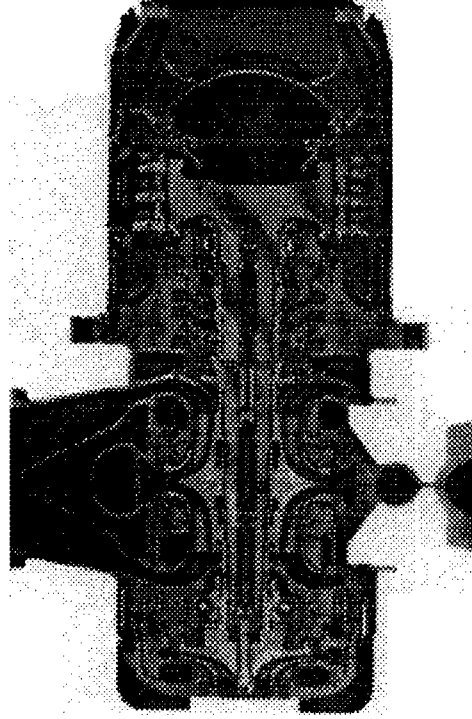
Water Flow Testing to Assess Suction Performance and Cavitation Dynamics



CFD Analysis of Flow Angles and Blade Loads



MSFC Inducer Test Loop ATD HPOTP Inducer Test - 100 % Design Q/N 14.6° β CB: Tip Clearance Effects Discharge Kistler 1N Amplitudes vs. Suction Specific Speed



Characterization and Minimization of Hydrodynamic Forcing Function of Synchronous Vibration

Figure 31. ATD HPOTP synchronous flow dynamics.

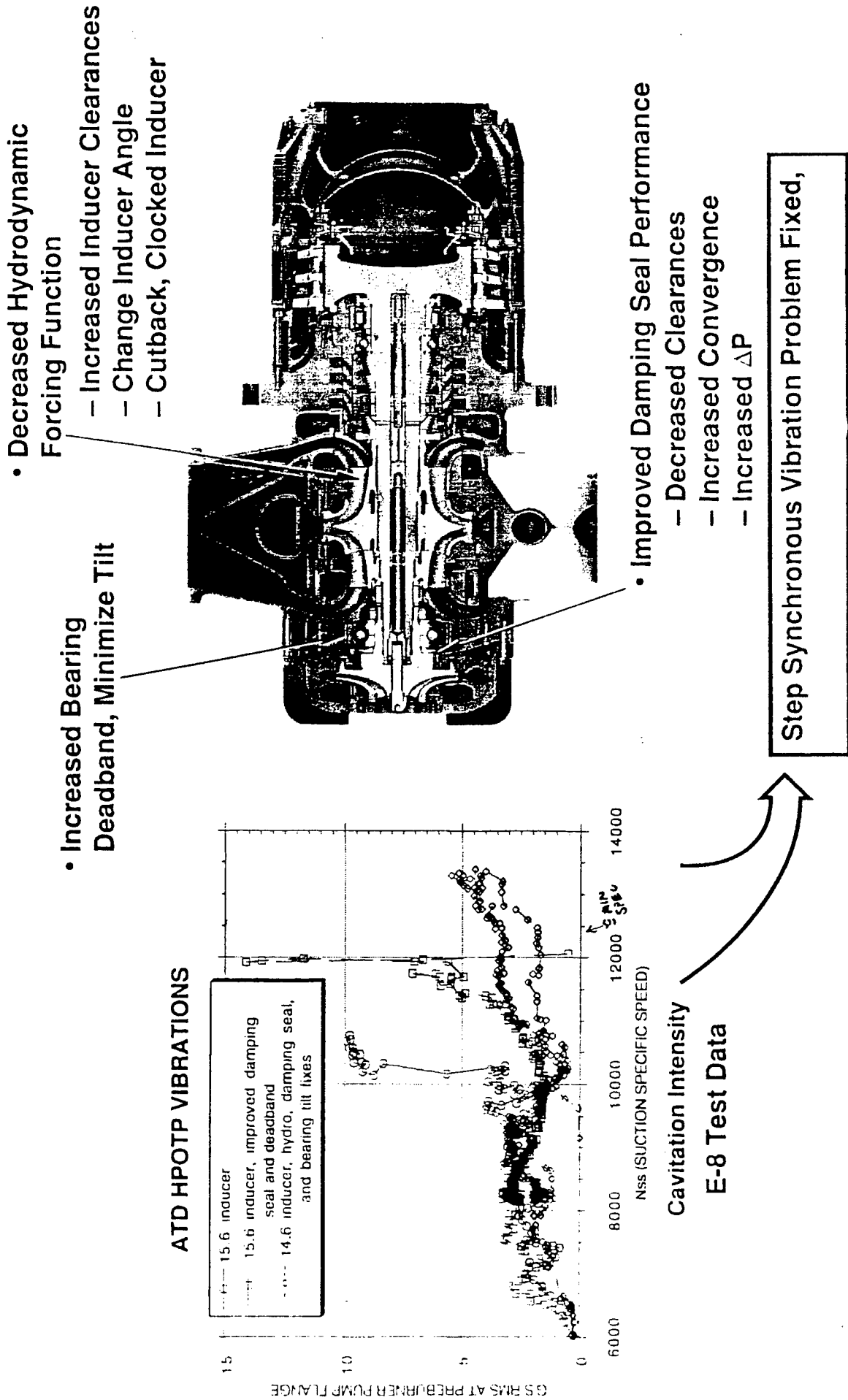


Figure 32. ATD synchronous vibration fix summary.

made to the pump and also repeats the change in synchronous hydroforcing function for three different inducer tip clearances. The 0.030-in radial tip clearance reduced the synchronous forcing function by a factor of three. This explained why there was a sensitivity to the net suction specific (NSS) (fig. 32). The problem can be further complicated by the factor that the force is nonlinear in that the amplitude is not just a function of clearance and rotor speed, but is a function of the radial rotordynamic amplitude and the axial location relative to the housing. This implies that the rotordynamic amplitude needs to be contained or damped; however, it was concluded for the ATD lox pump that the amplitude nonlinearity did not occur.

c. System Evaluation. Using this information developed by analyses, lab tests, and hot-firing the pump, a problem resolution plan was developed. Figure 33 is a matrix of potential problem fixes proposed for evaluation. Not all were tested; however, the indepth scope of the investigation is indicated by the list. Because the problem was caused by a system critical in the operating range, and the larger-than-predicted hydrodynamic forcing function, correcting sections should be incorporated that would produce margins in the system. This was done by building a convergent damping seal, providing a flat and stiffened housing support, increasing the bearing deadband and the 0.030-in inducer tip clearance thereby reducing the hydrodynamic forcing functions.

This design provided margins for the vibration problem. Figure 34 shows the margin demonstrated for HPOTP unit 06-2 that exceeds any NSS expected during flight. Figure 35 shows the same type information for the pump configurations before any fix pump configuration (left graph). The minimum NSS operating conditions are shown as well as the points where vibration occurred. Notice the vibration line (boundary line), which shows that these configurations are unacceptable. Pump 03-1A did not have the increased inducer tip seal clearance, but had the larger ball bearing deadband and convergent damping seal. Notice the improvement over the 03-1 configuration. However, there were still vibration problems for higher NSS conditions, as shown on figure 35. When all the enhancements are included in configuration 06-1, the vibration response is acceptable. Figure 36 is a bar graph showing the vibration history of pumps prior to the uncovering of the bearing wear problem.

Since the bearing problem occurred, several bearing changes have been tried to solve this problem that have aggravated the vibration sensitivity. In these cases, the vibration has not been excessively high, but has large variations (factors up to 5) at the same power level. Several potential areas were reopened in the fault tree to deal with vibration sensitivities. In all cases, it was hypothesized that it was a combination of a criticality in the operating range plus the hydroforcing function increasing with changing NSS. There are two sources for the criticality in the operating range. The first source is little or no ball bearing contact, hence the damping seal stiffness drives the pump support stiffness. In other words, the ball bearing acts as a bumper ball in a nonlinear manner. All ball bearings are nonlinear, but do not have the damper seal stiffness to retard its motion through the deadband as does the ATD lox pump. Much work was done by simulation and data evaluation to prove this theory; however, in this and for the other theories, there was some correlating and some refuting cases. For example, figures 37 and 38 are the vibration levels and pump speed plotted versus time. One can infer that there are two possible resonances on figure 37 that run B1-165 as the speed changes between 200 and 400 s. Figure 38 shows the vibration sensitivity spike. As a method of illustration, figure 39 shows the end-to-end test history of one of the pumps showing the characteristics across time of the vibration sensitivity. However, it was never possible with extensive simulations and hot fire data analysis to establish a firm correlation for a resonance caused by the pump end bearing, damping seal combination.

The second source for the vibration sensitivity is the turbine end roller bearing support changing due to thermal effects which could move a second critical mode into the operating range.

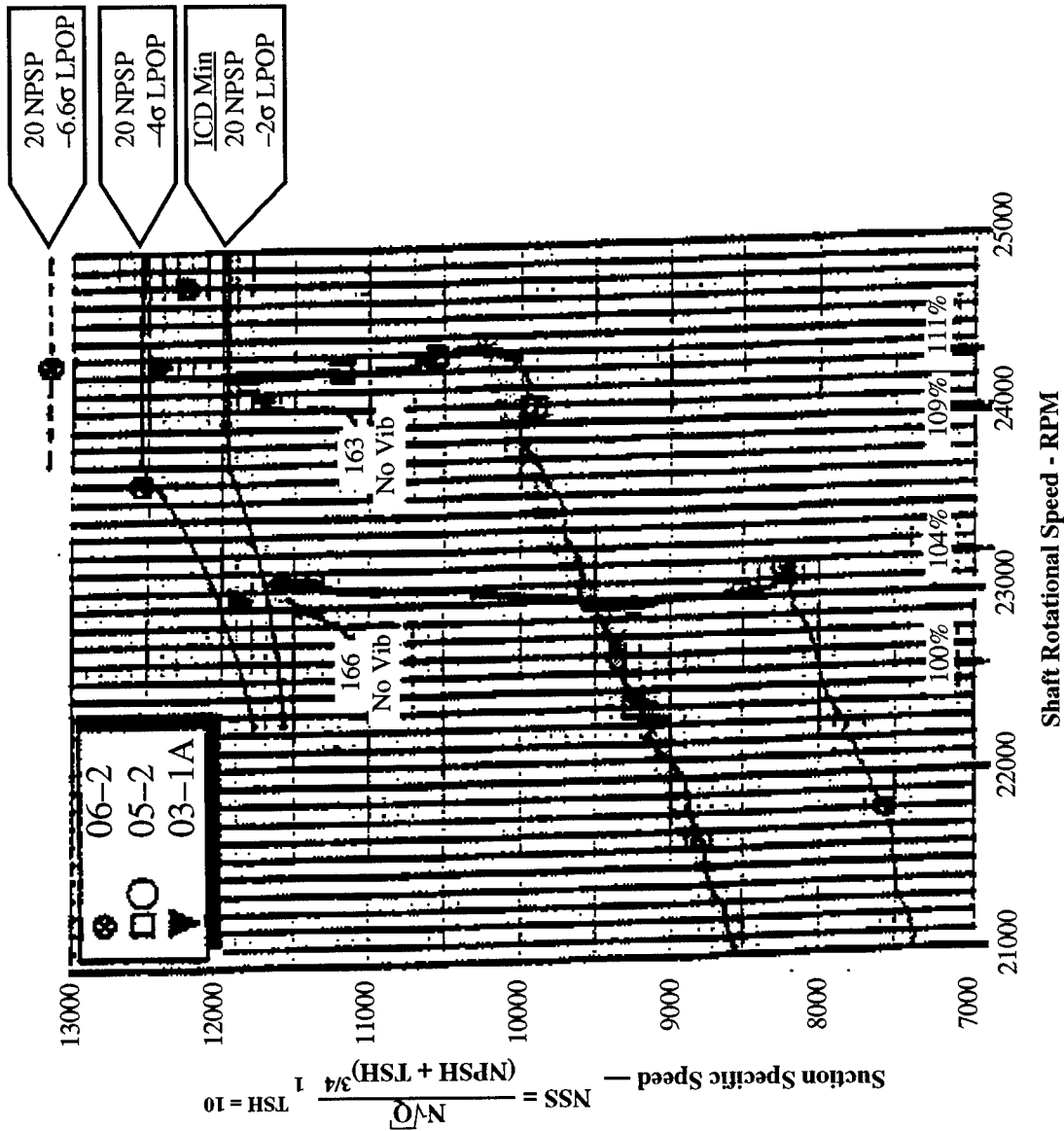
TURBOPUMP UNIT

Features	07-1F	03-1	06-1E	03-1A	05-2	06-2	02-3	07-2
Design								
- Optimize Damper Seal Convergence				A	B	B	B	B
- Stiffened Damper Support					X	X	X	X
- Increased Ball Bearing Preload Spring								
- PEBB Anti-Rotation Pin Removal				A	A	B	B	B
- Optimize Ball Bearing Deadband Clearance						X	X	X
- Chrome PEBB Deadband & Dry Lube				15.6	15.6	14.6	14.6	15.6
- Redesign Inducer		15.6						
- Inducer LE Shroud Flow Trip						X	X	X
- Inducer TE Axial Cutback & Clocking								
- Shrouded Inducer Damper Seal						X	X	X
- Optimize B/P Deswirl Vanes			A			A		
- Optimize B/P Orifice Overlap					X			
- Reduced Turbine End Roller Brg Deadband								
- Eccentric Inducer Shrouds					A	A	A	A
- Increased Inducer Tip Clearance								
Special Instrumentation								
- Ball Bearing Spring Strain Gage	X	X		X	X	X	X	X
- Inducer Inlet Pressure		PS, TS						
- Inducer Inlet Dynamic Pressure							PS, TS	
- Inducer Discharge Pressure	PS, TS	PS, TS		1-TS				
- Inducer Discharge Dynamic Pressure				1-PS	1-PS		TBD	
- Proximity Probes (B/P)	X							
• Axial								
• Radial								
- Balance Piston Cavity Dynamic Pressure	PS			2-PS	1-PS			
- Turbine End Roller Bearing Strain Gage						X		
- PEBB Outer Race TC								
- Turbine End Roller Brg Sleeve TC					X			
- Key Phaser							X	

Figure 33. HPOTP vibration configuration study plan.

Open Symbols Non Vibration
 Closed Symbols Vibration

03-114 No Fixes
 05-2 Deadband Changes
 06-2 Deadband Changes and Inducer Changes



- Unit 06-2 demonstrated vibration fix. High sync onset eliminated from operating range.

- Configuration includes:

1. 0.029" inducer tip clearance
2. Increased assy. taper PEBB deadband to operate straight with improved friction surface (Cr/Moly)
3. Increased assy. deadband (0.0165" pump-side)
4. Increased load PEBB axial perload spring
5. Relocated PEBB anti-rotation pin
6. Inducer trailing edge cutback

Figure 34. SSME/ATD HPOTP unit 06-2 vibration.

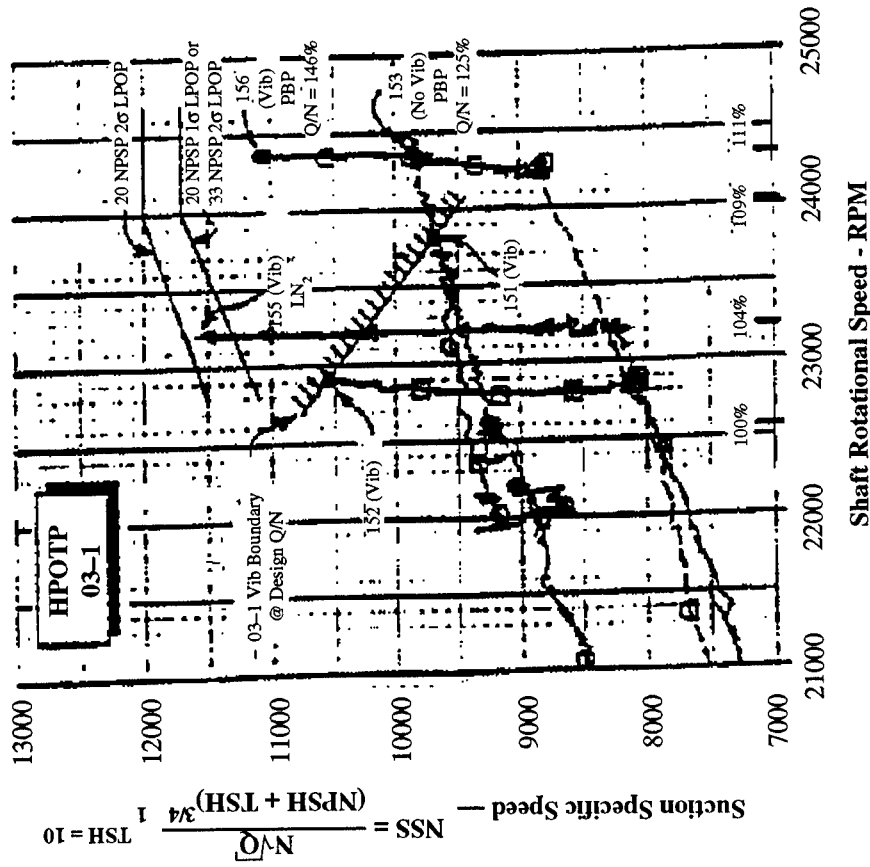
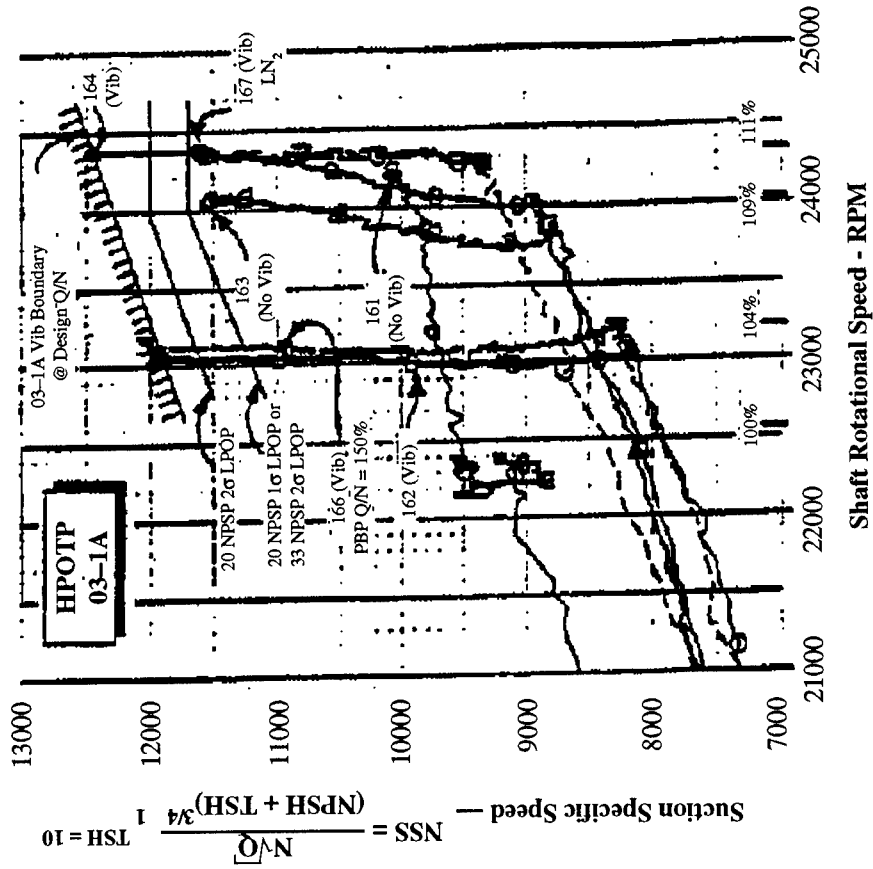


Figure 35. Unit 03-1A vibration envelope for turbopump without corrective fixes (03-1) and intermediate corrective fix (03-1A).

- Demonstrated E8 Tests:**
- 03-1A Exceeds Min Spec.
 - 05-2 Operated to Min Spec. (No Vib)
 - 06-2 Operated Beyond Min Spec. (No Vib)

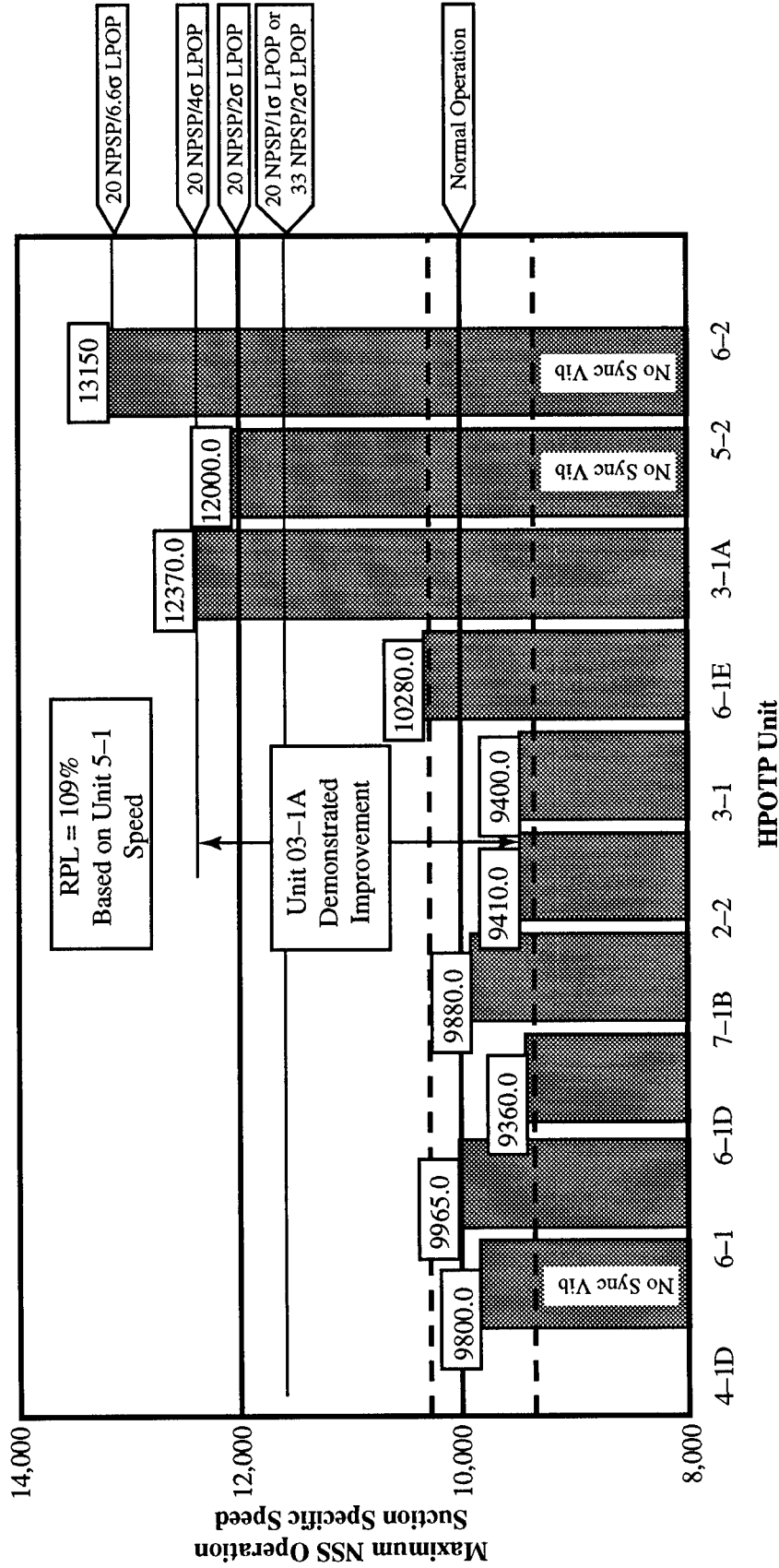


Figure 36. Synchronous vibration onset eliminated from operating range.

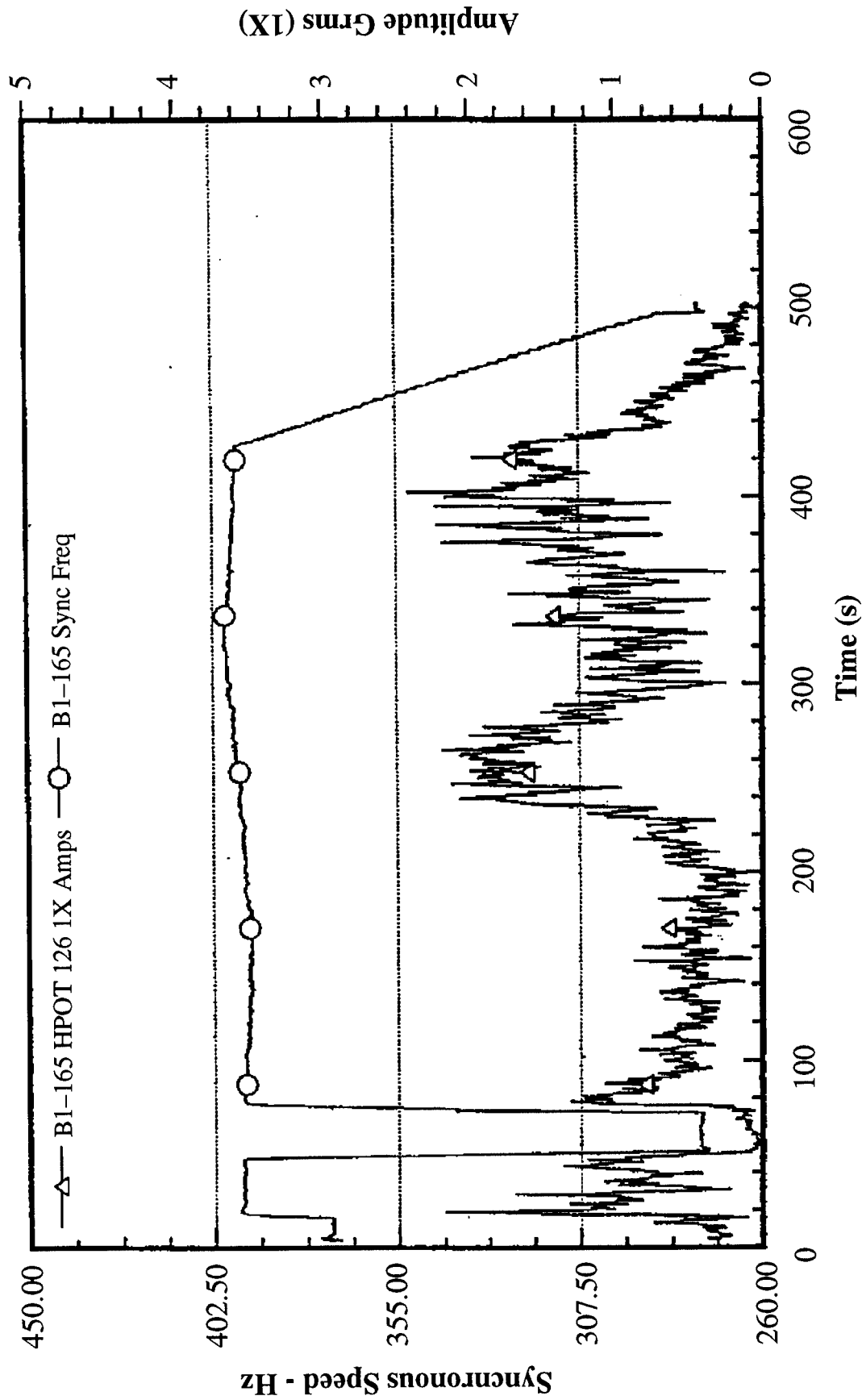


Figure 37. 1X synchronous trackings versus time.

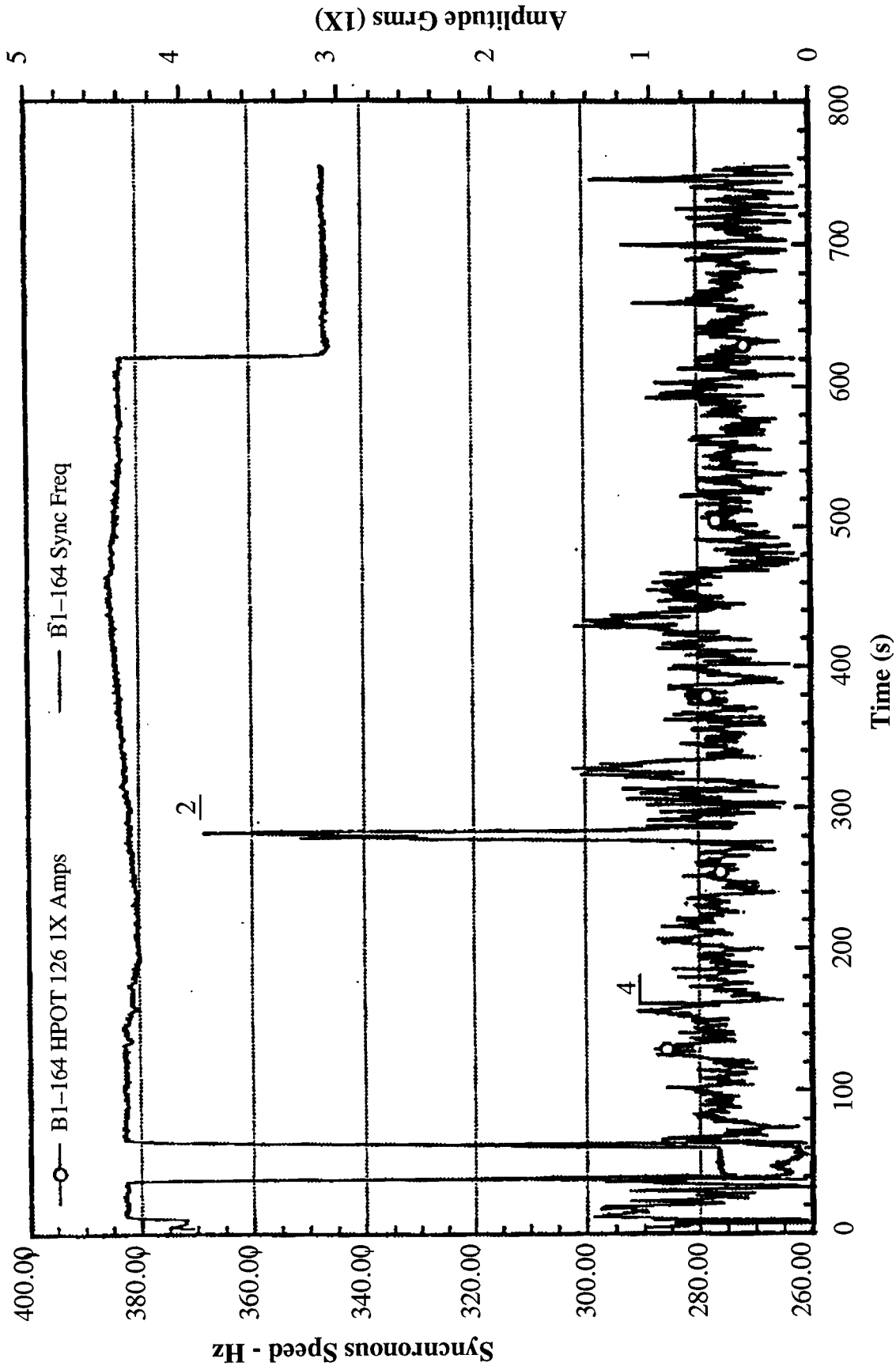


Figure 38. 1X synchronous trackings versus time—unit 7-2A.

Hot-fire data have shown that there is undesirable hot-gas leakage that is affecting the roller bearing support. Special instrumentation was installed in pump build 03-2 to assess the thermal environment. The data showed erratic hot-gas leakage that changed the roller bearing support temperature from the design predicted. The change in the housing temperature will alter the bearing support fits and thus change the support stiffness. A comprehensive effort was undertaken to provide a stable housing environment.

During this bearing solution development of the lox pump, prior to the evolution of the above critical design review (CDR) configuration, one pump configuration, 7-2D, experienced a high-g redline engine cutoff. This pump was being used to tune the bearing clearances, reducing the clearance in order to ensure less nonlinear bearing deadband effects. The bearing hung up, which caused the high-g shutoff, as discussed previously, was shown to be the cause through teardown inspection.

Since the vibration team was dissolved (solution of the high-synchronous spikes and bearing degradation problems), the turbine-end thermal excursions have been fixed and the CDR pump configurations built and tested. These pumps have not experienced any high-g spikes, and no vibration sensitivity.

V. BEARING WEAR

An HPOTP bearing distress problem first surfaced in September 1992 when long-duration engine testing was started after resolution of the synchronous vibration problem. The bearing which failed was the oxidizer-cooled pump-end ball bearing of the turbopump. With one exception (which will be discussed later) the bearing would fail after as little as a 100 s of operation to a few thousand seconds operation. Externally, a 2.5° step increase followed by a ramp increase in the coolant temperature rise across the bearing was noted (figs. 40 and 41). This event was assumed to be the bearing failure and is seen to be a discrete occurrence that does not take a long period of time to happen. Operation after this event showed continuing wear of the bearing as evidenced in the change in posttest rotor travel. When a turbopump teardown inspection of the bearing was done, the balls and races were found to be worn and thermally discolored, and the Salox-M® cage showed heavy fore/aft ball pocket wear. Comparison of the inner race surface color with test specimens heated in an oxygen environment indicated that the surface temperature reached 1,400 °F, a temperature well beyond design intent. Figure 42 is a bar graph of the bearing life experience for several pumps (numbers at top of bars) before the acceptable solution was implemented, showing that some bearings failed early and some ran a long time without failure.

In view of the design and development experience, the onset of the wear problem was unexpected. The static and dynamic loads carried by the bearing were kept low by careful attention to hydrodynamic and mechanical design of the turbopump. Posttest examination of the ball tracks on the bearing races verified that the loads were meeting the design. The bearing is cooled by approximately 16 lb/s of lox flow from the preburner pump discharge. The Salox-M® bearing cage is designed to provide cage-to-bearing transfer film lubrication. Extensive design verification testing at the component level of the bearing under simulated load and coolant were very successful. Several bearings were operated to twice the 7¹/₂ hour design life with no evidence of abnormal wear. A single failure in the component tests was isolated to a test rig misalignment problem. A similar design liquid hydrogen-cooled bearing used in the high pressure fuel turbopump (HPFTP) had successfully passed component test and was showing no problems in turbopump development, even though it runs 50-percent faster than the oxidizer pump bearing.

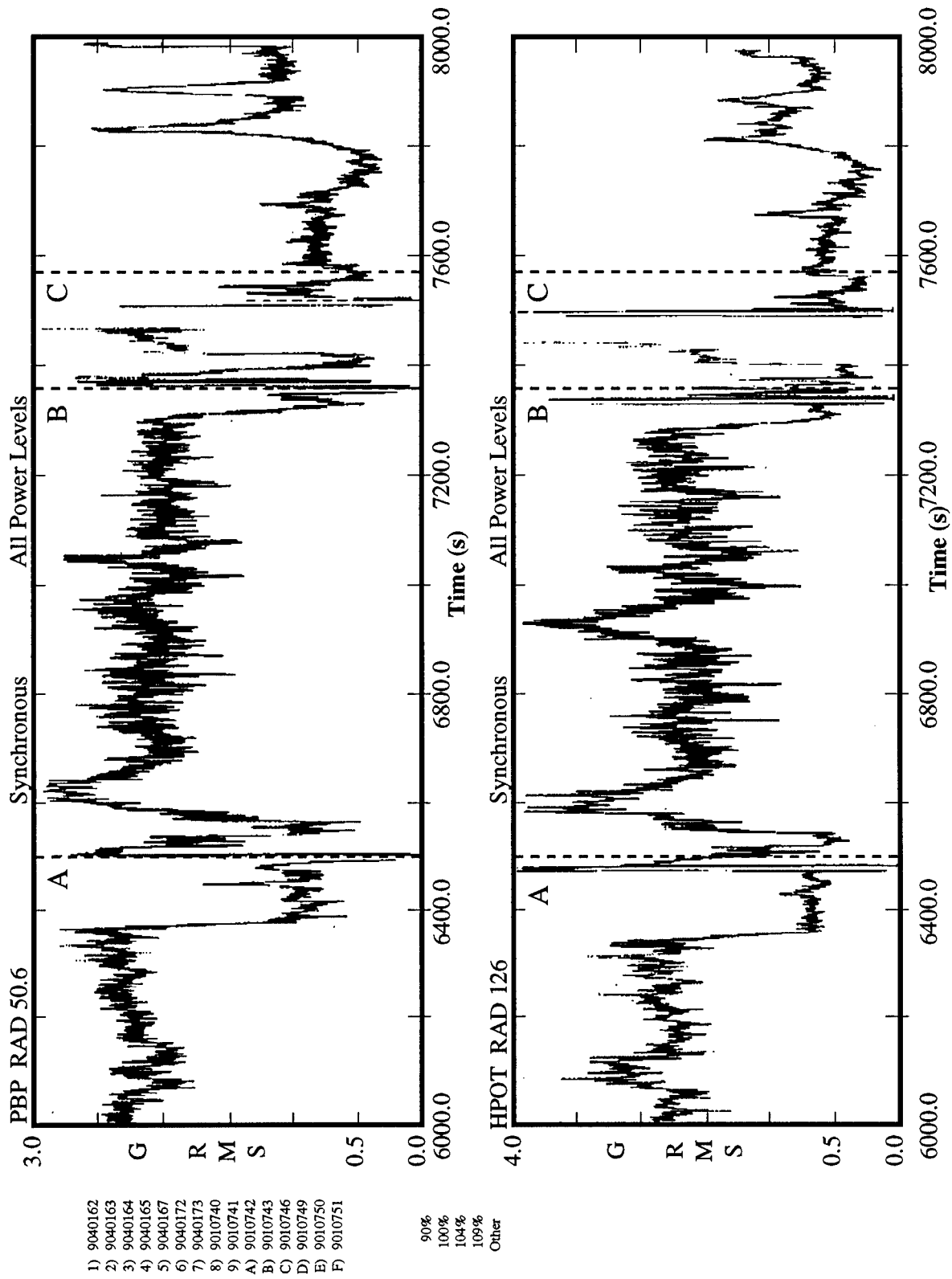


Figure 39. End-to-end runs of two of the development pumps.

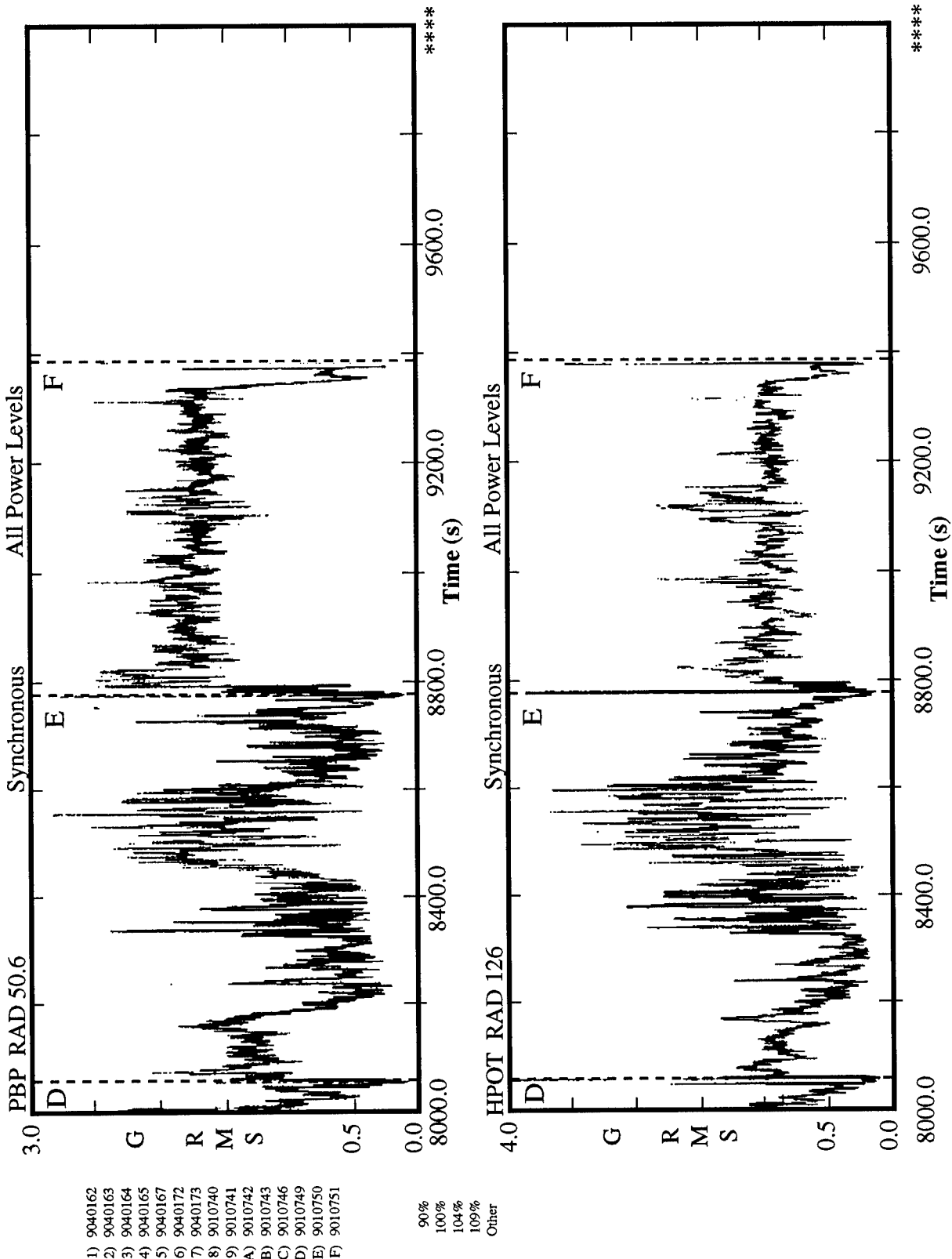
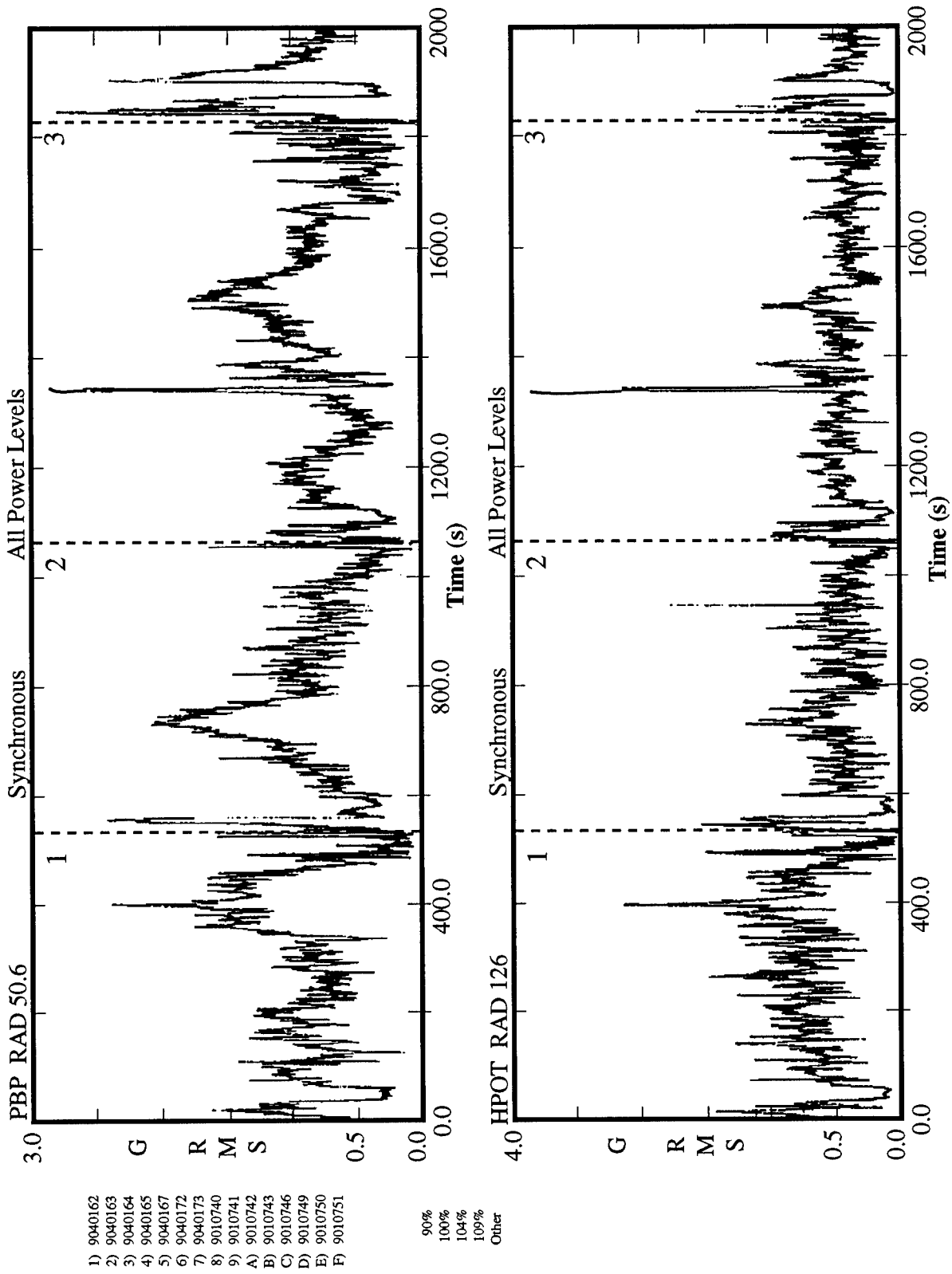
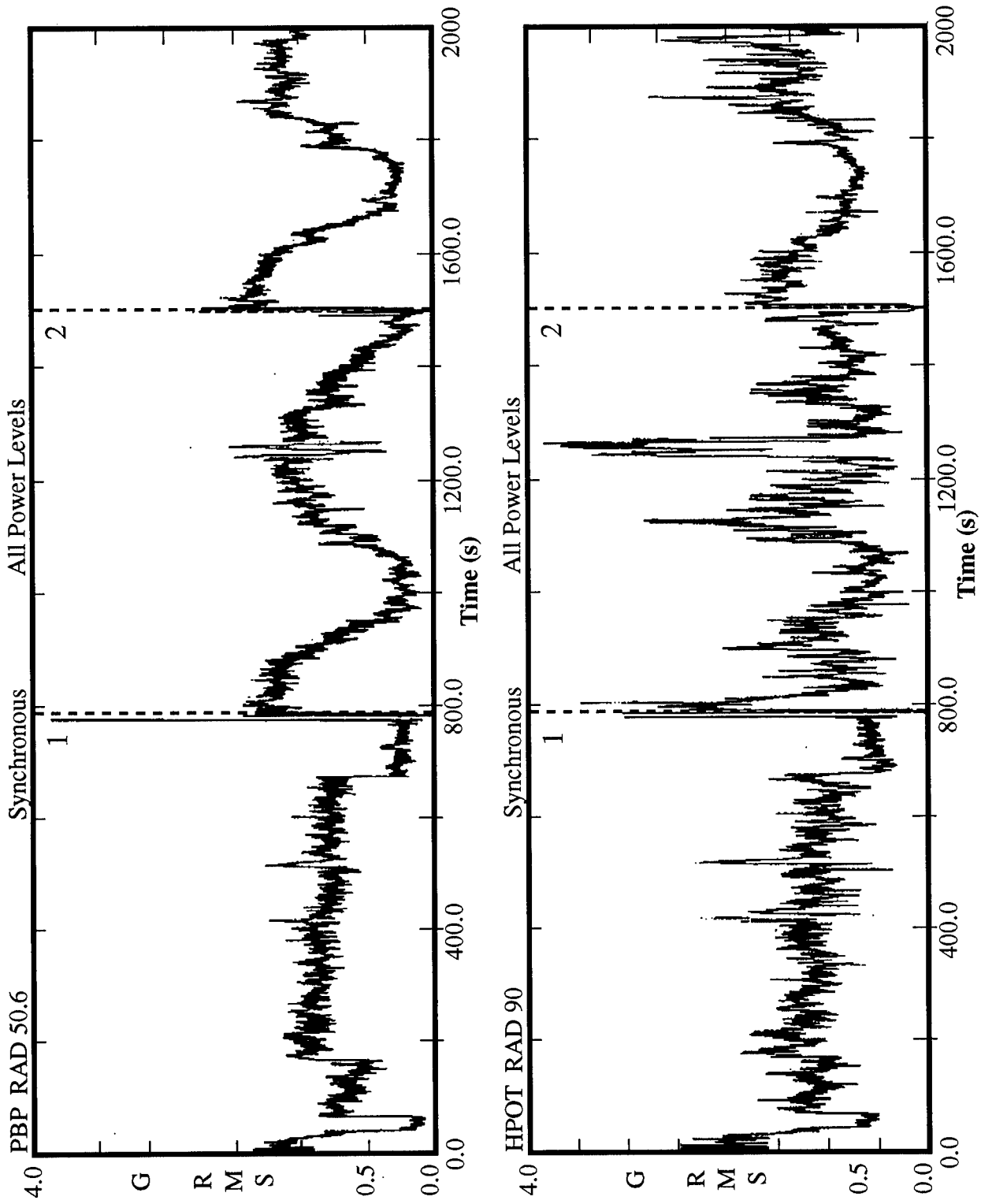


Figure 39. End-to-end runs of two of the development pumps—Continued.



- 1) 9040162
 - 2) 9040163
 - 3) 9040164
 - 4) 9040165
 - 5) 9040167
 - 6) 9040172
 - 7) 9040173
 - 8) 9010740
 - 9) 9010741
 - A) 9010742
 - B) 9010743
 - C) 9010746
 - D) 9010749
 - E) 9010750
 - F) 9010751
- 90%
 - 100%
 - 104%
 - 109%
 - Other

Figure 39. End-to-end runs of two of the development pumps—Continued.



- 1) 9010747
- 2) 9010748
- 3) 9040185
- 4) 9040193
- 5) 9040194
- 6) 9040195
- 7) 9040196
- 8) 9040197
- 9) 9040198

- 90%
- 100%
- 104%
- 109%
- Other

Figure 39. End-to-end runs of two of the development pumps—Continued.

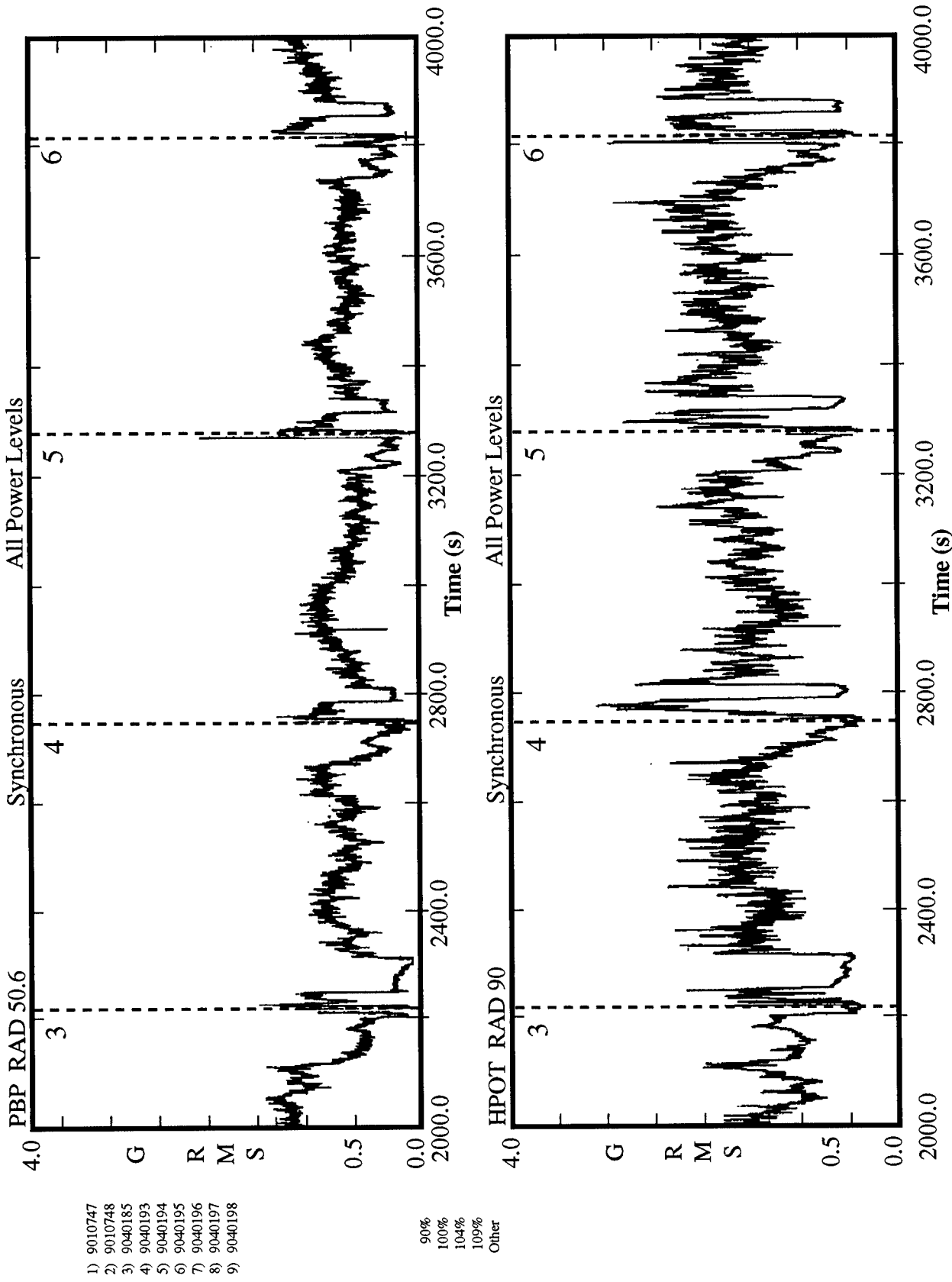
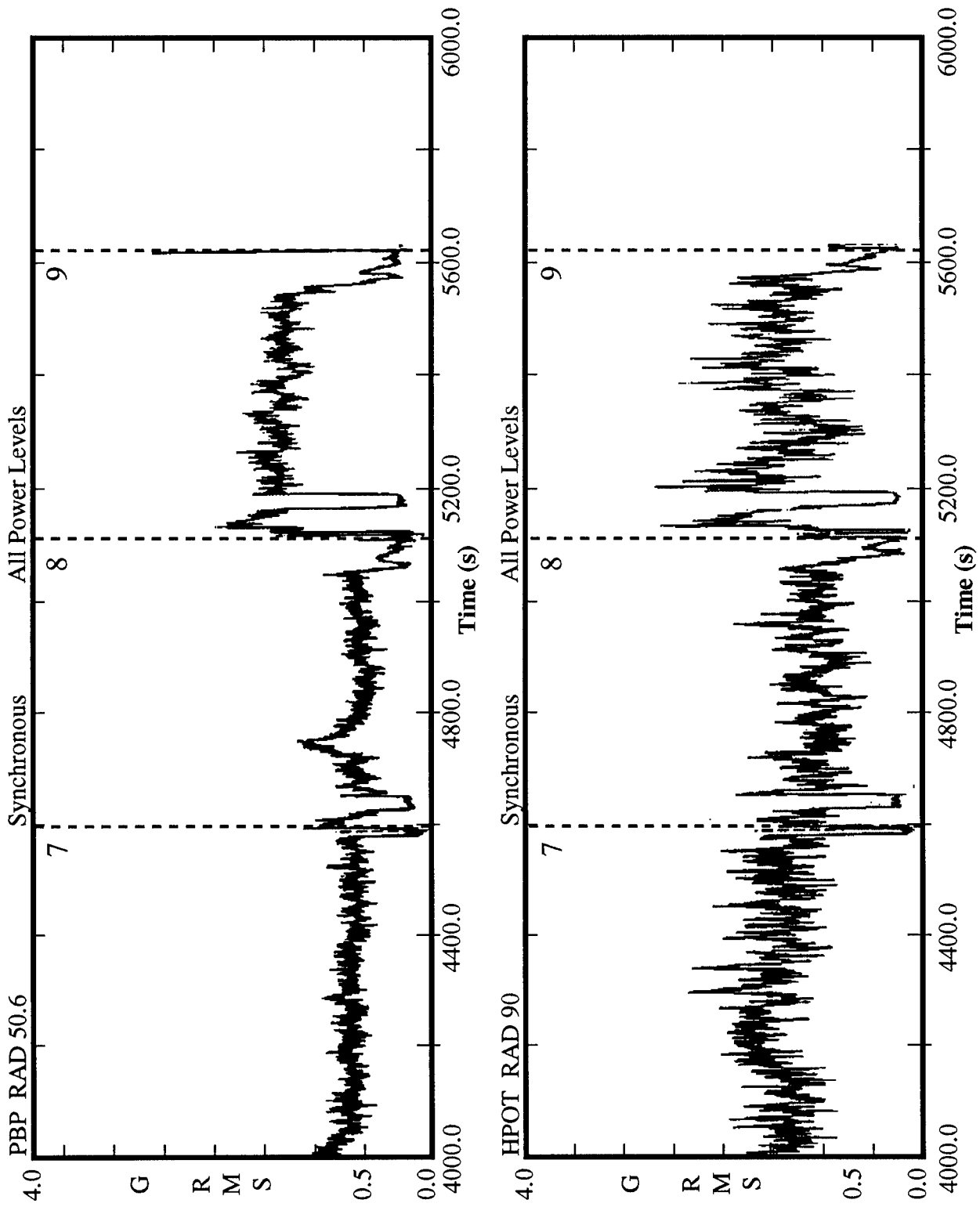


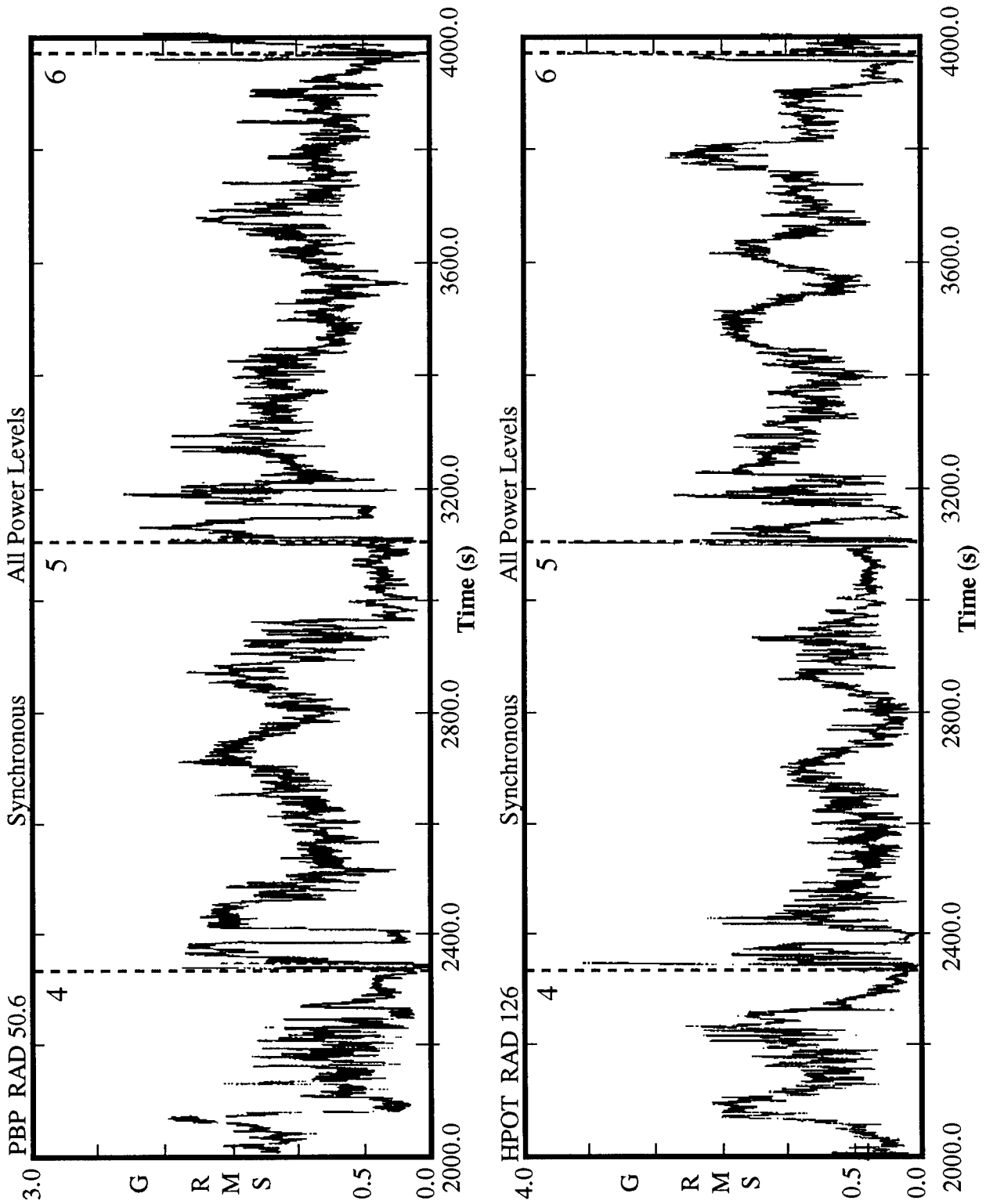
Figure 39. End-to-end runs of two of the development pumps—Continued.



- 1) 9010747
- 2) 9010748
- 3) 9040185
- 4) 9040193
- 5) 9040194
- 6) 9040195
- 7) 9040196
- 8) 9040197
- 9) 9040198

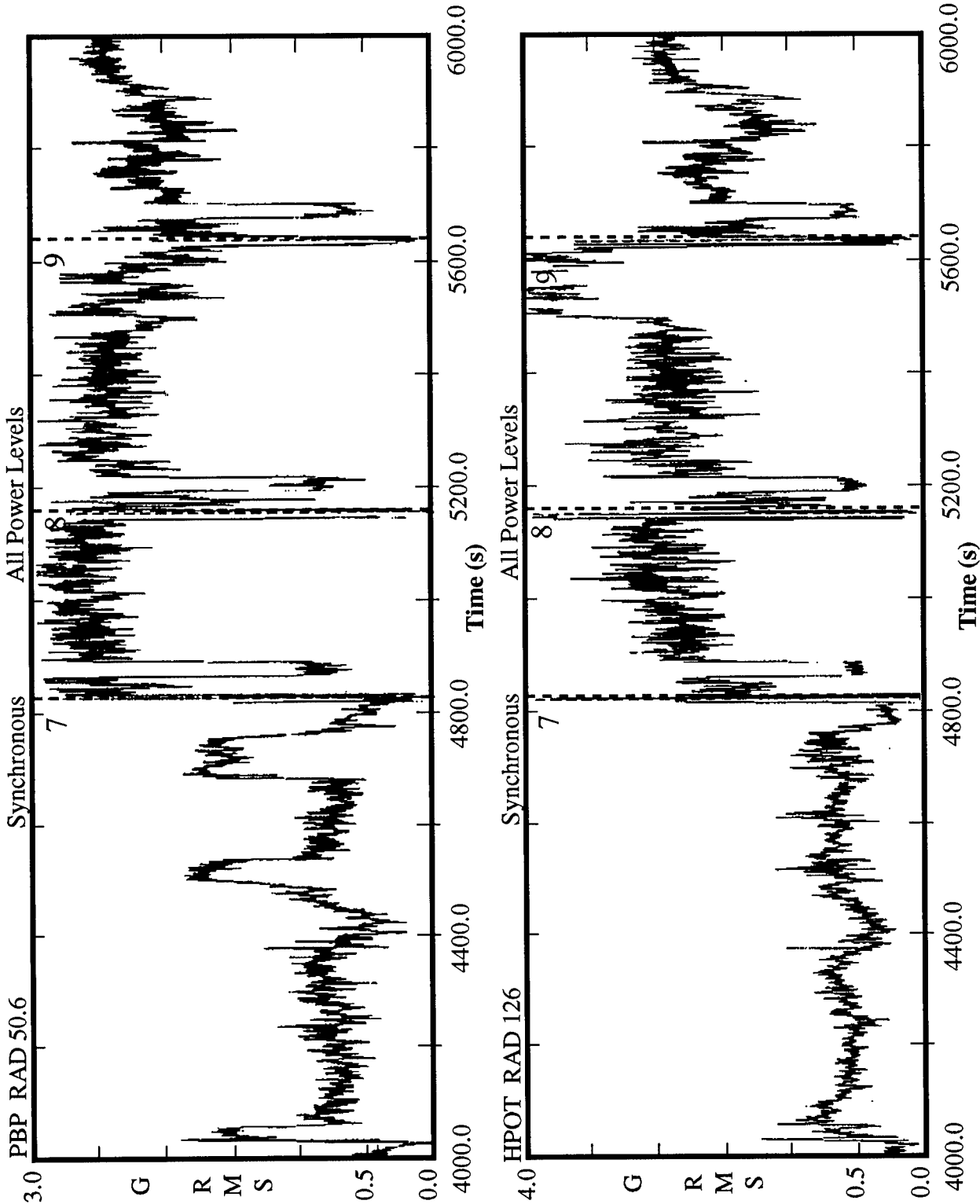
90%
100%
104%
109%
Other

Figure 39. End-to-end runs of two of the development pumps—Continued.



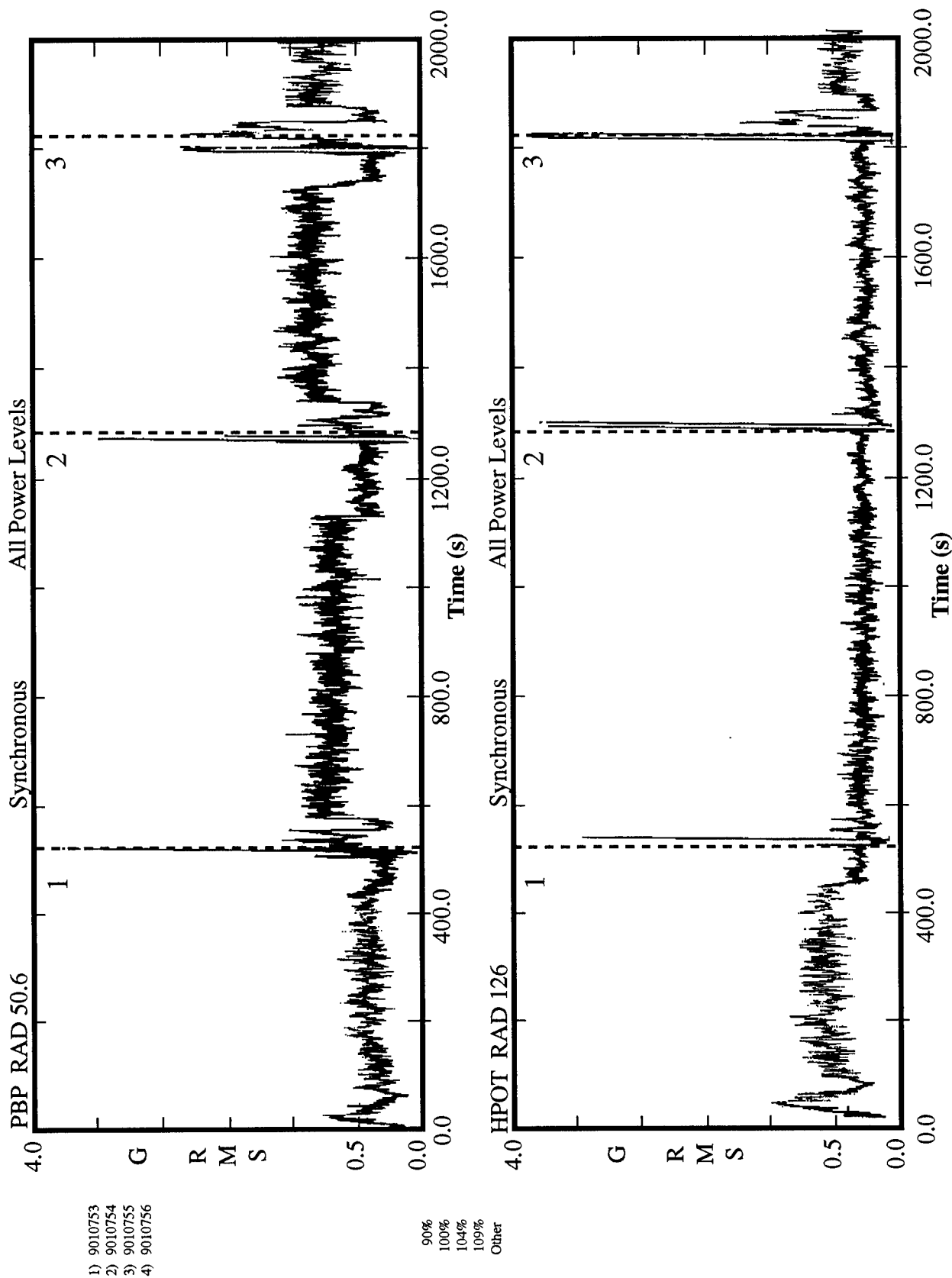
- 1) 9040162
 - 2) 9040163
 - 3) 9040164
 - 4) 9040165
 - 5) 9040167
 - 6) 9040172
 - 7) 9040173
 - 8) 9010740
 - 9) 9010741
 - A) 9010742
 - B) 9010743
 - C) 9010746
 - D) 9010749
 - E) 9010750
 - F) 9010751
- 90%
 - 100%
 - 104%
 - 109%
 - Other

Figure 39. End-to-end runs of two of the development pumps—Continued.



- 1) 9040162
 - 2) 9040163
 - 3) 9040164
 - 4) 9040165
 - 5) 9040167
 - 6) 9040172
 - 7) 9040173
 - 8) 9010740
 - 9) 9010741
 - A) 9010742
 - B) 9010743
 - C) 9010746
 - D) 9010749
 - E) 9010750
 - F) 9010751
- 90%
 - 100%
 - 104%
 - 109%
 - Other

Figure 39. End-to-end runs of two of the development pumps—Continued.



- 1) 9010753
- 2) 9010754
- 3) 9010755
- 4) 9010756

- 90%
- 100%
- 104%
- 109%
- Other

Figure 39. End-to-end runs of two of the development pumps—Continued.

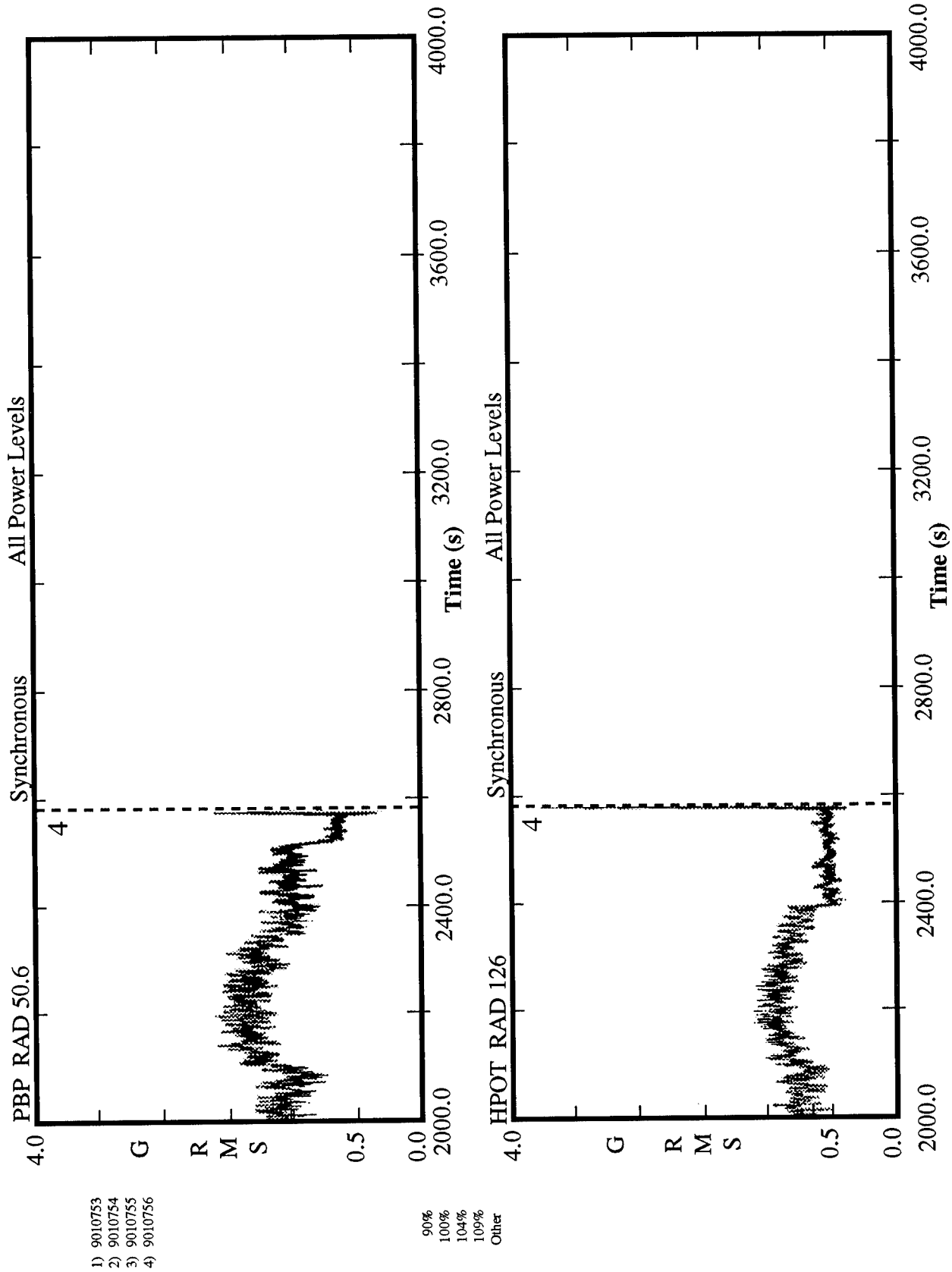


Figure 39. End-to-end runs of two of the development pumps—Continued.

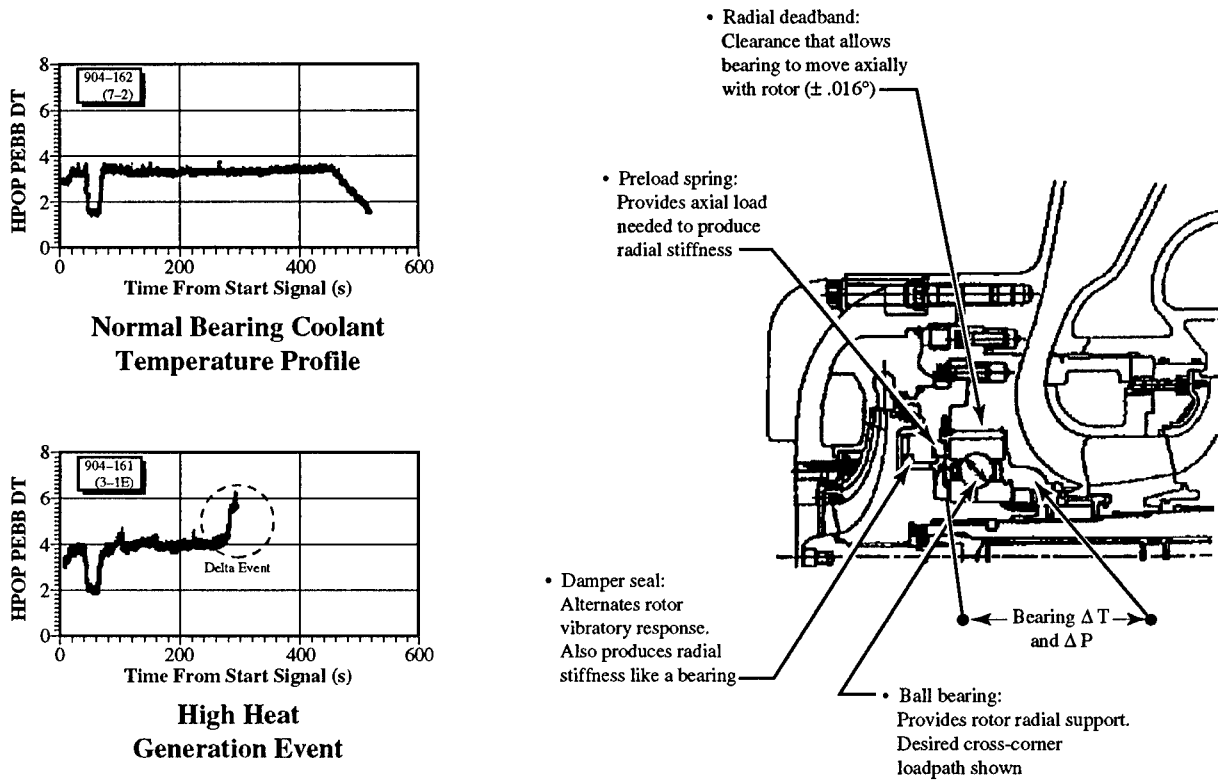


Figure 40. Bearing coolant flow temperature.

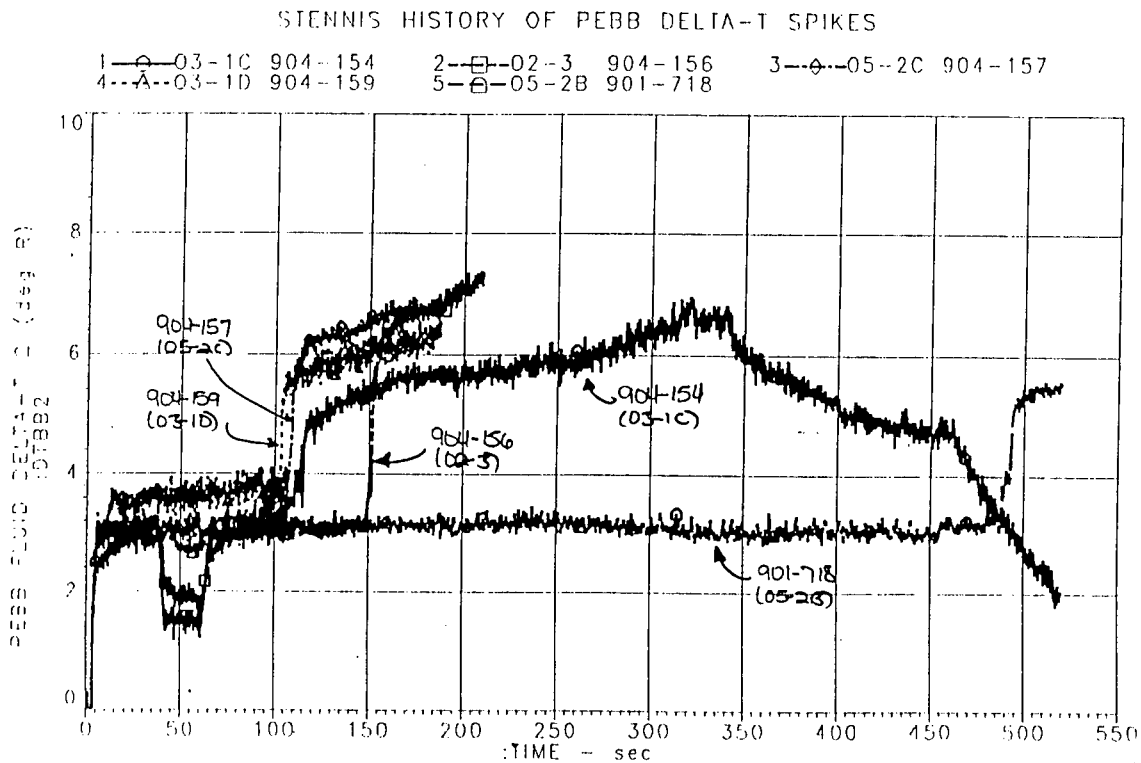


Figure 41. Bearing coolant temperature rise.

PEBB Accum Time at SSC

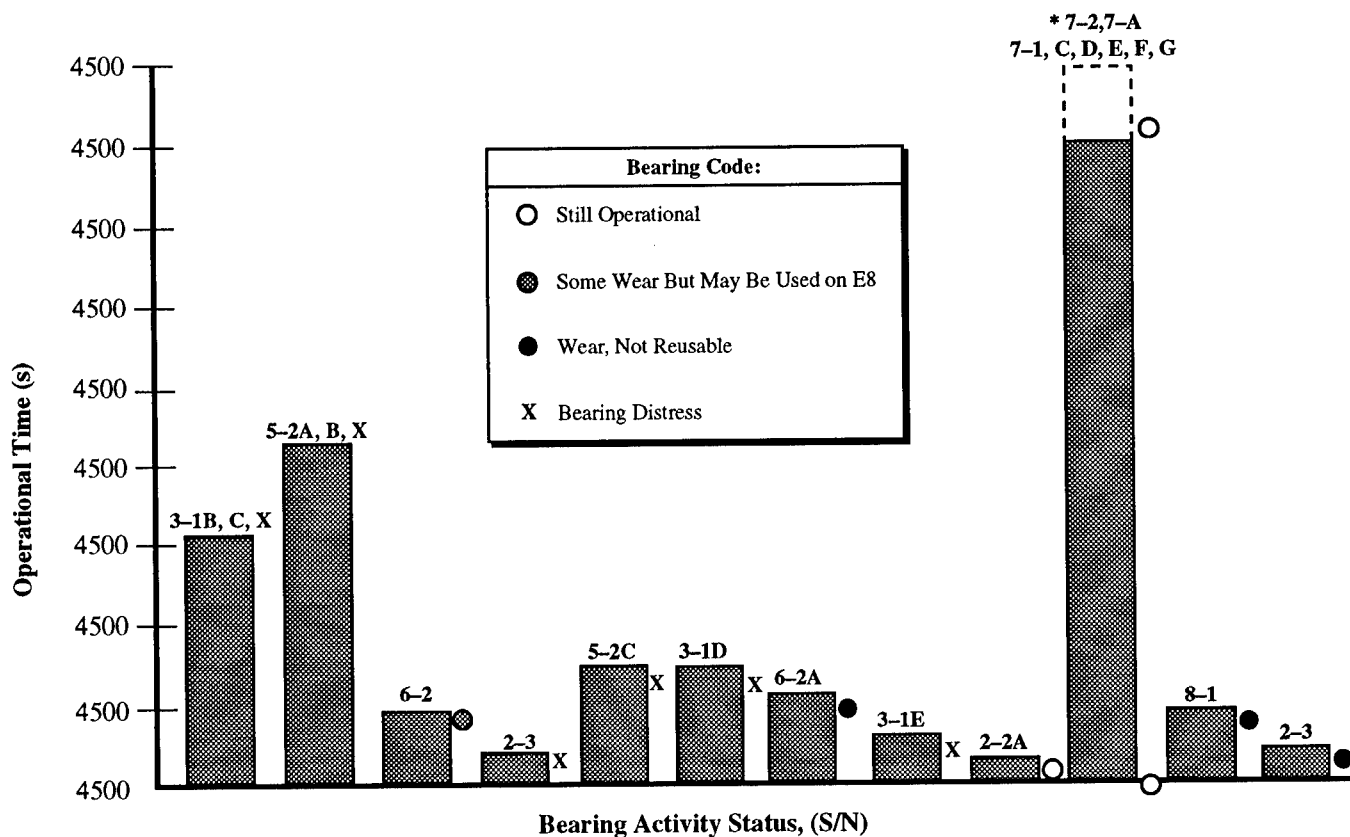
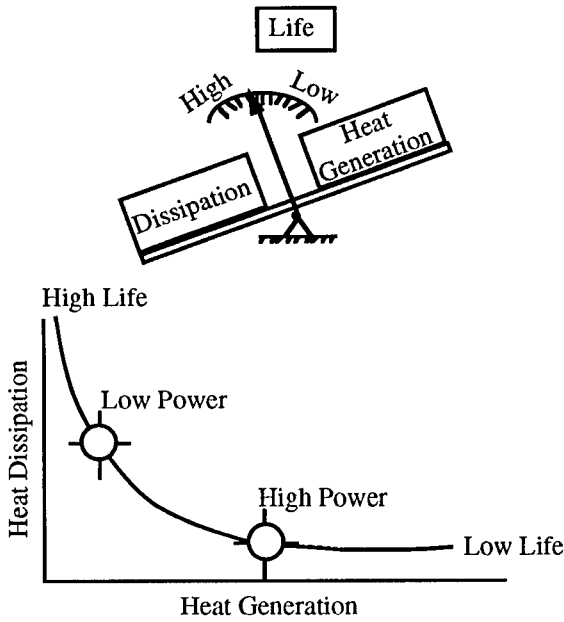


Figure 42. SSME/ATD HPOTP pump end ball bearing experience before corrective solution.

Reviewing, the life of rolling contact bearings is determined by many external factors such as dynamic and static radial loads, axial loads, bearing misalignment, instabilities in the rotor dynamics, lubrication, cooling and bearing geometry. Most research and engineering effort has been expended on oil-lubricated bearings. Cryogenic rocket engine turbomachinery cannot use oil lubrication due to the cold and the incompatible nature of the liquids being pumped. There have been major problems in developing adequate bearing life with lox and, to a lesser extent, liquid hydrogen-cooled bearings in turbopumps. The primary failure mode has been bearing wear and distress. Bearing fatigue failure, upon which the life predictions of well-designed oil-lubricated ball bearings are based, have not been the usual failure mode for bearings cooled and lubricated with cryogenic propellants. The problems of bearing design are compounded by the requirement that these pumps be lightweight and have a very high power density. In these turbopumps, the bearing life determining mechanisms have been heat dissipation and generation. Figure 43 shows how for a high power bearing a balance determines whether a bearing will operate successfully or will overheat. It is possible to put all the major parameters that influence bearing life under these two headings (fig. 44). Heat generation in the bearing is primarily from frictional contact between component surfaces, hysteresis losses because of cyclic stressing of the materials, and viscous fluid losses in the coolant. Heat dissipation is through convective heat transfer to the coolant in the flooded cryogenic bearing design. It should be pointed out that there is a strong interaction, or coupling, between heat dissipation and heat generation that is nonlinear in nature. As the heat generation exceeds the heat dissipation capacity,



$$\text{Bearing Life} = (\text{Dissipation}) - (\text{Heat Generation})$$

- Low bearing life (wear) is caused by inadequate heat dissipation for a given heat generation
- Heat dissipation and heat generation are coupled independent variables
- Heat generation with inadequate heat dissipation results in excessive inner race temperature which is the prime source of bearing wear

Figure 43. Bearing life.

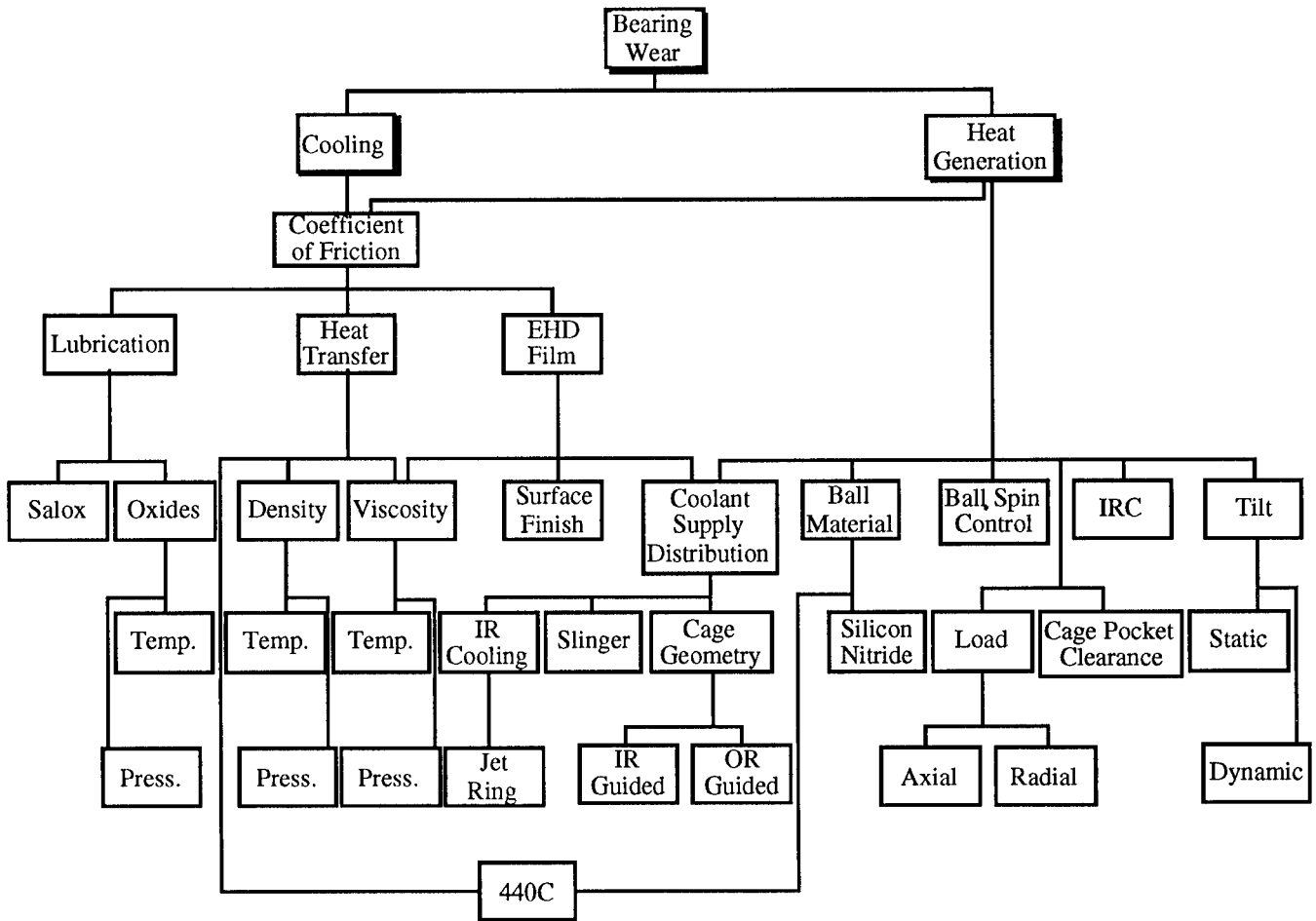


Figure 44. Bearing wear parameters.

abrasive surface oxide formation starts, the thickness of the elastohydrodynamic film is reduced, ball-to-cage interactions increase, inner race clearance (IRC) is reduced, prelubrication breaks down, and cage-to-ball-to-race lubrication transfer diminishes. All of these factors further increase heat generation, leading to what is often termed "thermal runaway" of the bearing.

Thus, a situation had evolved in which all bearings placed into service were failing within a few hundred seconds of operation for no apparent reason. Development of the turbopump was being delayed and significant cost increases were being incurred because of the inability to resolve the bearing failure. At the end of 1992, development termination was threatened unless the problem could be solved within 3 months. A team of Government and contractor specialists was formed with a directive to take all reasonable steps to resolve the problem by the deadline. Because of the limited time available to correct the problem, a concurrent approach was taken. Design and procurement of potential fixes was undertaken based on best engineering estimates of their potential for solving the problem. Fixes that were not viable based on increased understanding of the failures were dropped and new designs were added. While this approach is not the most cost effective, it does give the quickest engineering response time. The steps this team took, starting with a detailed fault tree analysis, are reviewed in the following paragraphs.

The detailed fault tree developed by the investigation team is shown in figure 8. The viable candidate failure mechanism that devolved from the fault tree analysis were:

- (1) Misalignment
- (2) Prelubrication
- (3) Cage instability
- (4) Inadequate IRC
- (5) High loads—fixed and dynamic
- (6) Inadequate cooling
- (7) Inadequate lubrication
- (8) High ball/race heat generation
- (9) Bearing material and configuration
- (10) Other potential causes.

All but items (6), (7), and (8) were eventually dispositioned as not being a cause or at the most being a secondary factor in the bearing wear. The failure scenario that most closely fit analyses, test results, and hardware evidence involved a combination of these three items on the list. A discussion of each of the mechanisms and the assessment of its involvement in the wear mechanism follows.

(1) Bearing Misalignment

Inspections of the first distressed pump-end ball showed evidence of bearing misalignment (tilting), i.e., angular displacement between the inner and outer races. The evidence was pronounced fore and aft cage pocket wear that will occur as the balls of the misaligned bearing speed up and slow down as they orbit the inner race (fig. 45). These data initiated investigations to understand how misalignment might affect bearing heat generation and thus bearing life. As a result, detailed sensitivity studies using various bearing codes were conducted.

The results of these studies showed that if the bearing misaligned more than 4 milliradians, the temperature would rise as the cage pocket clearance was used up. This temperature rise was found to rise to the sublimation temperature of Salox-M[®] at the cage/ball interface, which could render the Salox-M[®] transfer film ineffective. This could increase the ball-to-race friction quickly, causing potentially large temperature delta T's and bearing distress. Figures 46 and 47 show this data. Figure 46 shows the heat in Btu's versus milliradians. Figure 46 illustrates the cage pocket temperature, while figure 47 shows the temperature delta T if the friction coefficient is linearly changed from Salox-M[®]-on-steel to steel-on-steel.

Two facts argued against excessive misalignment of the bearing. Inspections of the race tracks of bearings after turbopump operation did not show indications of misalignment. A turbopump bearing was also instrumented for outer race misalignment. These measurements did not show excessive misalignment. For these reasons, this failure mechanism was discredited.

(2) Prelubrication

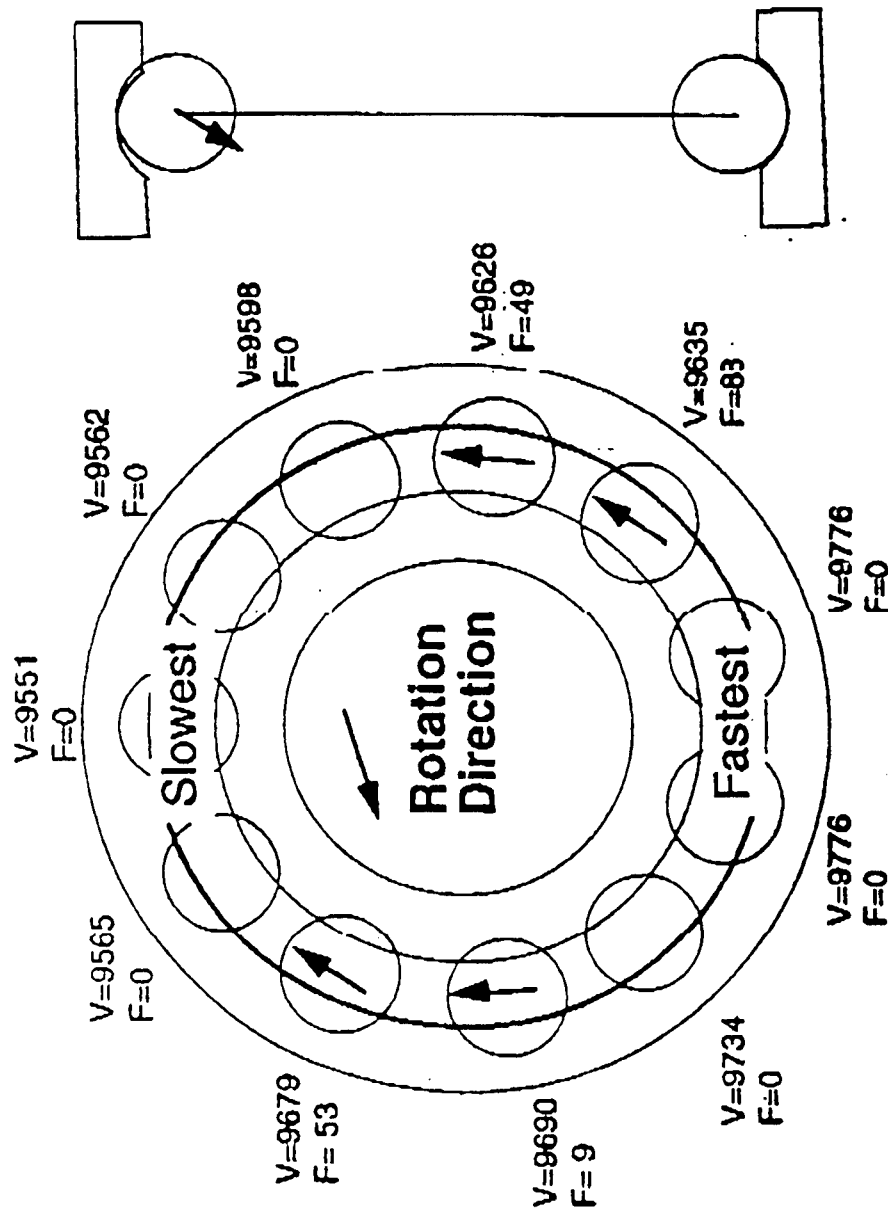
As previously mentioned, there was one exception to the general early failure characteristic shown during turbopump operation. Early in the investigation, one turbopump (unit 07-2) ran successfully for over 5,000 s with no bearing distress and marginally acceptable ball and race wear. This tended to confirm that the bearing design was acceptable as demonstrated in the component test. This result caused an intensive study of the factors contributing to successful operation of this bearing. Two factors stood out: (1) it had been run for over 1,700 s before high speed operation was undertaken, and (2) it, as was also the case of the component design demonstration bearings, had not received a prelubrication of the races until the first 1,700 s of operation were completed. Inspection showed the inner race of this bearing to be very smooth and polished relative to the outer race. This is contrary to the experience of the failed bearing where the inner race showed severe distress.

It was also observed that the ball track wear on the races showed that some failed bearings had switched from outer race ball spin control to inner race ball spin control. Theory allows this to happen with an increase in the friction factor at the inner race over that at the outer race by a factor of three. Thus, attempting to isolate the factors which maintained the low surface friction at the inner race of this particular bearing was given a great deal of attention. These efforts were not successful and a full understanding of the characteristics that made this bearing and turbopump unique were not achieved. Prelubrication of the bearing races was baselined as an improvement that could only improve bearing operation. It was also concluded that the reversing of ball spin control was the accelerator of the bearing distress, not the initiator.

(3) Cage Instability

All pump-end ball bearings have shown evidence of some contact between the inner diameter of the cage and the inner race land. This evidence could possibly be explained by an

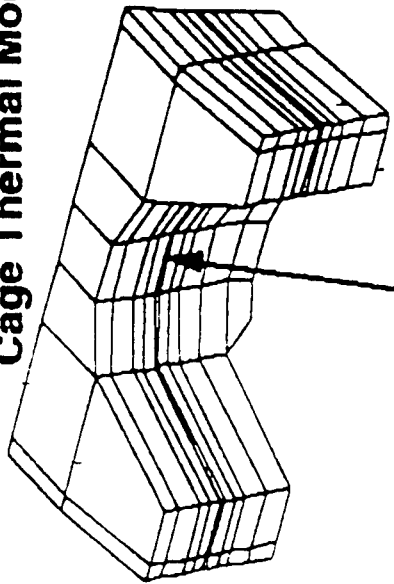
V= Orbital velocity of ball, RPM
 F= Ball-to-cage force
 Arrow shows direction of ball-to-cage force.



- Ball has to move to accommodate to outer race tilt. This changes the contact angle at each ball, which changes each ball's velocity.

Figure 45. Operation of misaligned bearing.

Cage Thermal Model



Max Surface Temp (T193)

- When bearing is misaligned, cage web surface temperatures can exceed sublimation temperature of teflon. This will effectively stop the transfer of lubrication from the cage to the ball. Cage pocket clearances do not change significantly due to extra heat.

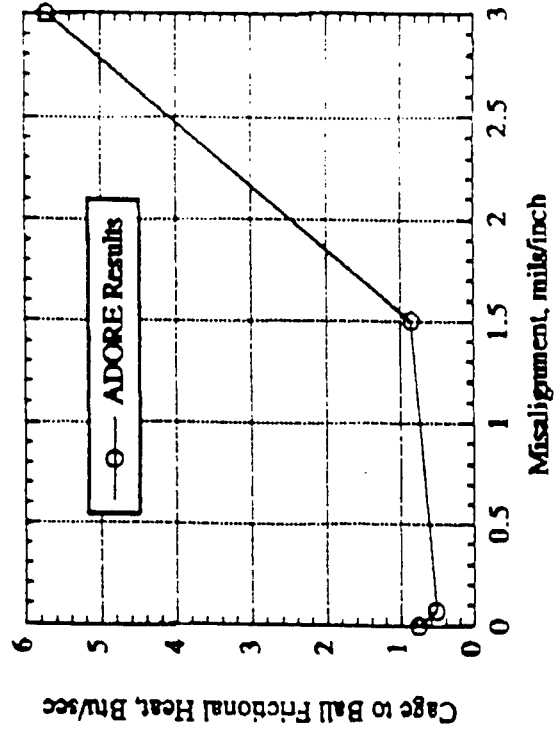
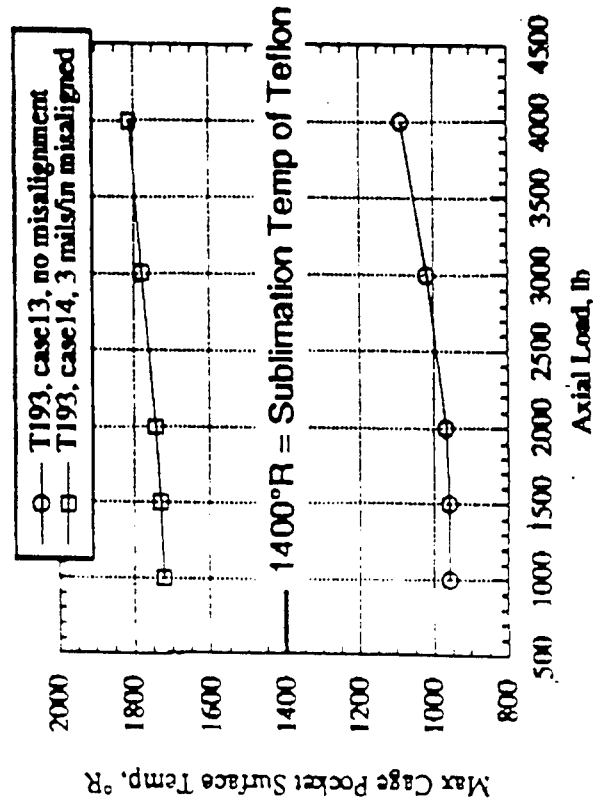


Figure 46. Cage thermal model of bearing distress scenario.

- Bearing failure can be simulated with a loss of lubrication. Simulated bearing had a 2000 lb axial load and no radial load. During 30 seconds prior to event, f was increased from 0.1 to 0.2. At 30 seconds, f was increased to 0.5 for rest of simulation. Speed was 24,000 RPM and outer race was tilted 0.003 radians.

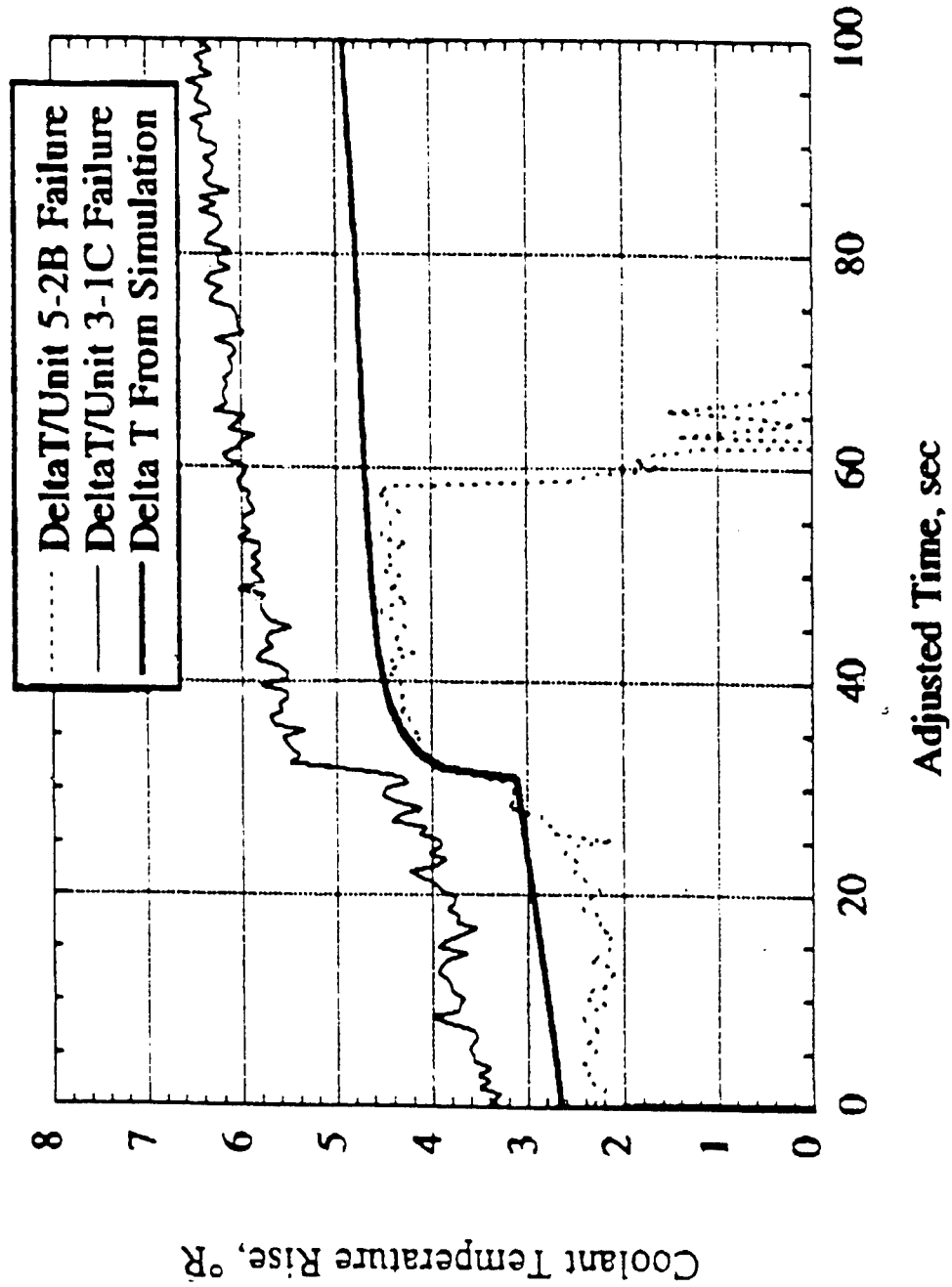


Figure 47. Loss of lubrication bearing failure simulation.

unstable cage which in effect "hula hoops" during rotation. The influencing factors for the instability are: (1) ball-to-cage pocket clearance, (2) cage balance, and (3) cage to land clearance. Other evidence to support the instability was the fore and aft wear on the cage pockets, which indicates excessive movement of the balls relative to the cage. The effect of the instability would manifest itself in cage frequencies in the dynamic data and in an increased temperature rise in the bearing. Analysis results showed that with the existing clearances and unbalance the cage should be stable. In fact, the ball-to-pocket clearance can eventually be doubled from the baseline clearance before instability is a problem. Examining the dynamic data for cage instability and correlating it with the bearing coolant delta T shows that the cage frequency is pronounced only after the step event of the delta T. During the initial slow rise of the delta T where heat generation is increasing, the cage appears to be stable. This leads one to believe that the cage frequency is a result of the accelerated wear process and not a cause. Because of this evidence, the cage instability scenario was dismissed as not credible.

(4) Inadequate Internal Radial Clearance (IRC)

The proper design of a ball bearing requires that the internal radial clearance at operation be sufficient to allow the balls to load against the races at the proper contact angle and provide sufficient margin against a thermal or mechanical loss of radial clearance. Inadequate IRC allows the ball-to-race contact angle to be less than design (ball track will be low on the inner race). This condition promotes increased heating of the balls and inner race due to higher contact stresses, and provides less margin against thermal runaway.

Examination of the inner races of the units which did not fail (low time units) showed that the ball tracks were at the proper contact angle. Failed units had ball tracks which were not too low; however, the track was very wide—some nearly touched the inner race high shoulder corner. This is believed to be due to post-accelerate wear damage and not an indication of the as-built or pre-event contact angle. Based on this evidence, the inadequate IRC scenario was judged as not credible.

(5) High Bearing Loads: Fixed and Dynamic

While the inspections of distressed bearings did not show overt signs of either high radial or axial loading, the unknowns in the design and our previous experience with ball bearings in cryogenic turbopumps did not allow us to immediately close out overload as a potential failure mechanism. In the turbopump design, the bearing cartridge must move axially in response to all operating point changes to ensure acceptable axial thrust balance. The cartridge (sleeve) has tight clearances, with the pump housing making a design that could potentially bind and introduce high axial loads into the bearing. In addition, the uncertainty in the hydrostatic loads acting on the rotor of a high pressure turbopump can be very large and as yet cannot be accurately predicted for a design. Dynamic loads on the bearing, especially in a turbopump which has exhibited high vibration sensitivity, are always a bearing load concern.

Strain gauges were mounted on the pump-end ball bearing preload spring on several development turbopumps to give a direct reading of the axial static and dynamic loads. They showed that the bearing axial load was as predicted and that the bearing was moving axially as required to accommodate pump operating points changes. The axial dynamic loads measured were very low. A subsequent turbopump with radial position measurements of the bearing sleeve deadband showed the sleeve to be moving radially, which confirmed that the radial loads were close to design. Again the dynamic load indications as seen by these gauges were low. Based on these data along with

continuing inspections of bearings removed from test which showed no loads higher than anticipated, it was concluded that bearing load was not a contributor to the distress problem.

(6) Inadequate Cooling

The bearing is cooled with the leakage flow from the preburner impeller back shroud which drains into the main pump inlet. The source pressure is approximately 6,000 lb/in² and pump inlet pressure is approximately 350 lb/in². The coolant temperature is 230 °R which is the temperature of lox at the preburner impeller discharge. The coolant flow (~16 lbm/s) first passes through the damping seal before entering the bearing. The pressure in the bearing compartment is approximately 1,800 lb/in². The bearing uses a flooded cooling system; the coolant is not guided or directed in its passage through the bearing.

Bearing development tests were successfully run on a rig which simulated the turbopump operating cycle to the maximum extent possible. The most significant differences were a coolant flowrate of about 5 lbm/s, a pressure of 200 lb/in², and a temperature of 180 °R. The turbopump conditions were not duplicated because of facility limitations and, in the case of flowrate, a large increase in the design flowrate after rig testing was completed dictated by the requirements of the vibration problem corrective actions. The rig-bearing fixed loads were comparable to the turbopump, but the dynamic loads are believed to be lower. The only failure in the testing occurred on a bearing which was inadvertently built with severe misalignment. This bearing still ran 27,466 s before it showed thermal distress. The successful rig bearings had almost no measurable wear and no evidence of thermal distress.

Heat transfer analysis showed that as long as the heat generation remained low (frictional heat generation consistent with experience) the bearing cooling system was adequate to remove the heat and maintain the ball and race temperatures close to the coolant temperatures. As the bearing distress investigations progressed, thermal analyses that degraded the heat transfer at the inner race surfaces (a condition which would be expected with the inner race guided cage configuration used) showed that the temperature at the inner race/ball contact point could rise as much as several hundred degrees, depending on the assumptions made as seen in figure 48. Later computational fluid dynamics (CFD) analysis and bearing model tests confirmed that there is little coolant circulation at the inner race/ball contact and that the temperature will locally rise significantly. While this temperature rise is not deleterious to the bearing materials, it was found that it can cause a significant reduction in the elastohydrodynamic (EHD) film at the inner race/ball contact. If the thickness of the EHD film is reduced so that as ball/race surface asperity contact occurs, the friction coefficient will rise significantly as noted in the Stribeck curve in figure 49. It is not possible to precisely locate where the pump-end ball bearing operates on this curve (the characteristics for lox must also be questioned because it was developed for oil lubrication), but calculation of the EHD film thickness for the ATD bearing conditions show that the inner race/ball contact operates in the region where friction coefficient is very sensitive to fluid conditions. Small changes in fluid temperature can cause a significant change in the EHD film thickness as seen in figure 50. An increase in friction and thus heat generation at the ball/race contact will be an unstable condition and will cause a further increase in friction.

(7) Inadequate Lubrication

Bearings for cryogenic rocket turbopumps have traditionally depended upon the transfer of a polytetrafluorethylene (PTFE) film from the cage by rubbing to the bearing balls and races. Adhesion of the PTFE to the contact surfaces has provided limited, but adequate lubrication for these applications. The ATD bearing uses a bronze filled PTFE cage (Salox-M[®]) to provide this

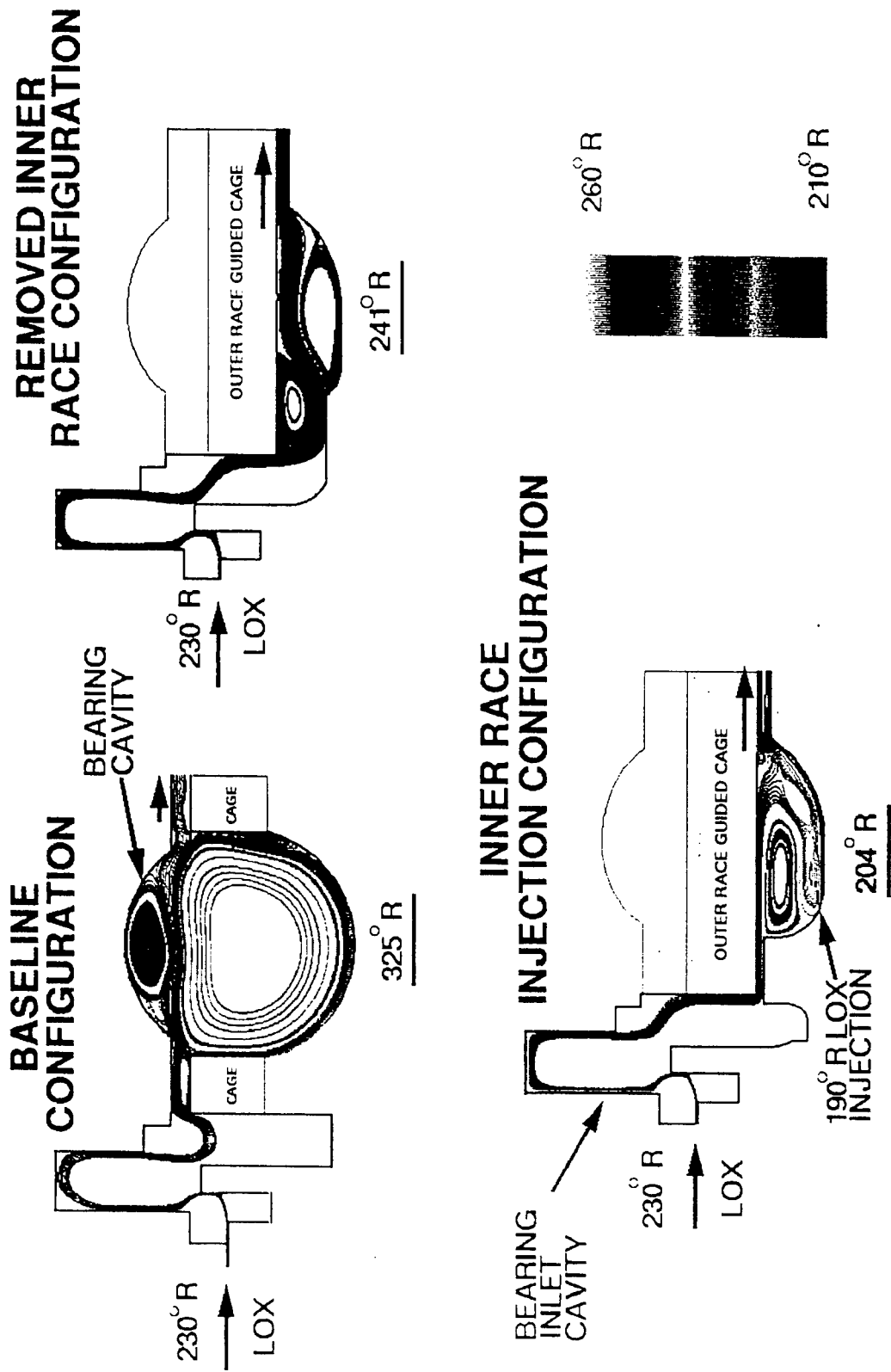


Figure 48. CFD analysis of ATD bearing coolant flows.

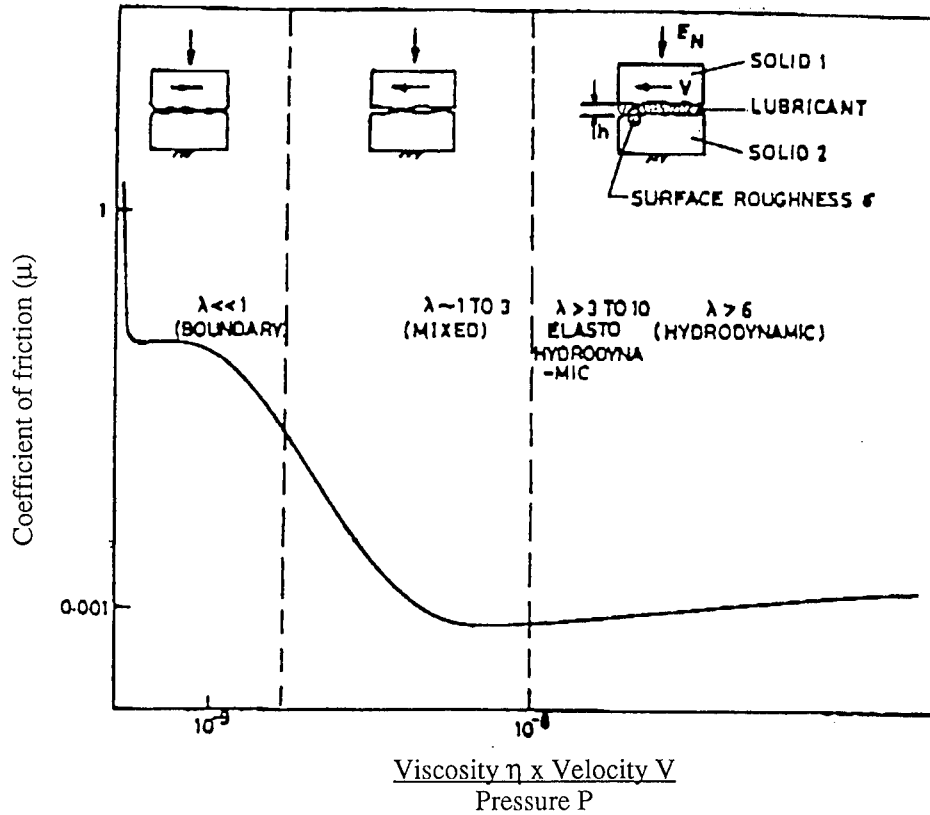


Figure 49. Stribeck curve (coefficient of friction versus viscosity by velocity/pressure).

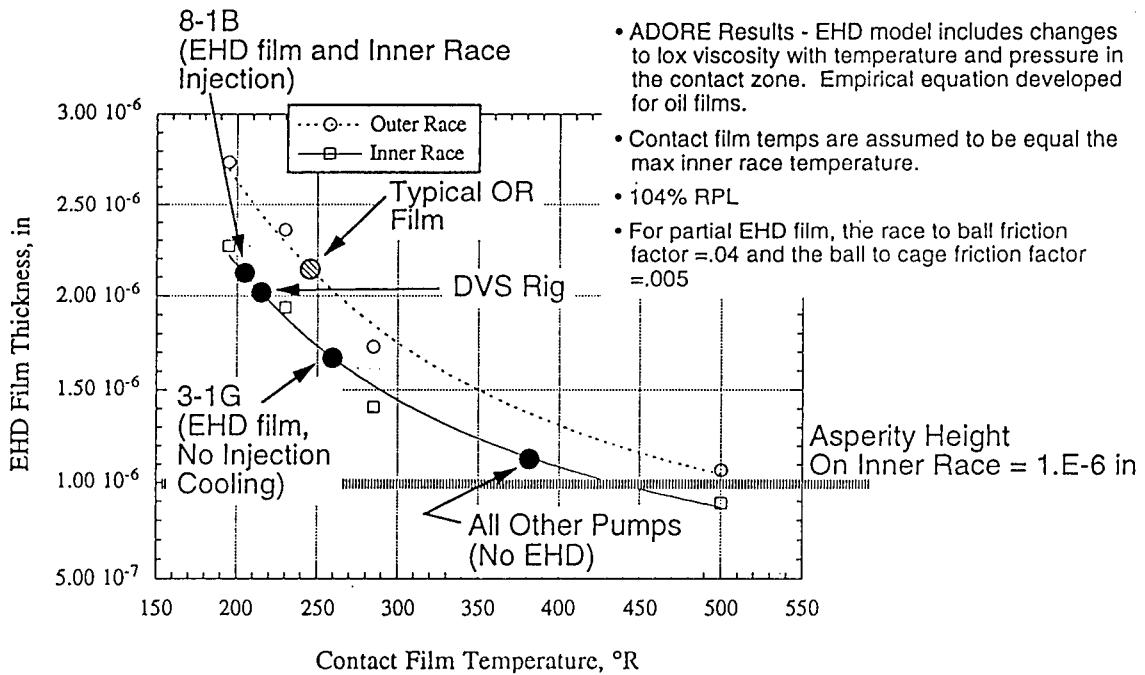


Figure 50. LoX EHD film thickness analysis.

lubrication function. Inspection of bearings from the rig testing showed that an adequate film of PTFE was being transferred as evidenced in the copper shading of the ball track on the races. Inspection of bearings from the early turbopump tests substantiated these results, and it was concluded that the lubrication intent was being met.

After the onset of the bearing distress problem, a prelubrication process for initially the inner race and later for both races was developed. Prelubrication was initiated to insure that an adequate lubrication film was present at the ball/race contact from the start of turbopump operation. The races were burnished with a Salox-M[®] block on the race contact surfaces.

During the failure investigation, the adequacy of the Salox-M[®] lubrication was questioned and several efforts were initiated to further improve the prelube and to provide a low speed run-in of the bearing. No definitive answers on the effectiveness of the prelube or on the worth of the run-in were reached. It was concluded that the worth of the prelube was most modest. The low speed run-in was dropped because of inconclusive test results.

As previously noted, the EHD film lubrication is significant in the successful operation of the ATD bearing. Again, small changes in lox properties can be shown to dramatically change the friction factor as seen in figure 49. The increased coolant temperature from the successful rig tests to turbopump would cause a significant decrease in the EHD film thickness, and thus, a tendency for operation in the boundary lubrication region (fig. 49). Traction tests run at MSFC showed a friction factor of less than $f = 0.1$, with conditions simulating the pump-end ball bearing, except that normal boiling point oxygen was used as a coolant. When the test was repeated with higher loads and lower speeds, the friction factor increased to $f = 0.2$. This is a clear indication of a sensitive EHD film contributing to the rig coefficient of friction.

Based upon these results, it was concluded that bearing distress could not be correlated to any breakdown or failure of the cage transfer film. The effectiveness of the transfer film is, however, open to question, and it is the opinion of many of the team members that it contributes little to the bearing lubrication.

(8) High Ball/Race Heat Generation

Excessive heat generation, which by itself or in conjunction with another failure mechanism, was considered as a potential cause of the thermal distress seen on the balls and races. Heat is generated by relative motion between the ball and races at the point of contact. The heat generated is thus a function of the friction factor of the materials, the contact loads, and bearing geometry, which will contribute in establishing the magnitude of relative motion. As noted earlier, the bearing loads were determined to be within the design limits. The bearings were determined to be as designed, and the load tracks on bearings that had not failed showed that the bearings were operating as designed geometrically. The friction factor at the contact is set by the surface finish and the EHD film established. The bearing balls and race contact area were being finished to $< 1 \mu\text{in}$, a value consistent with low rolling friction operation. The EHD film, as previously discussed, was believed to be marginal and for this reason excessive heat generation was a viable failure mechanism.

A simplified fault tree that concentrates on the viable interrelated failure mechanisms is shown in figure 44. There are several paths through this fault tree leading to a distressed bearing. The bearing team was unable to isolate the failures to a single mechanism. It is uncertain that there is a unique mechanism which will fit all of the failures. A combined mechanism with the several elements making differing contributions depending on the circumstances may be quite appropriate.

The fault tree approach served this failure investigation well. The most difficult and time-consuming part of the investigation was developing data to close out several branches of the fault tree.

(9) Bearing Material and Configuration

The other main emphasis of the investigation was in the area of the bearing material and bearing configuration. Bearing materials were considered to play a minor role in the failure cause; the heavier steel balls with their friction and heat transfer characteristics could have been part of the cause along with improper coolant. Bearing configuration characteristics that were studied and ruled out as a primary cause were IRC, inner race guided cage, cage pocket-to-ball clearance, and ball diameter. As solutions to the bearing distress problem were explored, all these areas were used to improve margins as well as solve the problem cause. The final configuration has outer race guided cage (fig. 51), stiffened housing, silicon nitride balls, lower preload spring, larger ball-to-cage pocket clearances, and auxiliary cooling (fig. 52).

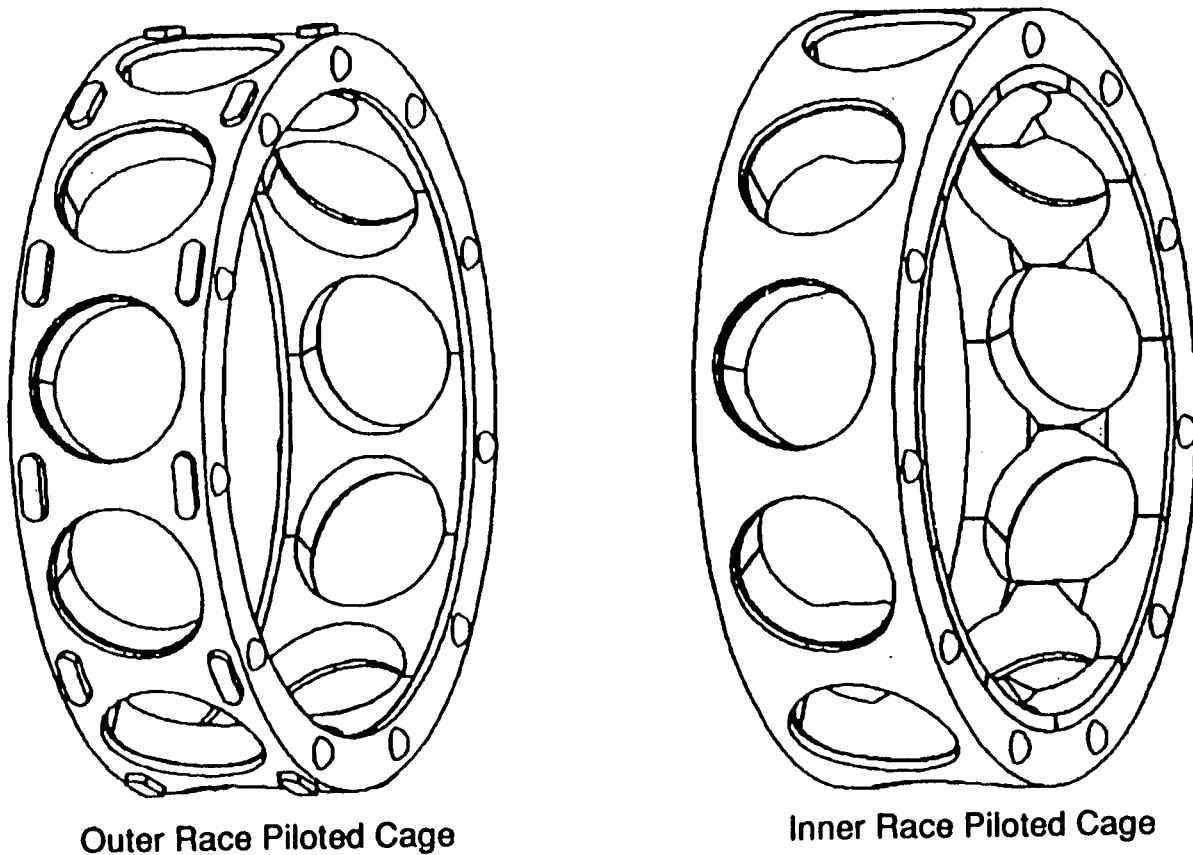


Figure 51. PEBB outer race piloted cage.

(10) Other Potential Causes

The team methodically pursued many other causes from balance position control authority, axial preload, high-radial load, surface sliding, plastic deformation, manufacturing, plus the other items discussed.

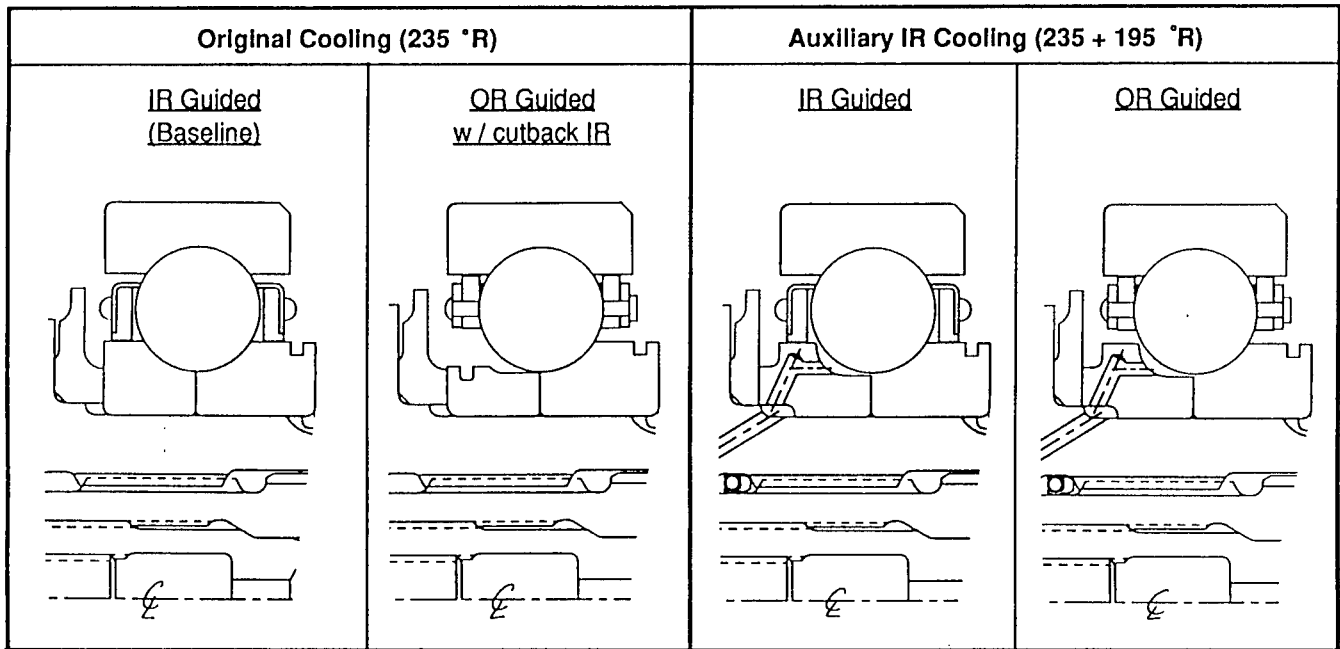


Figure 52. SSME/ATD HPOTP bearing configuration.

(11) Conclusion

The bearing problem was caused by excessive ball/inner race friction which in turn was caused by inadequate lubrication.

The bearing degradation scenario is:

- (1) The basic cause of the problem is high heat generation and poor heat dissipation.
- (2) Inadequate coolant temperature and distribution are the prime mechanisms for the heat dissipation. Heat generation is also improved by increasing the thickness of the EHD film (which reduces the ball/race contact coefficient of friction) and enhancing the Salox-M® transfer and retention.
- (3) The EHD film generated by cold lox is very sensitive to:
 - (a) Coolant temperature (viscosity)
 - (b) Surface finish
 - (c) Beneficial oxides created by cold lox
 - (d) Contact pressure
 - (e) Velocity.

A breakdown of the EHD film and loss of the Salox-M® transfer film caused by higher temperature lox is believed to be the trigger mechanism that initiates the rapid wear phenomenon.

- (4) The ball raceway control is a secondary event caused by the sudden increase in coefficient of friction at the inner race, and contributes to the rapid rise in delta T and bearing wear.
- (5) The use of silicon nitride ball material lowers the heat generation and improves heat transfer, enhancing bearing life. Silicon nitride balls also minimize the potential for breakdown of the EHD film and Salox-M[®] transfer film and reduces the loads due to lower mass. The ball material can also tolerate much higher temperatures than can 440C steel balls.
- (6) The success of unit 7-2 is explained by the low power run-in operation early in the testing of its bearing. Operation at 65-percent RPL results in a 40 °R reduction in coolant supply temperature, which is highly beneficial to creating the improved surface finish before extended operation at high power with the higher heat generation.

The corrective actions to eliminate wear are: to improve the coolant supply at the inner race ball contact, to use an outer race guided cage, and to use silicon nitride balls. In development of the corrective measures, the silicon nitride bearing balls and the outer race guided cage were introduced into the turbopump together. All turbopumps with these two modifications ran successfully and showed no measurable ball, race, or cage wear when inspected. Subsequently, the inner race ball contact cooling modification was added and again pumps with the three changes have operated with no wear. A single turbopump was built with only the outer race guided cage and inner race ball contact cooling modifications. The bearing was found to be worn and thermally distressed after 400 s of operation. Bearing coolant temperature rise data indicate the distress started after only 40 s of operation. Based upon this result, it must be concluded that the cooling improvements of themselves were inadequate to correct the problem. The silicon nitride ball characteristics, high elasticity, low centrifugal forces, reduced race contact heat generation, higher thermal conductivity, and a lower friction coefficient, when used with metal races, are crucial to successful operation in the ATD HPOTP application. No additional work was undertaken in this program to further understand the contribution to successful bearing operation of each of the design improvements. Based on this experience and several previous unsuccessful attempts to develop lox cooled bearing, dependence on only a transfer and/or an EHD film is too marginal and uncertain for successful bearing operation. The benefits of the silicon nitride balls are required.

Bearing technology and turbomachinery understanding were certainly advanced. The team's final fix for the bearing problem is:

- (1) Silicon nitride balls with steel races
- (2) Outer race-guided cage
- (3) Larger ball-to-cage pocket clearances
- (4) Inner race prelubrication only
- (5) Colder coolant directed to inner race.

These changes were completely successful in correcting the wear problem. No bearing wear has been observed since these incorporations.

The team did pursue other solutions such as better prelubrication, and hydrostatic damper seal bearings. Although the hydrostatic damper seal bearing had many merits, it is probably a good bearing for the future.

Even if the better coolant was fundamental to the bearing distress solution, depending on it to create EHD film is not prudent. Therefore, it is mandatory that the benefits silicon nitride balls bring be part of the solution in order to guarantee bearing life.

VI. OVERALL CONCLUSION/SUMMARY

The rotordynamics of high-performance turbomachinery are a very complex, nonlinear system composed of the pressure vessel and rotor support system, the hot-gas turbine drive system, the cryo-liquid pump system, system damping devices, and the bearings. The hot gas and hydroforces can be both periodic forcing functions and unstable (negative damping sources). Because of the high-performance requirements and the weight/volume constraints, there is a very fine tuning (balancing act) between performance requirements and rotordynamic characteristics. This means that sophisticated analysis tools, component tests, and a comprehensive hot-fire margin test program should be established. Due to the analytical complexity and the inability to properly quantify forces such as hot-gas environments, hydro environments, structural characteristics, bearing characteristics, and only limited analytical verification (trend/sensitivity prediction only) the margin test program is mandatory.

The solution to the ATD LO₂ turbopump problems were possible only because of the foresight of NASA leadership over the years to build test facilities (air and water flow, propulsive), analysis technology in bearings, heat transfer, rotordynamics and CFD, bearing materials development, and bearing lubrication. This includes MSFC development as well as the Pratt & Whitney E-8 test stand.

In future systems, it is highly desirable that the dual support system (ball bearing/damping seal) be replaced with either a hydrodynamic damping bearing or foil bearing, eliminating the main source of nonlinearities or move the damping seal and provide system damping at another location—possibly using a different source which allows full development of the ball bearing for stiffness potential. The damping seal hydro bearing is unique in that it simultaneously provides both damping and stiffness.

The only total answer to what is transpiring in a turbopump is found by testing in pump stands or engine systems with adequate data obtained by special instrumentation and posttest hardware inspection. In the final analysis, the hardware has the answer, our job is to read it. Work needs to be continued to accurately provide the hot gas and hydroforces characteristics so that the analytical models can be more heavily depended on for design verification and operations. Better instrumentation needs to be developed to verify these forces and determine in hot fire actual rotor responses.

Bearing technology development must continue. The silicon nitride ball bearing technology saved the ATD program. It is certainly a lesson learned that new programs are highly dependent on the technology programs. The same is true of special test facilities. These were critical in the vibration and bearing degradation solutions: (1) the E-8 hot-fire pump test, (2) MSFC bearing testers, and (3) MSFC cold-flow facilities.

It is very important that the design and the manufacturing process allow very quick changes in order to properly evaluate parameter sensitivities and cause/solution hardware characteristics. This ability allowed the team to accomplish its mission.

Sensitivity analysis as well as off-nominal testing are key to understanding problems and arriving at solutions. This couples with the proven approach of searching for deviation and their effects. Playing the two together shows understanding of problem.

For future programs, sensitivity analysis and testing (cold flow, dynamic, and hot fire) should be done early in the program to eliminate most of the problems downstream. It is doubtful, however, that this would have caught the bearing wear problem; but, it would have certainly eliminated the vibration problem.

The use of a concurrent engineering team in conjunction with the use of formal fault trees is mandatory for cause identification and problem resolution. The team members' selection is critical in that teaming brings no magic elixir to the table, thus the team is no stronger than the skills of the team members. This implies that organizations must vigorously develop the total person of its personnel.

All future systems should be designed with the goal of robustness.¹⁵

Silicon nitride balls provide substantial margins to the ball bearing life.

Through the results of the team's efforts, it is concluded that the ATD LO₂ turbopump is acceptable for certification from both bearing life and vibration sensitivities and high-g vibration. However, for management of the pumps operationally requires that an extensive vibration database of both ground and flight test be maintained.

REFERENCES

1. Biggs, R.E.: "Propulsion System Failure Analysis-A Methodology." AIAA/SAE/ASME/ASEE 28th Joint Propulsion Conference and Exhibit, July 6-8, 1992, Nashville, TN, pp. A1492-3796.
2. Ehrich, F.F., and Childs, D.: "Self-Excited Vibration in High-Performance Turbomachinery." *Mechanical Engineering*, May 1984, pp. 66-79.
3. Rao, J.S.: "Rotordynamics." Second edition, J. Wiley, 1991.
4. SSME Alternate Turbopump Development Program, Supplemental Report HPOTP PEBB Investigation, United Technologies, Pratt & Whitney.
5. Ryan, R.S., Gross, L.A., Mills, D., and Mitchell, P.: "The Space Shuttle Main Engine Liquid Oxygen Pump High-Synchronous Vibration Issue, The Problem, The Resolution Approach, the Solution." AIAA Paper 94-3153, June 1994.
6. Huzal, D., and Huang, D.: "Modern Engineering for Design of Liquid Propellant Rocket Engines." AIAA 1992, ISBN 1-56847-43-6111-147.
7. Csomor, A., Faulkner, C., and Ferlite, F.: "ALS Turbomachinery Technology." SAE International Aerospace Technology Conference and Exposition, Long Beach, CA, October 1-4, 1990.
8. Ehrich, F.F.: "Shaft Whirl Induced by Rotor Internal Damping." *Journal of Applied Mechanics*, June 1964.
9. von Pragenau, G.: "Damper Seals for Turbomachinery." NASA TP-1987, March 1982.
10. Childs, D.W., and Kim, C.H.: "Testing for Rotordynamic Coefficients and Leakage: Circumferentially-Grooved Turbulent Annular Seals." Proceedings of the IFToMM International Conference on Rotordynamics, Tokyo, Japan, September 1986, pp. 609-618.
11. Childs, D.W., and Kim, C.H.: "Test Results for Round-Hole Pattern Damper Seals: Optimum Configurations and Dimensions for Maximum Net Damping." *ASME Transactions, Journal of Tribology*, vol. 108, October 1986, pp. 605-611.
12. Matthew, E.K.: "Solving Subsynchronous Whirl in the High Pressure Hydrogen Turbomachinery of the SSME." *AIAA Journal of Spacecraft and Rockets*, vol. 17, No. 3, Article No. 78-1002R, June 1980.
13. Childs, D.W., and Kim, C.H.: "Analysis and Testing for Rotordynamic Coefficients of Turbulent Annular Seals with Directionally Homogeneous Surface-Roughness Treatment for Rotor and Stator Elements." *ASME Journal of Tribology*, vol. 107, July 1986, pp. 298-308.
14. Ryan, S.G.: "Limit Cycle Vibrations in Turbomachinery." NASA Technical Paper 3181, December 1991.
15. Ryan, R.S.: "Robustness." NASA Technical Paper 3336, March 1993.

BIBLIOGRAPHY

- Metals Handbook Ninth Edition, Volume II, Failure Analysis and Prevention, Failures of Rolling-Element Bearings, pp. 490–514.
- Bacht, D.G., Hawkins, L.A., Scharrer, J.K., and Murphy, B.T.: “Suppression of Subsynchronous Vibration in the SSME HPFTP.” Presented at the Sixth Workshop on Rotordynamic Instability Problems in High Performance Turbomachinery, College Station, TX, May 1990.
- Black, H.F. and Jenssen, D.N.: “Dynamic Hybrid Properties of Annular Pressure Seals.” *Journal of Mechanical Engineering*, vol. 184, 1970, pp. 92–100.
- Black, H.F., and Jenssen, D.N.: “Effects of High Pressure Ring Seals on Pump Rotor Vibrations.” ASME Paper No. 71-WA/FE-38, 1971.
- Black, H.F.: “Effects of Hydraulic Forces in Annular Pressure Seals on the Vibration of Centrifugal Pump Rotors.” *Journal of Mechanical Engineering Science*, vol. 11, No. 2, 1969, pp. 208–213.
- Bursey, R.W., et al.: “Incorporation of Silicon Nitride Rolling Elements Into the Pratt & Whitney High Pressure Oxidizer Turbopump for the Space Shuttle Main Engine.” Conference on Advanced Earth-to-Orbit Propulsion Technology, May 1994.
- Childs, D.W., and Garcia, F.: “Test Results for Sawtooth Pattern Damper Seals: Leakage and Rotordynamic Coefficients.” *ASME Journal of Tribology*, vol. 109, January 1987, pp. 136–143.
- Childs, D.W.: “The Space Shuttle Main Engine High Pressure Fuel Turbopump Rotordynamic Instability Problem,” ASME Paper 77-GT-49, 1976.
- Den Hartog, J.P.: “Mechanical Vibrations.” McGraw Hill Book Co., New York, NY, 1956.
- Dillis, M.K.: “Development and Application of Cooling Injection for the Pratt & Whitney High Pressure Oxygen Turbopump for the Space Shuttle Main Engine.” Conference on Advanced Earth-to-Orbit Propulsion Technology, May 1994.
- Janney, J.R.: “Guide to Investigation of Structural Failures.” American Society of Civil Engineers, New York, NY, 1979.
- Jenssen, D.N.: “Dynamics of Rotor Systems Embodying High Pressure Ring Seals.” Ph.D. Dissertation, Harlot-Watt University, Edinburgh, Scotland, July 1970.
- Kim, C.H., and Childs, D.W.: “Analysis for Rotordynamic Coefficients of Helically, Grooved Turbulent Annular Seals.” *ASME Transaction Journal of Tribology*, vol. 109, January 1987, pp. 136–143.
- Lomakin, A.: “Calculation of Critical Speed and Securing of Dynamic Stability of the Rotor of Hydraulic High Pressure Machines With Reference to Forces Arising in the Seal Gaps.” *Energomashinostroenie*, vol. 4, April 1958, pp. 1–5.

- Marmol, R.A., Smalley, A.T., and Tecz, J.A.: "Spline Coupling Induced Nonsynchronous Rotor Vibrations." ASME Paper 79-DET-60, September 1979.
- McCarty, J., Murphy, J.M.: "An Assessment of Liquid Propulsion in the United States." AIAA Paper, July 1989.
- Mitchell, J.P., and Prive, J.L.: "Space Shuttle Main Engine (SSME) Alternate Turbopump Design and Development." 43rd Congress of the International Astronautical Federation, Washington DC, August 1992.
- Nolan, S., Hibbs, R., and Genge, G.: "Hot Fire Testing of a SSME HPOTP With an Annular Hydrostatic Bearing." AIAA Paper 93-2358, 1993.
- O'Hara, K.: "Liquid Propulsion System Reliability, Design for Reliability." AIAA Paper 89-2428, July 1989.
- Petroski, H.: "Design Paradigms, Case Histories of Error and Judgment in Engineering." Cambridge University Press, 1994.
- Pugh, S.: "Total Design." Addison-Wesley Publishing Co., New York, NY, 1991.
- Pye, D.: "The Nature of Design." Reichold Book Corporation, New York, NY, 1969.
- Rieger, N.: "Balancing of Rigid and Flexible Rotors." The Shock and Vibration Information Center, USA Dept. of Defense, 1986.
- Roseau, M.: "Vibrations in Mechanical Systems." Springer-Varlay, New York, NY, 1984.
- Scharrer, J., and Nunez, D.: "The SSME HPFTP Wavy Interstage Seal: Part I-Seal Analysis." Machinery Dynamics-Applications and Vibration Control Problems, ASME Pub. DE-vol. 18-2, 1989, pp. 95-100.
- Scharrer, J., and Nelson, C.: "Rotordynamic Coefficients for Partially Roughened Pump Annular Seals." ASME Journal of Vibrations and Acoustics, vol. 113, No. 2, 1991, pp. 240-244.
- Scharrer, J., and Nelson, C.: "Rotordynamic Coefficients for Partially Tapered Annular Seals: Part I—Incompressible Flow." ASME Journal of Tribology, vol. 113, No. 1, 1991, pp. 48-52.
- Scharrer, J., Rubin, N., and Nelson, C.: "The Effects of Fixed Rotor Tilt on the Rotordynamic Coefficients of Incompressible Flow Annular Seals." ASME Journal of Tribology, vol. 115, No. 3, 1993, pp. 336-341.
- Scharrer, J., Tellier, J., and Hibbs, R.: "A Study of the Transient Performance of Hydrostatic Bearings: Part I—Test Apparatus and Facility." STLE Paper 91-TC-3B-1, 1991.
- Scharrer, J.K., Hibbs, R.I., and Nobs, S.A.: "Extending the Life of the SSME HPOTP Through the Use of Annular Hydrostatic Bearings." AIAA Paper 92-3401, July 1992.
- Spanyer, K.: "Characteristics Pertaining to a Stiffness Cross-Coupled Jeffcott Model." ASME Paper 85-DET-144, September 1985.

Wallace, P.J.: "The Technique of Design." Sir Isaac Pitman & Sons Ltd, London, England, 1952.

Zaretsky, E.: "Life Factors for Rolling Bearings." STLE Publication SP-34, 1992.